AD-A079 654 OKLAHOMA STATE UNIV STILLWATER FLUID POWER RESEARCH --ETC F/G 11/8
WEAR IN FLUID POWER SYSTEMS.(U)
NOV 79 N00014-75-C-1157

UNCLASSIFIED ONR-CR169-004-2 NL

1 OF 2
AD A079654

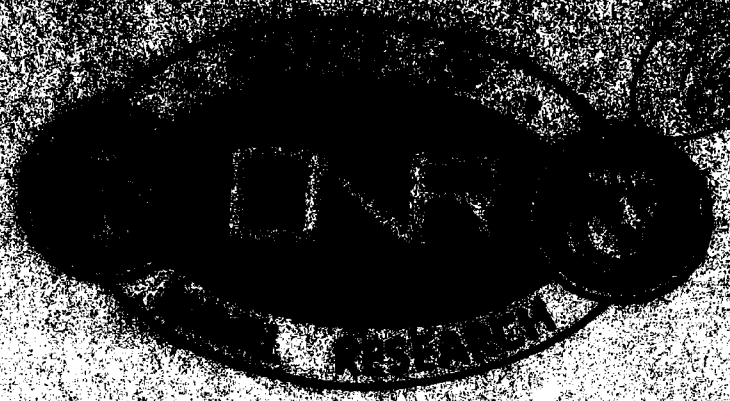

WEAR IN FLUID POWER SYSTEMS

FLUID POWER RESEARCH CENTER
OKLAHOMA STATE UNIVERSITY
STILLWATER, OKLAHOMA
74074

Contract No. N00014-78-C-1157

1 July 1978 - 30 June 1979

FINAL REPORT

Approved for public release; distribution unlimited.

PREPARED FOR THE
OFFICE OF NAVAL RESEARCH, 800 N. QUINCY ST., ARLINGTON, VIRGINIA

REPORT ONR CR169-004-2

WEAR IN FLUID POWER SYSTEMS

FLUID POWER RESEARCH CENTER
OKLAHOMA STATE UNIVERSITY
STILLWATER, OKLAHOMA
74074

Contract No. N00014-75-C-1157

1 July 1978 - 30 June 1979

FINAL REPORT

PREPARED FOR THE

OFFICE OF NAVAL RESEARCH ● 800 N. QUINCY ST. ● ARLINGTON ● VA ● 22217

SECURITY CLASSIFICATION OF THIS PAGE (When Data Entered)

REPORT DOCUMENTATION PAGE

READ INSTRUCTIONS BEFORE COMPLETING FORM

1. REPORT NUMBER (6)	2. GOVT ACCESSION NO.
3. RECIPIENT'S CATALOG NUMBER	
4. TITLE (and Subtitle) (9) Wear in Fluid Power Systems.	5. TYPE OF REPORT & PERIOD COVERED FINAL REPORT. 1 Jul 78 — 30 Jun 79.
6. PERFORMING ORG. REPORT NUMBER ONR CR169-004-2	
7. AUTHOR(s) Fluid Power Research Center (15)	8. CONTRACT OR GRANT NUMBER(s) N00014-75-C-1157
9. PERFORMING ORGANIZATION NAME AND ADDRESS Fluid Power Research Center Division of Engineering, Technology, and Architecture - Okla. State Univ. Stillwater 74074	10. PROGRAM ELEMENT, PROJECT, TASK AREA & WORK UNIT NUMBERS
11. CONTROLLING OFFICE NAME AND ADDRESS Office of Naval Research Attn: Hal Martin 800 N. Quincy Street Arlington, VA 22217 (11)	12. REPORT DATE 30 Nov 79 13. NUMBER OF PAGES
14. MONITORING AGENCY NAME & ADDRESS (if different from Controlling Office) (12) 122	15. SECURITY CLASS (of this report) Unclassified
	15a. DECLASSIFICATION/DOWNGRADING SCHEDULE

16. DISTRIBUTION STATEMENT (of this Report)

Approved for public release; distribution unlimited.

17. DISTRIBUTION STATEMENT (of the abstract entered in Block 20, if different from Report)

(18) ONR / (19) CR169-004-2

18. SUPPLEMENTARY NOTES

19. KEY WORDS (Continue on reverse side if necessary and identify by block number)

Contamination	Hydraulic Systems
Contaminant Wear	Wear Particles
Hydraulic Components	Ferrography
Hydraulic Pumps	TTCP

20. ABSTRACT (Continue on reverse side if necessary and identify by block number)

407 263 JM

DD FORM 1 JAN 73 1473 EDITION OF 1 NOV 65 IS OBSOLETE

Unclassified

SECURITY CLASSIFICATION OF THIS PAGE (When Data Entered)

Contaminant wear is one of the critical factors in component life and reliability. Therefore, the detection and analysis of this wear is extremely important. In this study, it was determined that ferrography is an effective tool for this detection and analysis.

A theoretical method was developed by which the behavior of both magnetic and non-magnetic particles in the fluid stream on the ferrogram can be predicted. This method indicates that very few magnetic particles will not be deposited on the ferrogram. This was verified experimentally.

Tests were conducted on gear pumps, a hydrostatic transmission, and complete hydraulic systems to verify the effectiveness of the ferrographic technique. These tests showed that changes in the wear rate of a system or component could be readily detected by the ferrograph.

The lack of standardization of ferrographic procedures is delaying the acceptance of the ferrograph as a critical decision making instrument. A very advanced draft procedure has been prepared and is ready for consideration by the appropriate committee of the Society of Automotive Engineers.

FOREWARD

This report was prepared by the staff of the Fluid Power Research Center at Oklahoma State University of Agriculture and Applied Science. The study was sponsored by the office of Naval Research at Arlington, Virginia, under Contract Number N00014-75-C-1157. The time period covered by this report is 1 July 1978 - 30 June 1979.

This study was effectively monitored by Lt. Commander Harold Martin, whose guidance and participation contributed significantly to the overall success of the effort. The program was conducted at the Fluid Power Research Center under the direction of Dr. R.K. Tessmann, with guidance and consultation from Dr. E.C. Fitch, Center Director.

TABLE OF CONTENTS

LIST OF FIGURES

LIST OF FIGURES

LIST OF TABLES

I. INTRODUCTION

The degrading effects of particulate contamination on the components in fluid power systems have been a topic of discussion in the fluid power world for years. Literally hundreds of papers have been published extolling the virtues of fluid cleanliness and dangers of fluid "uncleanliness". Conferences and symposia have repeatedly provided a forum for debating the value of the multitude of particle counting equipment, patch tests, sampling procedure, etc. The type and locations of, and even the need for, filters has sparked frequent heated debate. Throughout all of this, the authors, speakers, and combatants, for the most part, have considered particles only as particles and have paid considerably less attention to their sources than to their presence.

Certainly there were some who were interested in identifying the sources of contamination. Significant advances in this area were made through the use of both optical and scanning electron microscopy and spectrometric oil analysis programs (SOAP). These methods, however, were primarily concerned with identifying the materials present in a fluid sample. Under certain conditions, a knowledge of the materials in the sample could lead a knowledgeable investigator to the component which was the source of the particulate. This, in fact, is the basis of the very successful SOA Programs which are used to provide an early warning of an impending failure of the rotating components in jet engines.

While SOAP is concerned with the type of debris material, and subsequently its source, it cannot provide any insight into the mechanisms that generated the debris. The development of the Ferrographic technique finally provided researchers the tool they needed to examine the morphology of particles and conduct meaningful studies into the mechanisms by which the particles were produced. A natural evolution of the ferrographic concept will provide the system operator or maintainer with the capability to accurately predict impending component failures long before the situation becomes critical.

An obvious advantage is that potentially troublesome components can be replaced at some convenient time rather than causing costly unscheduled system downtime. While this is one of the major benefits of SOAP, a recent Technical Memo published by the U.S. Air Force on the results of an Air Force sponsored investigation into the laboratory testing of aircraft actuators implied that the ferrograph showed failure debris long before it was detectable by SOAP [1]. This is not a wholly unexpected result. Although there have been several attempts to apply the SOA Program to fluid power systems, the results have never been encouraging. This stems, at

least in part, from the inability of currently employed spectrum analyzers to cope with particles larger than 2 μm.

The Office of Naval Research recognized the potential advantages of the ferrograph very early in its development and has provided contract funding for research and the development of the ferrographic techniques by the Fluid Power Research Center (FPRC).

This report presents the results of the fourth year of activity on the program.

II. TECHNICAL BACKGROUND

The previous phases of this study have dealt with the practical applications of ferrography to fluid power systems.

The first two phases were investigations of the life improvements of hydraulic components brought about by the removal of particulate contamination entrained in the fluid of hydraulic systems. In this investigation, two basic test mechanisms simulating mechanisms commonly found in hydraulic systems - a rotary device and a linear reciprocating device - were constructed. These mechanisms were operated using hydraulic fluid which was contaminated with known quantities of AC Fine Test Dust. The resulting debris was analyzed ferrographically.

Several important results which were obtained from these tests are listed here:

1. The wear debris generated from rotary mechanisms is detectably different from that generated by linear reciprocating mechanisms.

2. In rotary mechanisms, the particle size distribution is very critical at high concentrations of contaminants.

3. In linear mechanisms, the greatest wear results from some critical size distribution which is related to clearances within the device rather than the concentration level.

4. Significant - and predictable - reductions in wear and the resultant increases in component life can be achieved by reducing both the level and the size distribution of the particles in the system.

5. Changes in wear rates brought about by variations in the concentration or distribution of contaminants in the fluid are readily detectable ferrographically.

Subsequent work extended these basic mechanism wear tests to hydraulic gear pumps. These tests showed that the results discussed above could be extrapolated to include the gear pump and quite possibly other similar hydraulic components.

During the gear pump testing, it was found that the wear debris generation from very low contaminant concentrations were detectable through the ferrographic density values. This has two important implications. The first is that component contaminant sensitivity testing could be conducted on a non-destructive basis. The second is that a routine fluid sampling program should allow

the early detection of wear debris in operating systems and facilitate preventive maintenance actions to preclude system failure.

Throughout these phases, the processes and procedures involved in ferrographic analysis were constantly being evaluated and revised to produce a repeatable and viable wear debris analysis method.

III. SCOPE OF EFFORT

This report covers the fourth phase of work under contract number N00014-75-C-1157. This phase had as specific tasks the standardization of the ferrographic procedure and the completion of a comprehensive field test program to investigate the wear debris generated within hydraulic systems in field service.

In an effort to promote an internationally accepted ferrographic oil analysis procedure, the FPRC has established an active liaison with the TTCP (Sub-Group P, Technical Panel 1, Active Group 4). Significant progress has been made. A highly advanced draft procedure is now available for presentation to the appropriate SAE sub-committee for advancement to the national standard stage.

When this project was proposed, it was the intention of all involved to select an appropriate hydraulic system of interest in Naval application to use for the field test program. Unfortunately, this could not be accomplished. However, the FPRC was able to conduct some brief field tests on some non-Naval equipment. The results of those tests are presented herein.

IV. THEORETICAL ASSESSMENT OF THE FERROGRAPHIC PROCESS

Since the introduction of the ferrograph in 1974, numerous questions have arisen concerning the particle dynamics and the behavior of nonmagnetic particles in the fluid stream. During the past year, the FPRC has expended considerable effort in producing theoretical analyses to answer these questions. The results of these analyses are presented in Appendices A, B, and C. By using the mathemetical models developed in these papers, the behavior of any given particle can be predicted.

One of the most significant points brought out by these papers is that the probability of a magnetic particle's not being deposited on the slide is extremely low. This has been verified experimentally at the FPRC by collecting the fluid used to make a ferrogram and using it to make a second ferrogram. This has been accomplished numerous times, and no appreciable number of magnetic particles has ever been found in the second ferrogram.

Appendix C discusses the behavior of non-magnetic particles and their effect on densitometer readings. It concludes that these particles can cause erroneous readings, especially when real-time monitoring is used.

V. CONTAMINANT WEAR

One of the primary objectives of this contract phase was to concentrate on the study of wear in complete hydraulic systems. This was to have been done by selecting candidate hydraulic systems (with guidance from the Navy sponsors) which would be operated under various conditions. Fluid samples would be extracted on a predetermined schedule and analyzed on both a particle size distribution and a ferrographic basis. Unfortunately, arrangements could not be made for the program as originally planned. However, to demonstrate the applicability of the ferrographic process to hydraulic systems, the FPRC conducted test programs on several non-Naval systems. The results of these programs are presented here. Work on the assessment of contaminant wear in gear pumps was completed during this phase. The results from that work are also included in this section.

Gear Pumps

The pump is considered by fluid-power engineers to be the heart of the hydraulic system. Therefore, forces and influences that tend to degrade the performance of hydraulic pumps are of great concern. A common occurrence that has a deleterious effect upon a pump is the presence of particulate contamination entrained in the fluid of the system. In the case of a pump, these particles are forced into the critical leakage paths between mating surfaces, which many times are in relative motion. Once these particles have entered this area, wear will probably occur. Two events occur as a result of this wear. First, the enlargement of the critical leakage paths will cause a decrease in the output flow of the pump. Second, the wear process will remove material from one or both of the surfaces. This material will become wear debris entrained in the circulating fluid.

Previous efforts to study the influence of various particle size distributions and contaminant concentrations have relied upon flow degradation measurement alone. There were several reasons for this dependency upon flow degradation data. A primary reason is that flow is the only performance parameter of importance associated with fixed-displacement pumps. Therefore, the use of flow degradation is directly related to performance degradation, which is the sole criterion in field applications. A second reason stems from the problems in attaining any other wear-related measurement—direct measurements of dimensional changes are impossible. In addition, there was no proven method of measuring the wear debris generation, and the weighing of entire pump parts was shown to be fruitless.

The use of flow degradation data to evaluate the contaminant wear of a pump presented several problems. The most important drawback was associated with contamination levels at which the test pump was exposed to several particle size ranges. To obtain a measureable flow degradation at the smaller particle size ranges, a fairly high concentration was used. However, the use of such a high contaminant level many times results in considerable pump wear at the larger particle size ranges. Therefore, to obtain the needed data at small size ranges but not destroy the pump, a more sensitive wear parameter was needed. One paramount requirement of such a new parameter was that it must correlate with flow degradation data at the higher contamination levels. This would permit the use of standard interpretation techniques such as the algorithm developed to calculate a contaminant tolerance profile [2] and the nomograph to determine an Omega rating for the pump [3].

With the introduction of the Ferrographic Oil Analysis System [4, 5, 6], evaluation of a wear process through an analysis of the generated debris became a practical consideration. In fact, the measurement of wear debris through Ferrographic techniques is much more responsive to the severity of the wear process than flow degradation and therefore may represent the key to pump contaminant sensitivity testing at a reduced contamination level. Ferrographic analysis can be used effectively for contaminant wear studies of most fluid components. This is particularly important when a single critical performance parameter is difficult to identify. For example, in the case of hydraulic valves, several parameters could be selected, where each is extremely critical in some given application. However, using them all to assess contaminant wear would be difficult, if not impossible.

This section presents the results of a study on the contaminant wear of pumps. The pumps were tested at various particle size ranges and contaminant concentrations. In addition to the flow data normally recorded during such testing, samples were extracted for Ferrographic analysis. The objective of the program was to assess the capability of the Ferrographic technique not only to produce useful data at contamination levels much lower than the 300 mg/litre used in the Standard Contaminant Sensitivity Test [7] but to correlate at various concentrations so that standard intrepretations methods could be employed. The results obtained should significantly advance the understanding of pump contaminant wear and will open the door to desirable improvements in contaminant sensitivity testing.

Experimental Methods

To keep the initial investigations of Ferrographic analysis of contaminant wear in hydraulic pumps to a manageable level, a

typical gear-type, fixed-displacement pump was selected. To explore the debris generation characteristics of these pumps, tests were conducted over a broad range of contaminant concentrations and sizes. The contaminant concentrations selected were 25, 150, and 300 mg/ℓ. Particle size ranges of 0-5, 0-10, 0-20, 0-30, 0-40, 0-50, 0-60, 0-70, and 0-80 micrometres obtained by classification using air elutriation from AC Fine Test Dust [8] were used in these pump tests.

Basically, the Standard Pump Contaminant Sensitivity Test [7] was used for testing with the exception of the contaminant concentrations that were employed. All test pumps were subjected to a break-in period based on rated conditions of 2500 rpm and 172 bars. In the wear tests, the pumps were operated at 2000 rpm and 138 bars. The test temperature was held constant at 65.5°C. The initial flow of the pump was accurately measured and then the pump was exposed to the desired concentration of contaminant (25, 150, or 300 mg/litre) that had been classified to a particle size range of 0-5 micrometres. The pump was operated at this entrained contamination level until the flow remained constant for 10 min or until a total of 30 min had elapsed. At this time, a fluid sample was extracted from the system for Ferrographic analysis, and the control or background filters were valved into the main system. The filtering system was used for 10 min after which the filtering subsystem was removed and the next particle size range was injected. The procedure was repeated sequentially for 0-10, 0-20, 0-30, 0-40, 0-50, 0-60, 0-70, and 0-80 micrometre particle size ranges or until the flow of the pump had decreased a total of 30% or more.

The samples extracted from the test system were analyzed Ferrographically. During preliminary Ferrographic analysis studies [9, 10] of samples from pump contaminant sensitivity tests, the optical density at the 54-mm location was found to be the most responsive to the wearing process accelerated by the entrained contamination. Therefore, Ferrograms were made from each sample, and the optical density was measured at the 54-mm position. This value was then normalized to reflect the concentration of wear debris in 1 mℓ of sample fluid. When a sample is only slightly concentrated with debris, several millilitres of the fluid may be utilized in preparing the Ferrogram. On the other hand, for heavily laden samples, only a fraction of a millilitre is required. Therefore, the normalization to a unit volume of sample fluid is necessary for comparison purposes.

Flow Degradation Test Results

Because output flow after each contaminant exposure was accurately measured during the testing program, the results could be modeled both as a function of particle size range and concentration. The flow readings were made using a turbine-type meter carefully

calibrated.

TABLE I. SUMMARY OF FLOW DEGRADATION DATA.

CONT. LEVEL	FLOW DEGRADATION AFTER INDICATED EXPOSURE, ΔQ (ℓpm)								
(mg/ℓ)	0-5	0-10	0-20	0-30	0-40	0-50	0-60	0-70	0-80
25	--	--	--	--	0.76	1.02	1.59	2.04	2.76
150	--	--	0.83	2.61	5.34	7.34	10.94	13.40	16.12
300	--	--	1.93	5.90	10.86	13.82	19.68	--	--

The flow degradation data obtained in the various tests are summarized in Table 1. The numbers within the table are total flow change after the particular exposure. For example, after exposure at 150 mg/ℓ of 0-40 particle size range, the flow rate from the pump was 5.34 ℓpm less than it was before any contaminant had been injected into the system. The numbers represent total flow loss and not the loss for the particular exposure under consideration.

TABLE II. SUMMARY OF EQUATIONS FOR FLOW DEGRADATION.

Cont. Level (mg/ℓ)	Equation
25	$\Delta Q = 6.81 \times 10^{-4} D^{1.88}$
150	$\Delta Q = 4.54 \times 10^{-3} D^{1.88}$
300	$\Delta Q = 9.46 \times 10^{-3} D^{1.88}$

The flow degradation data shown in Table 1 can be reduced to a functional relationship by a least-squares data-fit program, producing the flow degradation equation, Table 2. The general relationship that describes flow degradation as a function of the particle size range is the classical power function. The variable represented by D in the equations shown in Table 2 is the particle size range where D is the upper limit of the range. For example, for a particle size range of 0-20 micrometres, D would be 20.

Note that the coefficient of the power function is obviously some function of the concentration. The general power function used for the equations of Table 2 can be written:

$$\Delta Q = bD^{x} \tag{1}$$

where: ΔQ = total flow degradation, b = coefficient (some function of concentration), X = exponent = 1.88, D = upper limit of the particle size range. A plot can be made to evaluate the coefficient, Fig. 1. This figure illutstrates that the coefficient of the flow degradation equation is an excellent linear function of the concentration. the best-fit equation (least squares) for the function can be written:

$$b = 3.2 \times 10^{-5} C \tag{2}$$

where: C = contaminant concentration (mg/litre).

Thus, the complete equation describing the flow degradation data requires that Eq. (1) and Eq. (2) be combined:

$$\Delta Q = 3.2 \times 10^{-5} C\, D^{1.88} \tag{3}$$

Fig. 2 is a graphical illustration of Eq. (3) as well as all of the data shown in Table 1. The flow degradation model as represented by Eq. (3) is an excellent fit to the measured data. However, to develop a function that relates Ferrographic density to flow degradation, an equation similar to Eq. (3) must be developed for the Ferrographic data.

Ferrograhic Density Test Results

In conducting a contaminant sensitivity test, the pump is subjected to the various particle size ranges of contaminant on a

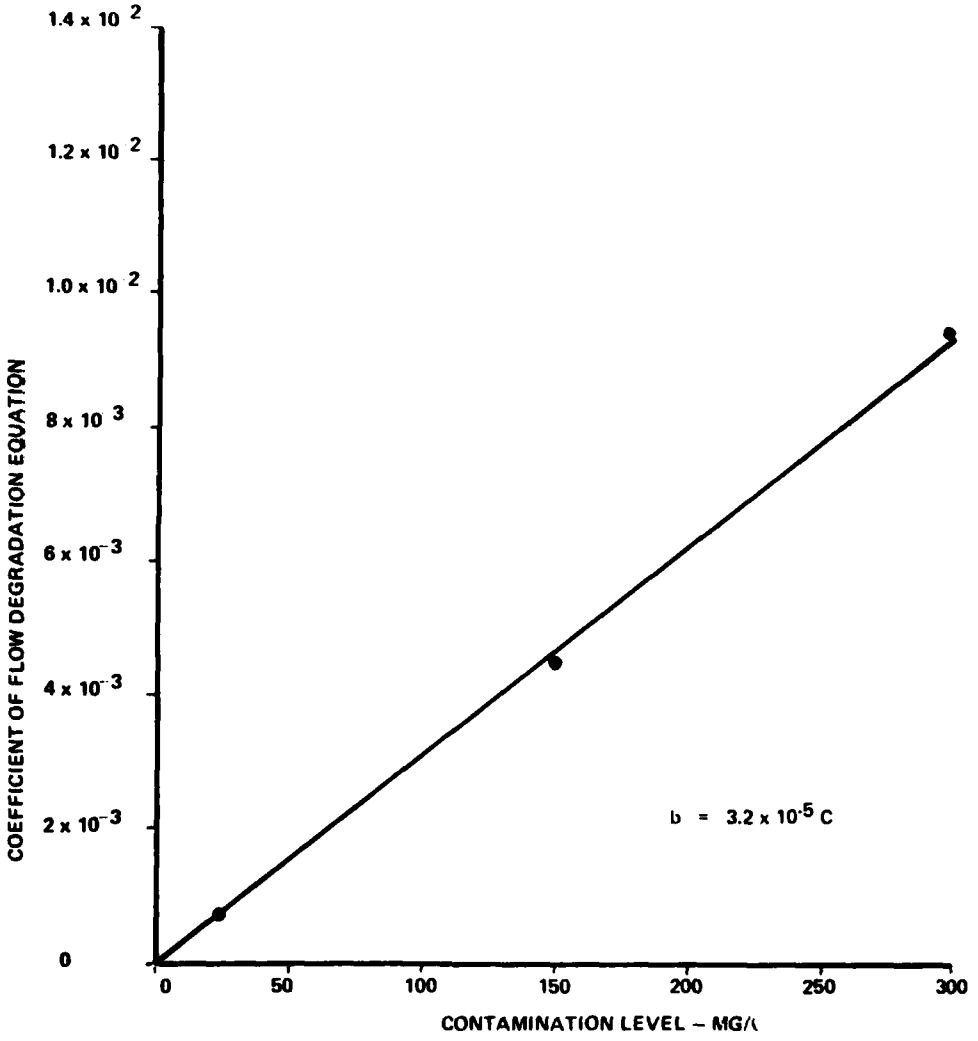

Fig. 1. Coefficient of Flow Degradation Function vs. Contamination Level.

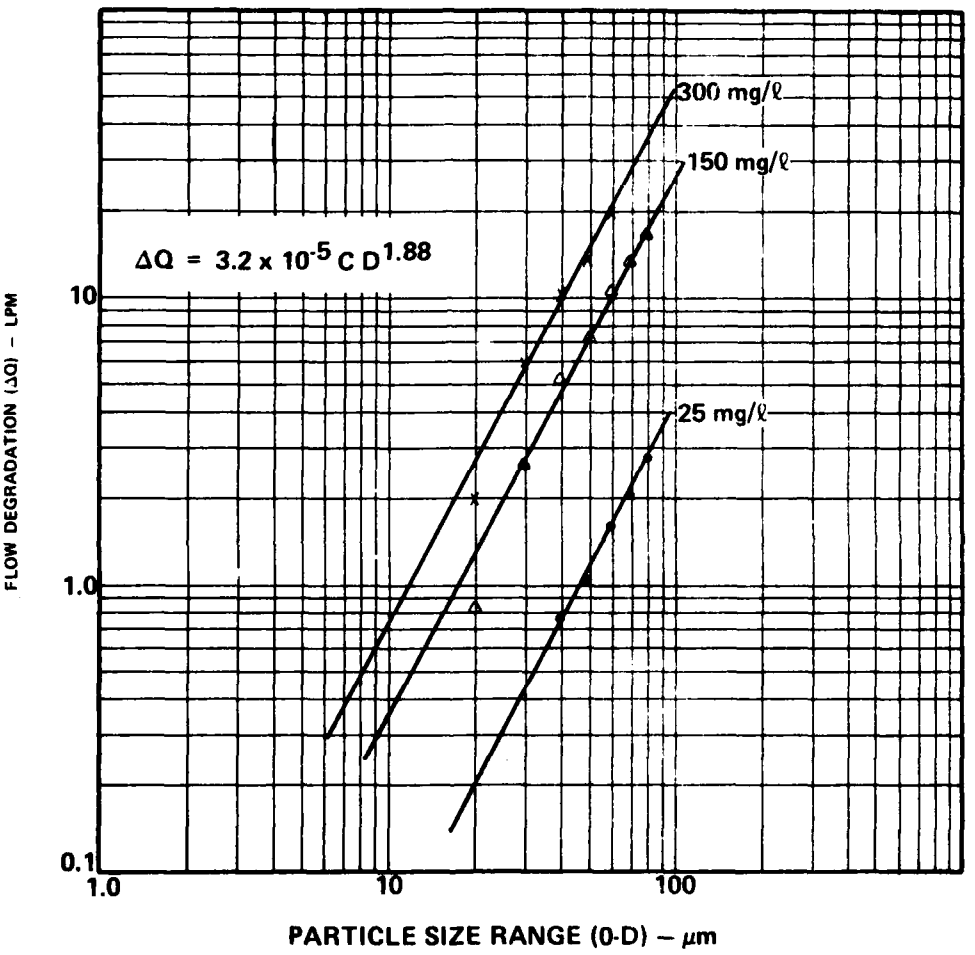

Fig. 2. Flow Degradation vs. Particle Size Range for Various Concentrations.

sequential basis. Therefore, the total wear of the pump is the summation of the wear caused by each and every particle size range that has been injected. After each exposure, the pump wear as expressed by flow degradation is the result of not only the most recent exposure but every preceding injection. For example, the change in clearances of the pump after it has been exposed to, say, 0-20-micrometre particle size range is the sum of the increases due to 0-5, 0-10, and 0-20. Because the flow degradation will be a function of the total clearance change, the Ferrographic data must be related in a similar manner to obtain a meaningful correlation.

If the amount of wear debris generated during the test is proportional to the increase in pump clearance, the Ferrographic density must be summed over particle size range to be on the same basis as the flow degradation. Furthermore, to obtain the most accurate Ferrographic density data, various fluid volumes were utilized, depending upon the debris concentration in the sample [10]. Therefore, the Ferrographic density values must be divided by the volume used to be comparable. In this case, all Ferrographic data have been normalized to 1 mℓ of sample fluid.

TABLE III. SUMMARY OF FERROGRAPHIC DENSITY DATA.

Cont. Level	Ferrographic Density After Indicated Exposure, $\sum$ D54/mℓ								
(mg/ℓ)	0-5	0-10	0-20	0-30	0-40	0-50	0-60	0-70	0-80
25	1.75	4.28	8.21	11.46	16.18	19.58	24.35	28.20	34.40
150	8.40	19.00	47.67	77.17	118.34	141.17	174.47	201.30	236.63
300	19.20	42.75	87.00	152.40	218.40	304.65	378.82	----	----

The Ferrographic data obtained from these pump tests are presented in Table 3, where the D54 density values have been accumulated over particle size range and normalized to 1mℓ, as indicated by Σ D54/mℓ. The data shown in Table 3 can be reduced to a functional form in a manner similar to that used for flow

TABLE IV. SUMMARY OF EQUATIONS FOR FERROGRAPHIC DATA.

Cont. Level (mg/ℓ)	Equation
25	$\sum D54/ML = 0.25D^{1.13}$
150	$\sum D54/ML = 1.57D^{1.13}$
300	$\sum D54/ML = 3.29D^{1.13}$

degradation data. Preliminary efforts [11, 12] have indicated the Ferrographic density is also best described by a power function. The best-fit (least squares) equations for the Ferrographic data are shown in Table 4. Here again, it is easy to see that the coefficient of the power function that describes the Ferrographic data is some function of the contaminant concentration.

Fig. 3 shows a plot of the coefficient from the power function describing the Ferrographic data vs the contaminant concentration used. This coefficient is as good a linear function of concentration as one would hope to find. The equation produced by a least-squares curve fit to the data graphically illustrated in Fig. 3 can be written:

$$a = .011C \tag{4}$$

where: a = coefficient of the Ferrographic power function.

Substituting Eq. (4) into the equations given in Table 4 produces a single relationship for the Ferrographic data:

$$\Sigma D54/ml = 0.011CD^{1.13} \tag{5}$$

Fig. 4 is a graphical representation of Eq. (5) as well as all of the data given in Table 3. As was the case with the flow degradation model, the Ferrographic model given by Eq. (5) is an excellent fit to the recorded data. Now that a model for both flow degradation and Ferrographic density has been derived as a function of both contaminant concentration and particle size range, a relationship for flow degradation as a function of Ferrographic density can be derived.

CORRELATION ΔQ vs $\Sigma D54/m\ell$

Both Eq. (3) and Eq. (5) can be solved for particle size range D:

$$D = \left[\frac{\Delta Q}{3.2 \times 10^{-5} C}\right]^{1/1.88} \tag{6}$$

$$D = \left[\frac{\Sigma D54/ml}{0.011C}\right]^{1/1.13} \tag{7}$$

Then, these two equations, Eq. (6) and (7), can be equal:

$$\left[\frac{\Delta Q}{3.2 \times 10^{-5} C}\right]^{1/1.88} = \left[\frac{\Sigma D54/ml}{0.011C}\right]^{1/1.13} \tag{8}$$

Reducing Eq. (8) produces the following relationship:

$$\Delta Q = 0.061 C^{-0.66} (\Sigma D54/ml)^{1.66} \tag{9}$$

Eq. (9) is the correlation that will provide the breakthrough necessary to conduct pump contaminant sensitivity tests at any contaminant level but still refer the data back to a 300 mg/ℓ base. Fig. 5 graphically illustrated the functional relationship as given by Eq. (9). In addition, the corresponding data from Tables 1 and 3 are shown to indicate the exactness of the model fit.

There has always been criticism of the pump contaminant sensitivity test because of the relatively high concentration required. Now, for the first time, a way has been found to reduce the contamination level of the test without losing any of its sensitivity.

Probably the greatest advantage that can be attained by low concentration contaminant sensitivity testing of components, lies in the greatly reduced destruction. In examining Table 1, note that the test had to be stopped after 0-60 exposure when 300 mg/ℓ was used: and, at that point, the leakage had increased by 19.68 ℓpm. However, when using 150 mg/ℓ, the total leakage increase was only about 16 ℓpm after 0-80. Furthermore, when

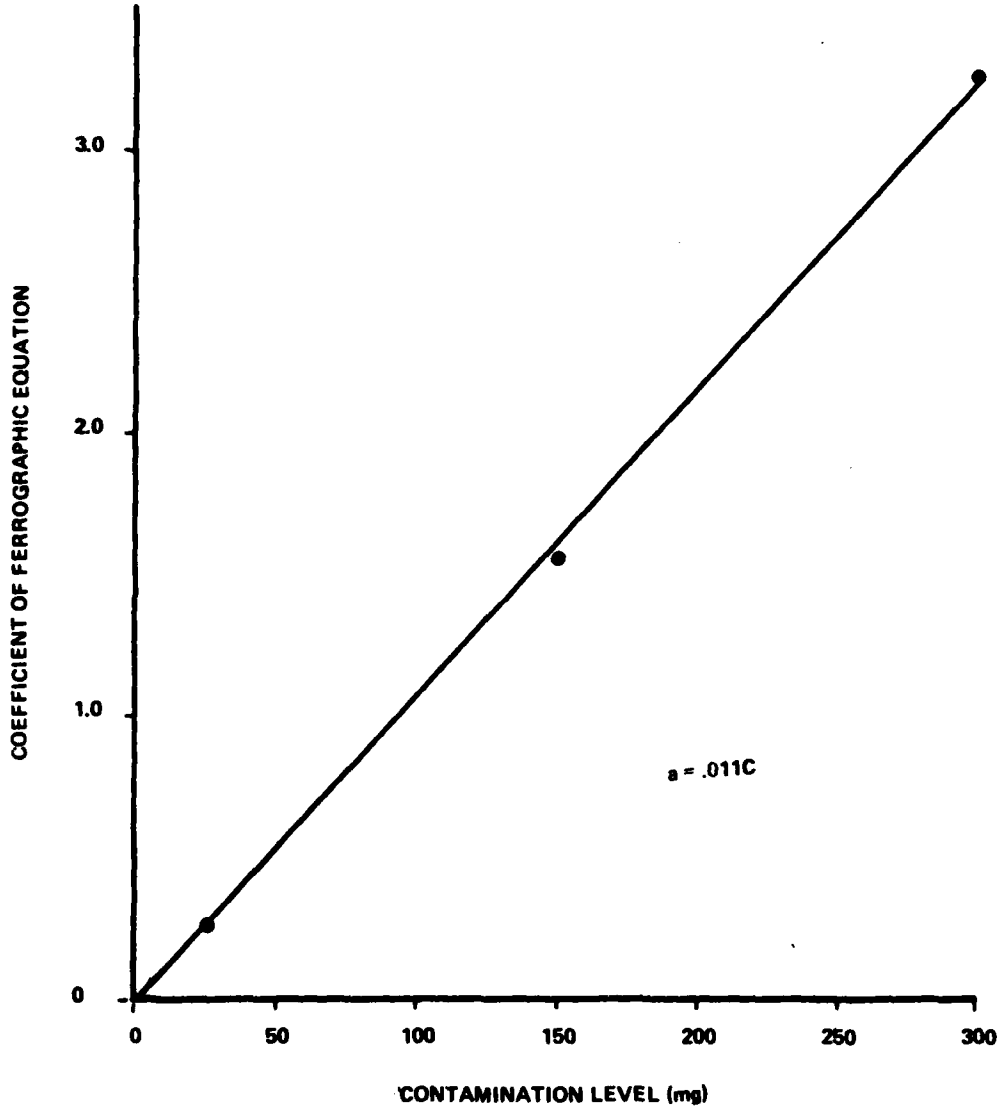

Fig. 3. Coefficient of Ferrographic Function vs. Contamination Level.

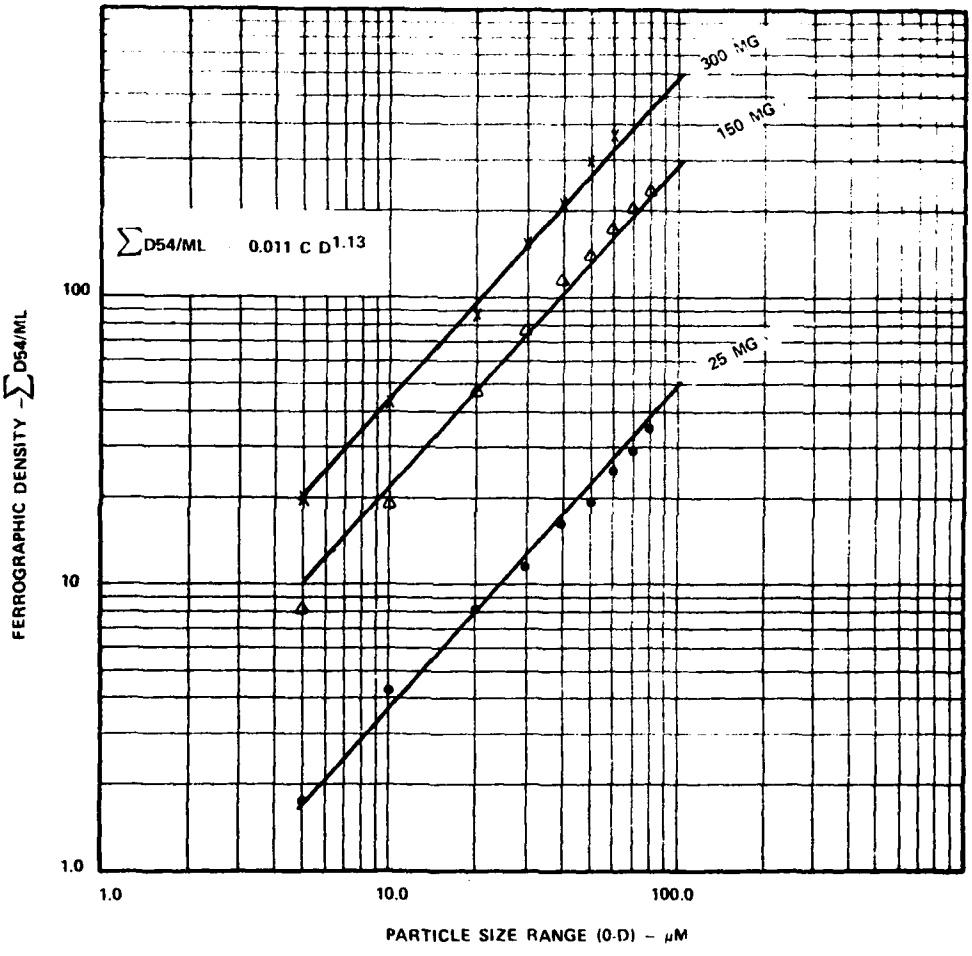

Fig. 4. Ferrographic Density vs. Particle Size Range for Various Concentrations

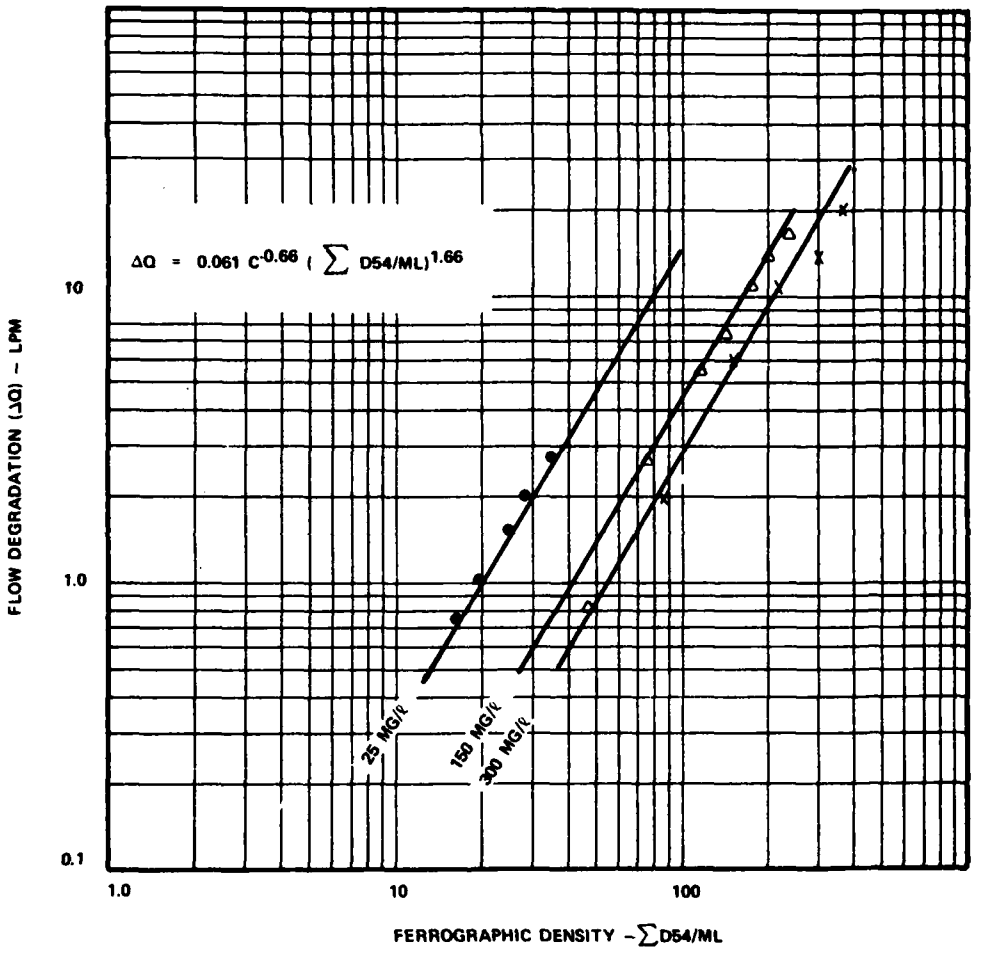

Fig. 5. Flow Degradation vs. Ferrographic Density Data at Various Contaminant Concentrations.

25 mg/ℓ concentration was utilized, only about 3 ℓpm increase had been observed after the 0-80 exposure. Almost seven tests through 0-80 cound be conducted on one pump at 25 mg/ℓ to reach the same total flow degradation at 0-60 in one test at 300 mg/ℓ. Thus, several tests could be conducted using one pump at the reduced concentration.

Hydrostatic Transmission

The objective of this project was to evaluate a hydrostatic transmission. In certain applications, the wear rate in this system was apparently sufficient to cause premature failure. Examination of the internal surfaces of a failed transmission revealed disastrous wear at the cylinder block/backplate interface and the piston shoe/swashplate area. Therefore, a plan of attack was devised in which wear information and duty cycle data were collected while the vehicle was operating in three different environments.

It was felt that the three test conditions would provide data which could be used to assess the severity of the terrain, the contamination levels of the transmission system, and the concentration of wear debris generated within the pump/motor system. Two of these tests were conducted with the vehicle operating in an actual field application. The difference between the two test runs was that one was considered "level" terrain operation, while the other was deemed to be "rough" terrain. The third test was conducted on a test track.

Each of the three tests had a duration of ten hours. Fluid samples were extracted every hour during each of the tests. These samples were analyzed to obtain the contamination level through the use of an automatic liquid particle counter calibrated per ISO approved procedures. In addition, the samples were evaluated Ferrographically to obtain wear data.

The operation of the unit during the track test is shown in Fig. 6. According to this driving procedure, the vehicle makes two 540^{o} turns - one to the left and one to the right. In addition, four 180^{o} turns are executed - two left and two right. Finally, there are eight 90^{o} turns - four left and four right. The terrain is level, and the surface is hard-packed gravel.

Ferrographic Results

The results of the Ferrographic analyses performed on samples extracted from the case drain of the pump which supplies oil to the right-wheel motor are given in Fig. 7, while that for the left-wheel drive pump is shown in Fig. 8. The numerical data are tabulated in

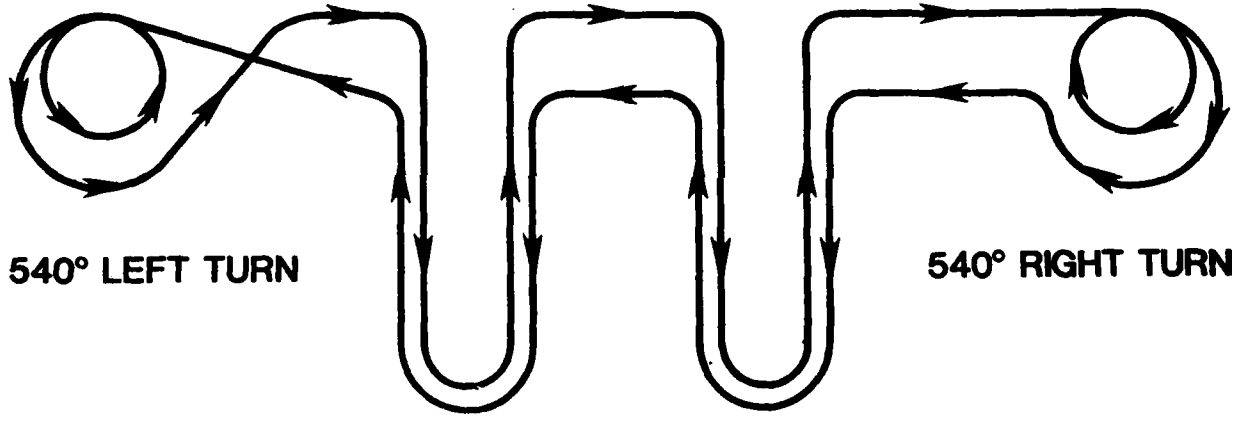

Fig. 6 Schematic of Test Track Operation.

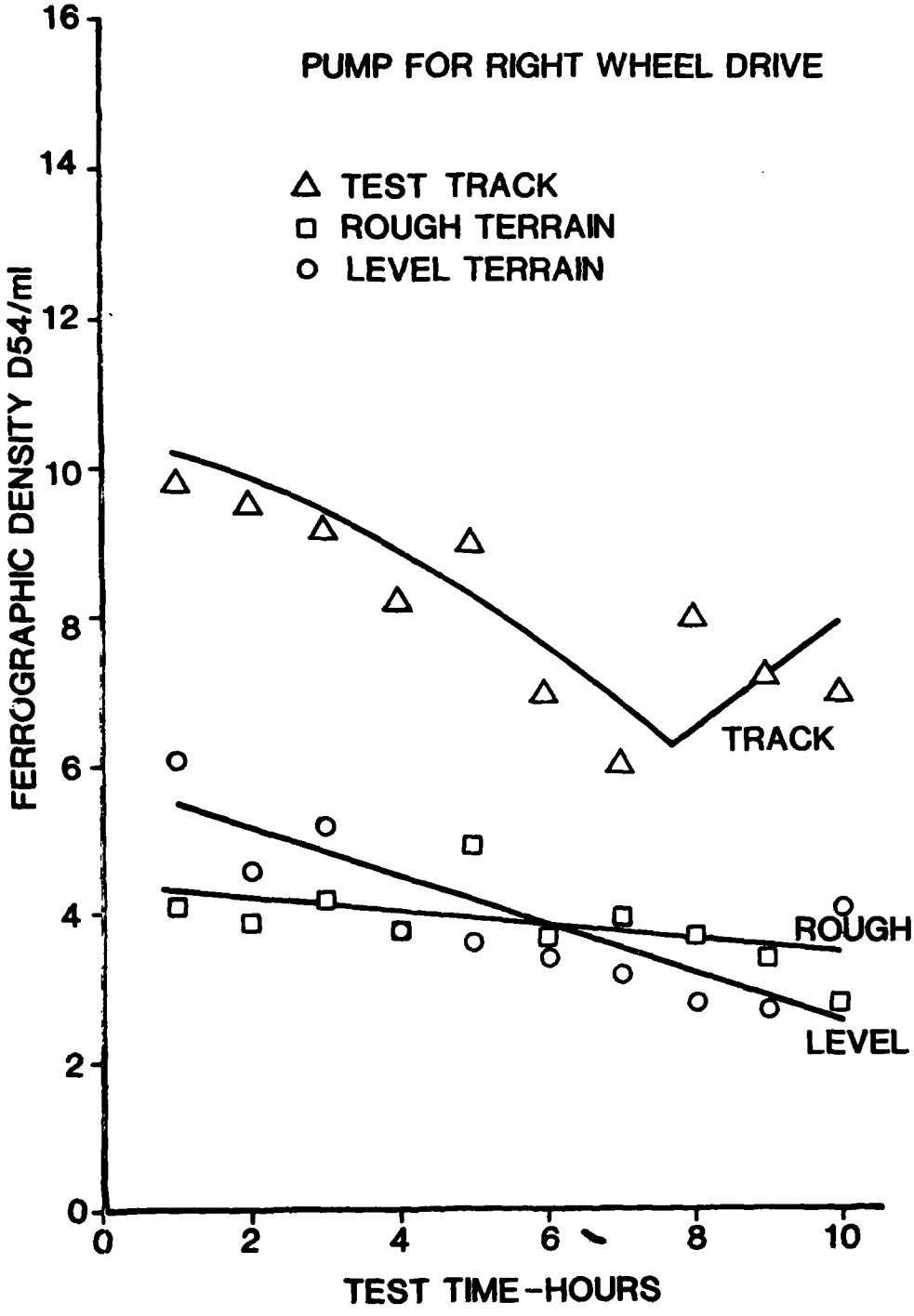

Fig. 7 Results of Ferrographic Analysis for Right Wheel Drive Pump.

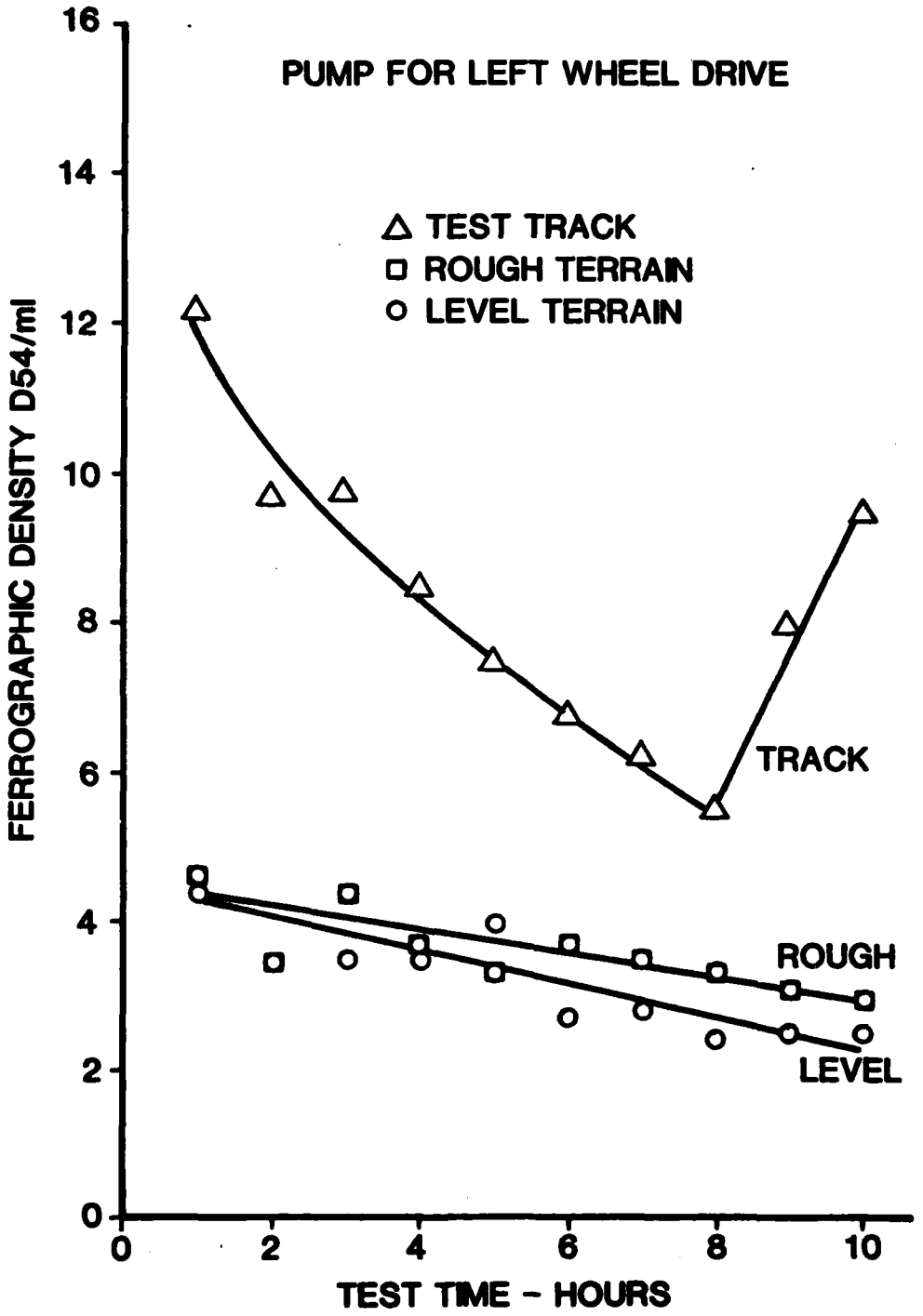

Fig. 8 Results of Ferrographic Analysis for Left Wheel Drive Pump.

Appendix D. Both of the figures illustrate the graphical relationship between the Ferrographic density at the 54 mm position on the Ferrogram and the test time when the samples were taken.

In general, it must be concluded that the wear in the transmission while operating in rough-terrain is only slightly higher than observed during level terrain operation. On the other hand, the amount of wear debris entrained in the case-drain oil was significantly higher during the track test than either rough or level operation. The density at 54 mm was chosen for this interpretation because other tests have shown that this value correlates well with the actual wear process. It is felt that the rapid increase in density reading during the track test after about eight hours is indicative of an imminent failure, probably in the left-wheel drive system.

The system was such that the leakage oil from the left pump actually flows into the right pump case and is relieved from there. This means that the wear debris from either system will be entrained in the case drain oil taken from the right-wheel drive pump. Therefore, the wear debris observed from the right pump should be higher than that from the left pump. In reviewing the data shown in the figures, it can be seen that the debris measurements from case drain oil of the right pump are not significantly different from those of the left pump. This could mean that most of the wear debris is generated from the left drive system or that the fluid communication obscures the differences between the two systems.

The results of the tests presented in this report reveal very little difference between what was termed level - and rough-terrain operation. The duty cycles are not significantly different, nor is the wear rate significantly higher in one than the other. The Ferrographic density values were slightly higher in the rough-terrain operation, but the difference was not of a sufficient magnitude to be impressive.

The closed-loop pressures during the test track operation were considerably different than those for field operation. The maximum pressure observed was very high indicating the severity of the turns. However, the system pressure level was below 500 psi for a large percentage of time, indicating the level, hard-packed characteristic of the track. The case drain temperature during the track test showed that some very high temperatures were encountered. Depending upon the characteristics of the hydraulic oil, these high temperatures could account for the increase in wear rate observed during track testing.

The particle count data revealed excellent control of the contamination level. The system filter was able to clean up the

system rapidly following the oil change and the system failure. The magnitude of the particle counts after the component failure was quite high. It would probably be good practice to initiate a system cleanup following any failure and subsequent to actually placing the system in service.

Overall, it is felt that the data acquired during these tests are excellent. They reveal the duty cycle which can be expected when operating the transmission in field service and provide a comparison of that duty and the test track operation. In general, the wear rates are useful from a comparative standpoint. That is, little data are available on actual wear debris concentrations from hydrostatic transmissions. However, the values of density measured can be compared between types of operation and on a trend basis to indicate potential failures. For example, the rapid increase in debris concentration after eight hours of track operation definitely indicates a disastrous change in the wear rates. This can be observed from trend analysis.

Other Selected Systems

Evaluations were conducted on five different selected systems, which included two complete vehicle systems, one steering system, one auxillary hydraulic functions system, and one transmission lubrication system. Each will be discussed individually, with the findings and conclusions from all five studies resummarized at the end.

System One - Complete Vehicle Hydraulic System

System One involved analysis of a complete agricultural tractor hydraulic system. Such functions as power assisted steering, transmission cooling and lubrication, and hydraulic lift assist are included, as well as numerous other auxillary hydraulic subsystems inherent to the particular vehicle design. Oil samples were taken just upstream of the main filter to allow collection of wear debris generated throughout the system. The sampling period for this vehicle encompassed approximately the first 1000 operating hours after assembly completion. Thus, close data inspection should also indicate field break-in characteristics of the vehicle.

Figure 9 indicates the Ferrographic D54 density values. Most obvious in Fig. 9 is the extremely high initial density reading. Initial vehicle shake down was conducted prior to this reading, and would account for the high results. Many normal rubbing wear particles (1-10 μm in size) and severe wear particles (approximately 20 μm) were present in this Ferrogram. However, with a filter replacement made prior to the second sample, the magnitude of the

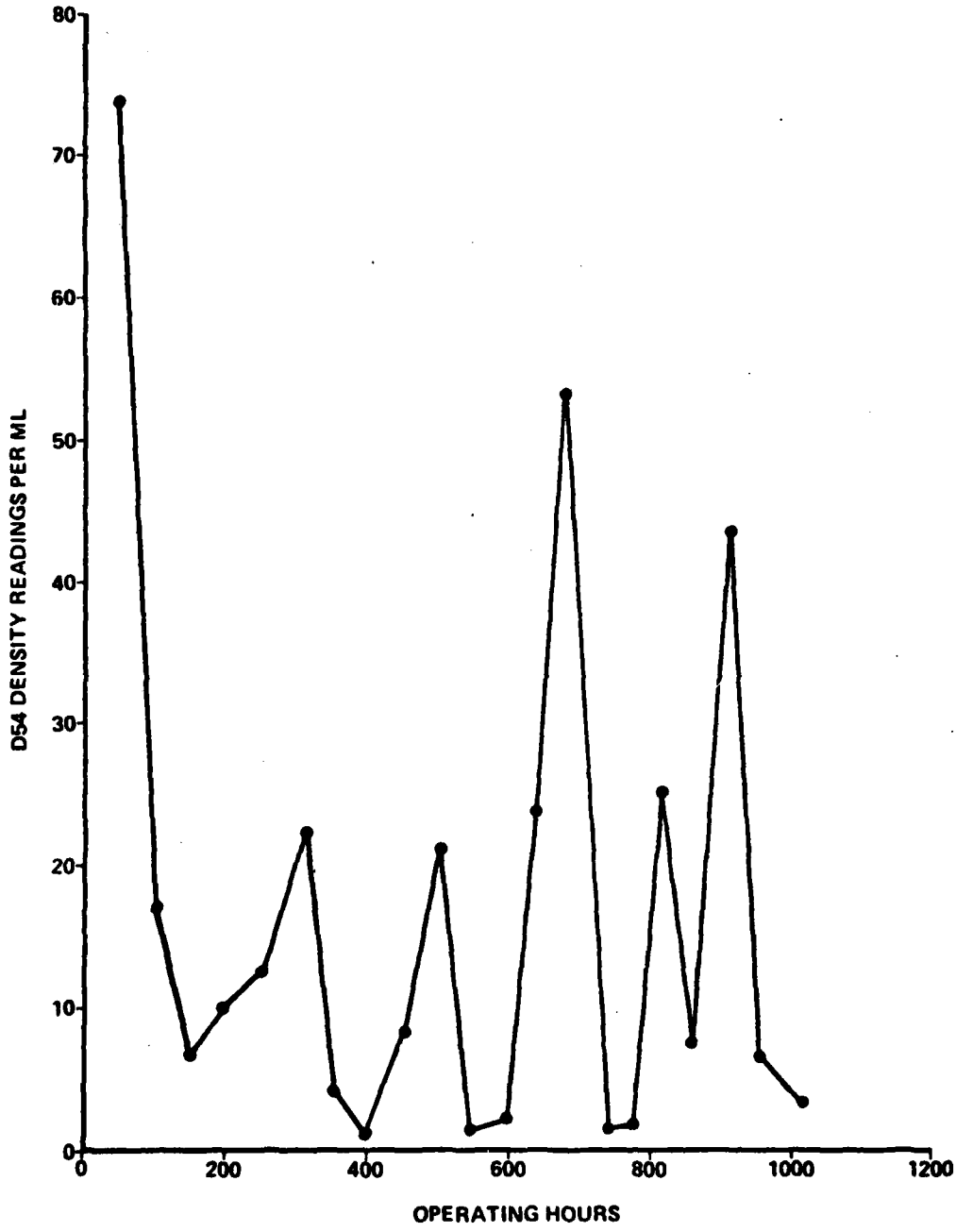

FIG. 9 D54 DENSITY VS. OPERATING TIME FOR SYSTEM #1 - COMPLETE VEHICLE HYDRAULIC SYSTEM

density value recorded dropped substantially.

The second pronounced peak in density readings occurs at approximately 700 hours. This sample was recorded during a substantial increase in vehicle loading, with approximately 50% of the operating hours between 600 and 700 hours occurring at 100% load and the remaining 50% at 70 to 80% vehicle load. Again, heavy amounts of severe wear particles are present in the Ferrogram. However, numerous metallic spheres were also recorded throughout with the majority near the exit end (indicating very small and/or high alloy material). The combination of severe wear and spherical particles is indicative of fatigue cracks located in rolling bearings, and in this case, most likely made of a high alloy material.

Investigation into the type of debris present throughout the evaluation period indicates several system changes. Evidence of oxidation through the presence of black and orange colored particles, and surface heating were evident generally after 500 hours. At approximately 800 hours,fibrous particles began appearing on the Ferrograms. The presence of corrosion or oil breakdown due to heat is again evident at 950 hours, with increasing severity noted at the final sampling (approx. 1020 hours).

In an overall assessment of the hydraulic system state, the Ferrographic analysis indicates the degradation of some component part consisting of a fibrous material in contact with ferrous particles, possibly brake or clutch disk facings. Secondly, the presence of an increasing number of tempered, oxidized, and corroded particles in the last three samples could possibly be identifying a breakdown of the hydraulic oil, and more specifically the additive package for that particular oil specification. Finally, the application of heavy system loading (80-100%) generates large amounts of spherical severe wear particles identifying the presence of fatigue cracks in rolling bearing surfaces. Recommendations for system maintenance would include replacement of system fluid and filter, and inspection of clutch or brake disk facings.

System Two - Complete Vehicle Hydraulic System

Vehicle System Two again involves the evaluation of an agricultural tractor hydraulic system. As in System One, all onboard hydraulic functions as well as any remote connect systems were analyzed by samples taken just upstream of the main filter. The time period for sampling encompassed 500 hours, with the first sample taken approximately 50 hours after initial vehicle shakedown.

Fig. 10 is the Ferrographic D54 density reading for each sample. Much in evidence is the extremely high density readings

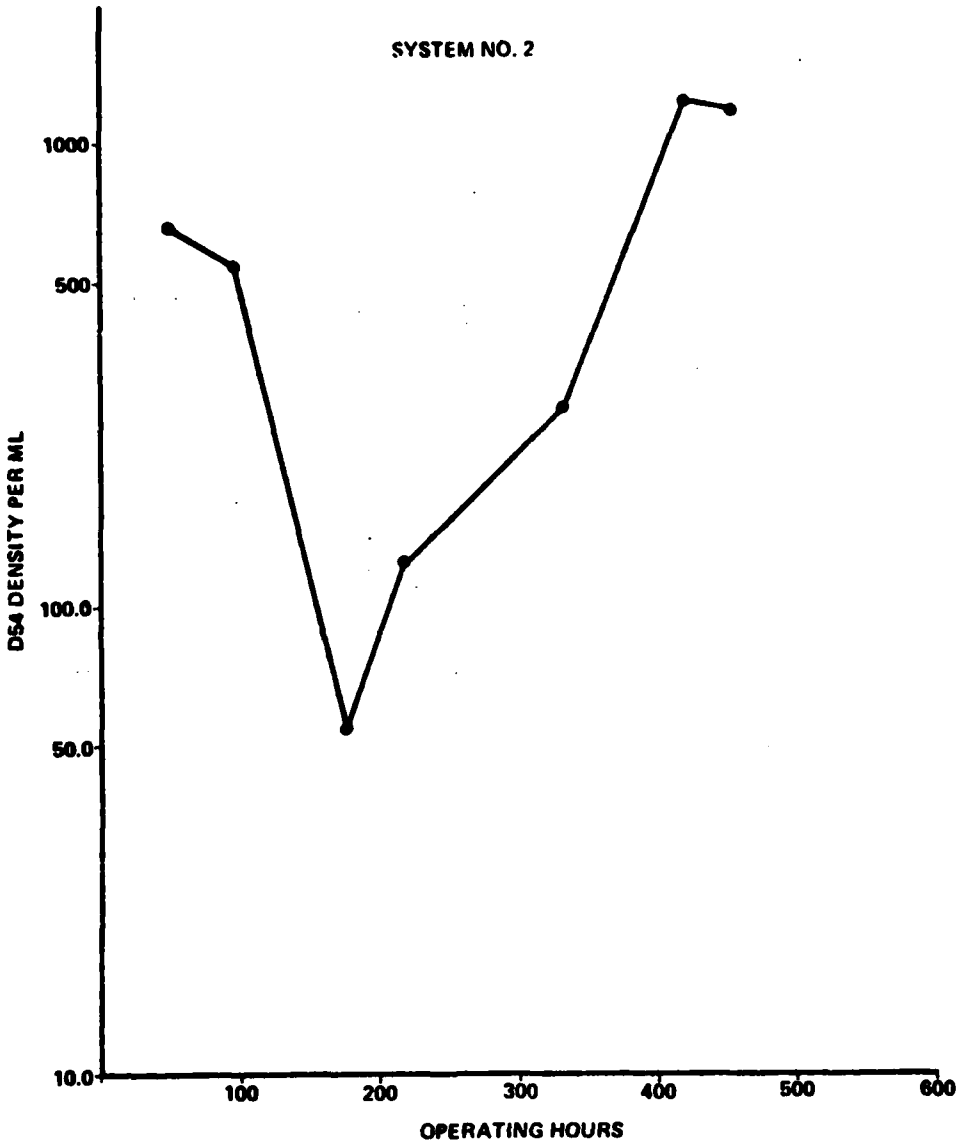

FIG. 10 D54 DENSITY VS. OPERATING TIME FOR SYSTEM #2
COMPLETE VEHICLE HYDRAULIC SYSTEM

obtained for this vehicle.

As in System One, high initial D54 density readings were measured during the first 100 hours of operation. Again this would seem to show the effects of vehicle break-in during initial operation at typical field contaminant ingression levels. Fig. 11 indicates the per cent of total operating time at 60, 70, and 90 per cent vehicle load. These curves indicate that approximately 90% of the total operating time (after 200 hours) occurred between 60 to 70 per cent of full vehicle loading. In relation to D54 readings, a dramatic increase in wear debris at this time is also observed. Particle inspection indicated moderate to heavy amounts of fatigue chunks present (typical gear surface fatigue). Thus, the gears used for 60 to 70 per cent vehicle loading during field operation most likely are the source of the wear debris generation.

A fibrous material of some sort begins appearing after approximately 200 hours. The increasing frequency and magnitude of these as operation continues would seem to indicate a growing ineffectiveness of the system filter element.

A general assessment of the internal system state indicates an impending failure. The areas of concern would be in the transmission for the gearing that supplies the 60 to 70 per cent power range. Also, any fiber containing components (clutch and/or brake disks) are suspect to failure. It is also recommended that the system filter and oil be replaced as soon as possible.

System Three - Hydraulic Steering System

The third system to be analyzed limits its size to include just the hydraulic steering sub-system of a field test vehicle. This system is independent of the hydraulic functions provided on the vehicle, therefore allowing the hydraulic fluid to possess the characteristics of only the wear debris generated and contaminant ingressed into the steering system itself. Samples again were removed just upstream of the filter element and taken over a period of approximately 1000 hours. The initial reading was recorded at 300 hours.

Fig. 12 shows the D54 density readings obtained from this system. Since no vehicle load history was available, only correlation to servicing and noted failures will be possible. First, the extremely low density readings are justified by the high safety and reliability factors involved in a steering system. Therefore, minor density increases (1 to 2 units per ml) in this system could mean impending failure. This fact is illustrated by the rise and peak between 400 and 500 hours. A failure was recorded at approximately 500 hours, and with component(s) replacement and system clean-up

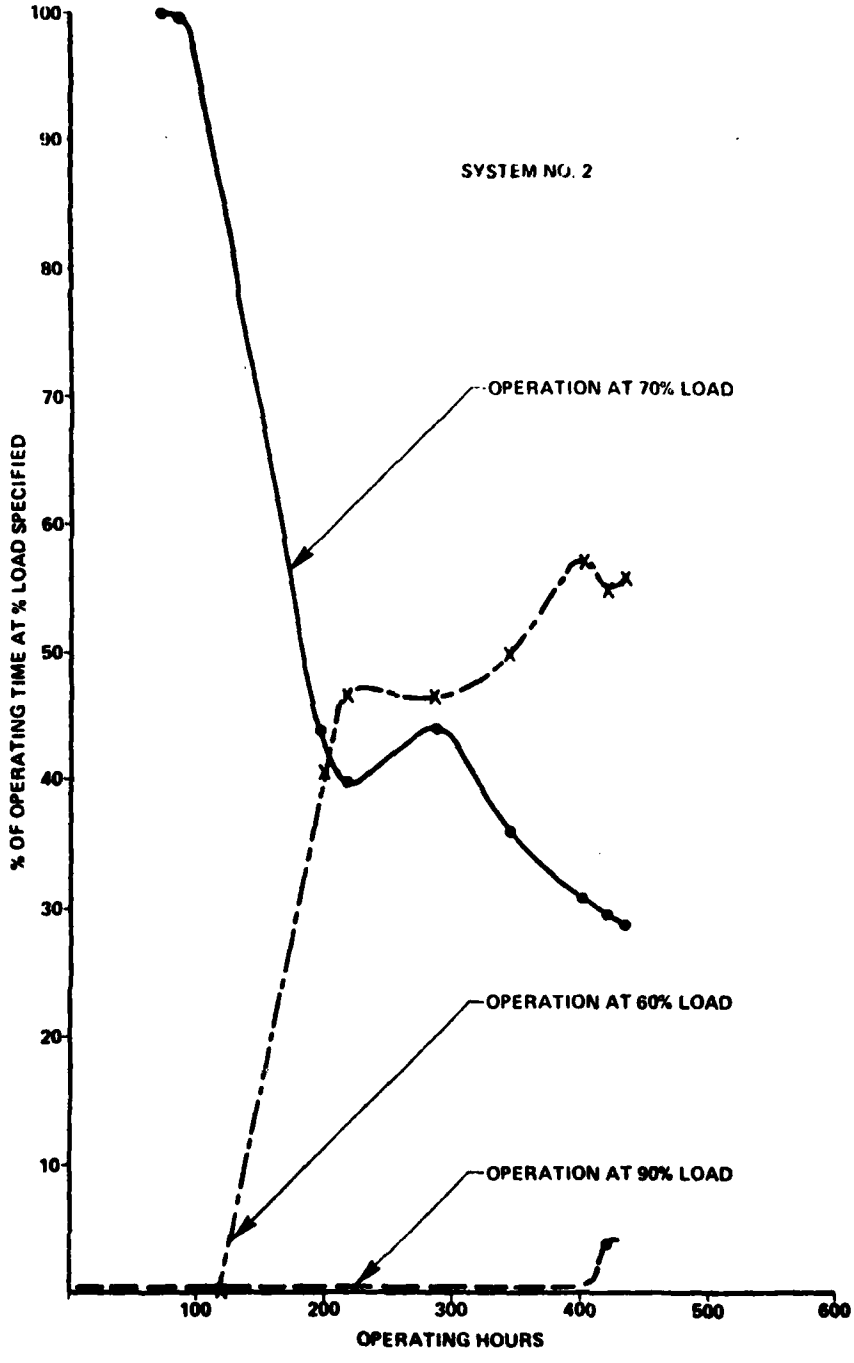

FIG. 11 PER CENT OF VEHICLE OPERATING LOAD VS. OPERATING TIME FOR SYSTEM #2

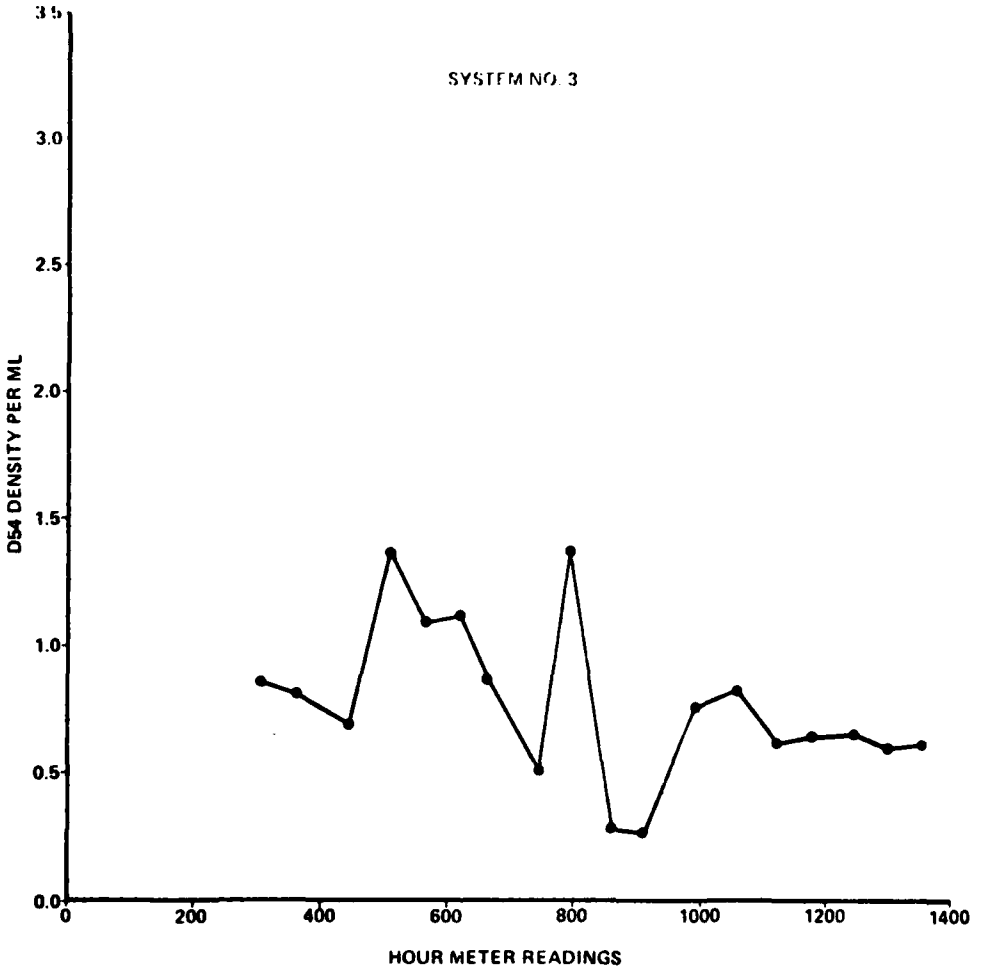

FIG. 12 D54 DENSITY VS. OPERATING TIME FOR SYSTEM #3 - HYDRAULIC STEERING SYSTEM

(filter and oil change) the readings declined. Particle analysis prior to this failure indicated the presence of fairly high alloy metal wear particles in moderate amounts. Also observed were crystals (silica possibly) of all sizes and colors, again in moderate amounts.

The second prominent peak at 800 hours was characterized by heavy amounts of laminar particles and spheres, with some approximately 20-25 micrometres in size. This suggests possible bearing fatigue beginning within the system. Indications of some surface heating due to the presence of iridescent particle coloring were also noted throughout the period.

Observed throughout the entire monitoring period was the presence of web-like or jelly-like substances within the samples. This is a possible indication of a breakdown in the hydraulic fluid additive package or the presence of water within the system thus affecting a barium additive.

Assessment of System Three suggests the wearing rate to be leveling off as indicated in the density readings after 1000 hours (Fig. 12). Points of possible concern are parts with high alloy metals and the problems associated with breakdown in the oil additive package. Recommendations are for replacement of the hydraulic fluid and improvement of the contaminant ingression level (check system sealing).

System Four - Transmission Lubrication System

The fourth system analysis was conducted on a vehicle transmission lubrication system. As with the hydraulic steering system, this lubrication system is also independent of the other hydraulic functions present on the vehicle, thus allowing isolation on the wear debris generated by the transmission and related lubrication circuit. The evaluation period ran from 300 to 1350 hours, with samples drawn approximately every 50 hours just upstream of the filter.

Fig. 13 indicates the D54 density data recorded during the evaluation. Again, no vehicle load history is available. Therefore, discussion of the wear generation will be centered around the type of particles present. The pronounced drop of D54 density values after 500 hours is due primarily to a filter replacement and oil change at this time. Prior to 500 hours, initial exposure to field ingression produced a "field break-in" period which resulted in initially high wear rates. The filter and oil replacement removed most of this debris, allowing the system to operate at a "normal" wear level as indicated after approximately 600 hours.

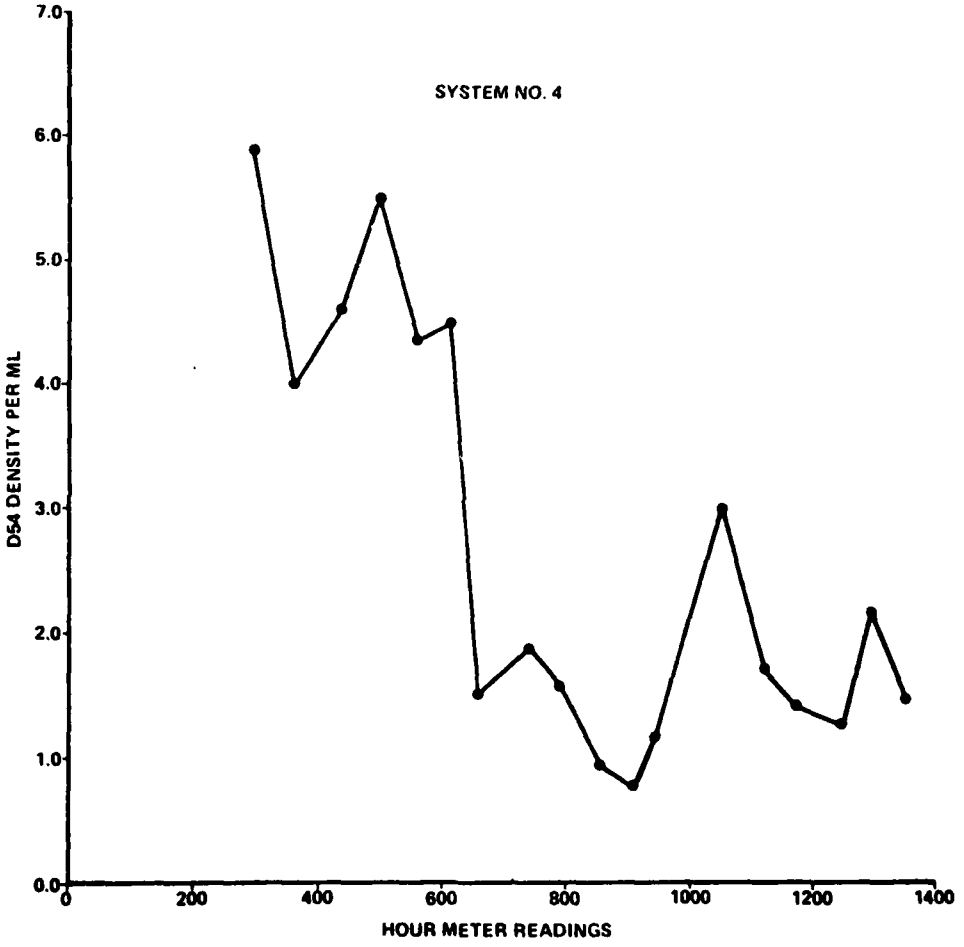

FIG. 13 D54 DENSITY VS. OPERATING TIME FOR SYSTEM #4 - TRANSMISSION LUBRICATION SYSTEM

The type of wear observed indicates a heavy amount of severe wear particles (due to rubbing) throughout the entire sampling period. These particles are ferrous in nature and appear both with striations and pitting. Early samples (before 700 hours) show the presence of a non-ferrous material, possibly aluminum. However, the frequency decreases after 700 hours. Similar to the steering system, a web-like or jelly-like substance is present in readings after 600 hours. The magnitude of this material varies, but is consistently observed.

Evaluation of the wearing condition in this transmission lubrication system would seem to identify a normal wear mode encountered by vehicle transmission. The relatively constant D54 density readings around two units per millilitre, as well as the presence of the same type and magnitude of particles throughout the sampling period, verify this. Abnormal rises in future samples would warrant inspection of transmission components. It is suggested that an analysis of the web-like substance in these samples be conducted. A decrease in filter life due to this material is quite possible, as well as its effect on wear rates if this is a breakdown in a wear additive.

System Five - Auxillary Hydraulics System

The final system to be analyzed involves the auxillary hydraulic functions available on a field operated agricultural tractor. Again separated from the other vehicle hydraulic functions, the samples taken for this analysis reflect the wear debris generated throughout these functions as well as the pumps supplying the power. The initial sample was taken at 300 hours, with periodic sampling conducted for the next 1000 hours.

Fig. 14 illustrates the recorded D54 density data for the testing period monitored. As has been typical of each system so far, the range of density magnitudes for this system is different from the other system levels. Thus, comparison of different hydraulic systems in relation to their wear status is generally difficult to obtain. The indicated extreme density readings recorded after 600 hours are somewhat misrepresented. Large amounts of the same web-like (jelly-like) substance, which were also present in Systems Three and Four, are located throughout these Ferrograms and are significantly altering the measured density readings. However, through visual analysis of the debris present, a moderate increase from the early readings (before 600 hours) is evidenced, approximately to the extent shown by the dashed line in Fig. 14.

The effect of this webbed substance on filter efficiency is most pronounced by the high recorded D54 density readings as

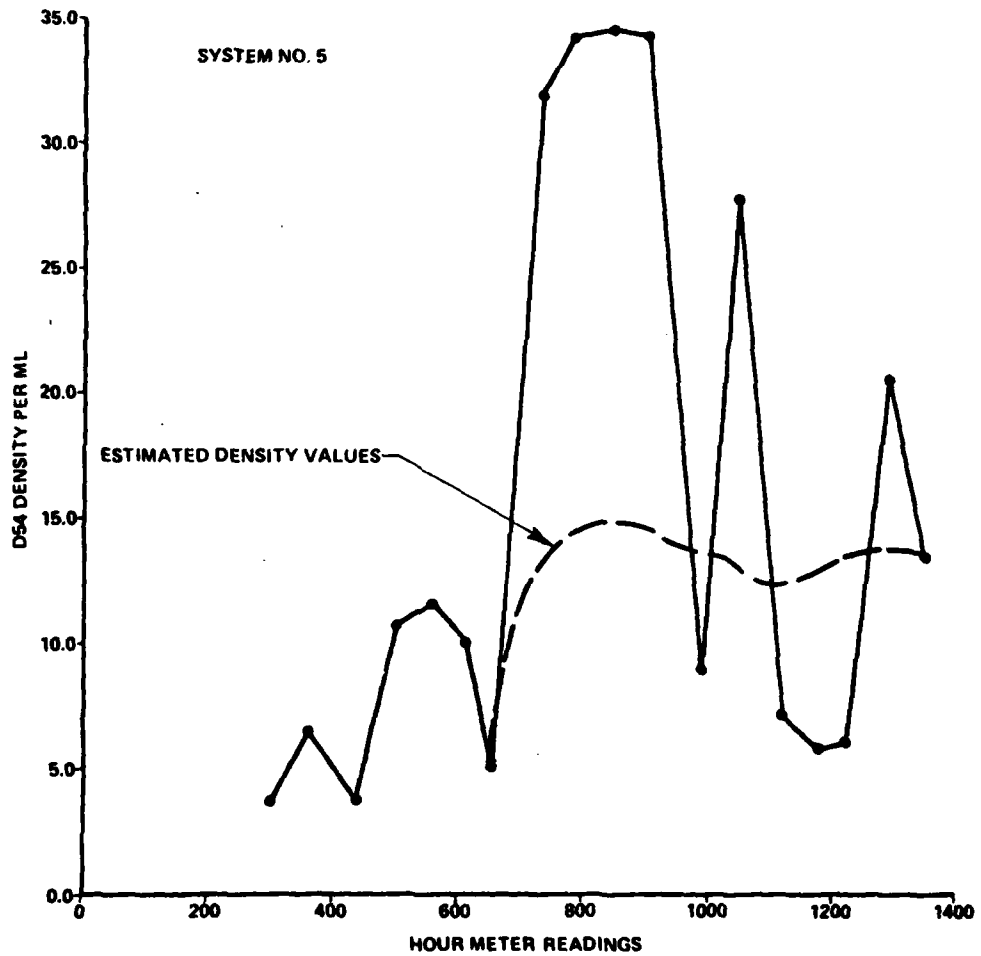

FIG. 14 D54 DENSITY VS. OPERATING TIME FOR SYSTEM #5 - AUXILLARY HYDRAULIC SYSTEM

well as the particle counts. A replacement element was installed at approximately 900 hours, and the resulting system clean-up is shown in Fig. 14. Suspecting this substance is due to a breakdown in the oil additive package, its affect on lubrication within the system is also observed by the presence of corrosive particles (mostly rust) and extreme surface heat which were present throughout the sampling period.

The main type of wear debris monitored during system operation indicates periodically heavy amounts of severe wear particles present. However, except for a short period of moderate amounts of laminar particles (indicating wear in rolling bearing devices), this seems to be a normal operating condition for the system.

The observed internal state for System Five definitely indicates the need for a complete oil and filter change. Due to the repetitive nature of the suspected additive breakdown in three evaluated systems, it is recommended that this oil be analyzed for the true nature of the webbed substance. The presence of severe surface heating and rust particles are most likely due to to the failure of the oil to adequately protect the system. However, an inspection for possible pump scoring and system exposure to water is suggested.

Summary of System Findings

System One - Complete Vehicle System

The presence of fibrous material in these samples indicate a possible breakdown of brake or clutch disk facings. Also observed were a number of tempered, oxidized, and corroded particles in the final three samples, suggesting a breakdown of the oil lubricating characteristics. And finally, the presence of large amounts of spherical severe wear particles during system loading at approximately 80 to 100% suggests fatigue cracks generating in rolling bearing surfaces. System evaluation suggests replacement of system oil and the filter element be made, with vehicle brake or clutch disks cited as possible source of impending failure.

System Two - Complete Vehicle System

The presence of fatigue chunks in large amounts occurring during operation at 60 to 70 per cent of vehicle loading suggests possible failure of gearing for that operating range. As in the previous system, the fibers present warrant an inspection of clutch and/or brake disks. Recommendations include system clean-up through oil and filter replacement as soon as possible.

System Three - Hydraulic Steering System

Assessment of system indicates a generally constant wear condition after an initial failure. Some presence of high alloy metal wear was observed, as well as problems associated with a possible breakdown in the oil additive package. It is suggested that the oil be removed, replaced, and analyzed. An improvement of the contaminant ingression level is also recommended by checking for possible system sealing problems.

System Four - Transmission Lubrication System

Evaluation of this system indicates a relatively constant wearing process at a fairly low density magnitude. At present, no immediate failures are indicated. However, if dramatic density increases are indicated, the probable cause would most likely be the transmission gearing due to earlier evidence of severe rubbing wear particles with striations and pitting. Indicated web-like substance (possible oil additive package breakdown) in samples warrants an analysis of this oil for causes. A possible decrease in filter efficiency may also be occurring due to clogging by this substance. Both oil and filter element replacement are desirable.

System Five - Auxillary Hydraulic System

The presence of the web-like sutstance in large amounts is the dominant characteristic. The suspected additive package breakdown accelerated the amount of severe surface heating and rust particles observed in the system due to the loss of adequate system lubrication. It is suggested that possible pump scoring has occurred. Inspection is also recommended for possible points of system exposure to moisture. Again, recommendation for a complete oil and filter element replacement and implementation of an analysis of the oil breakdown is suggested.

Conclusions

The five system evaluations have very clearly indicated the capabilities available through Ferrographic Analysis Techniques. In addition to identifying the magnitude and type of wear debris generation occurring, correlation with system operation data (load history, service records, and system description) allowed isolation of the possible source(s) and cause of wear without visual inspection of the entire system assembly.

It has also been shown that the Ferrograph has the ability to record the presence of non-metallic particles (fibrous material)

and breakdowns in hydraulic fluids (or fluid additive packages) which may occur during system operation. While these conditions may not be directly related to system wear, they do signify abnormal operation of some component or aspect of the system. Identification of their cause and source may prove to be just as valuable in the prevention of system failure due to non-wear sources.

The results have indicated that direct system analysis is possible and feasible for in-field evaluations. As the Ferrographic potential is realized, the possibility of manufacturer installed system sampling ports and scheduled vehicle oil sampling and analysis may become a standard maintenance procedure for future hydraulic power systems.

SYSTEM CONTAMINATION CONTROL CONCEPTS

From the preceding sections, the severe component degradation which results from the presence of particulate contamination is obvious. The implication, therefore, is that control of the particulate contamination - and subsequently the control of wear debris production - provides a simple solution to the problem of contamination initiated premature component or system failures. This seemingly simple solution seems to become rather complex, however, when the interaction of the contaminants, the components, and the system parameters are considered.

Contamination Control Balance

Figure 15 is a pictorial presentation of the interactions mentioned in the preceding paragraphs. The concept presented in the figure is based on the premise that the primary reason for the interest in contamination control is to increase the contamination service life of a component or system. A natural result of increased service life is increased reliability and availability and, perhaps, some maintainability advantages. These factors are depicted simply as hours in the middle of the figure.

The contaminant service life is ultimately dependent on just two factors. The first of these is the system contaminant level. The contaminant level, in turn, is a function of the system filtration. Obviously, higher filtration ratios (β) and flow rates (Q) are conducive to better filtration and lower contaminant levels, while higher rates of ingression of particles (Ri) have a detrimental effect on those levels.

The second factor affecting the contamination service life is the contaminant tolerance of the component (ω). Intuitively, it can be said that ω is a function of the wear resistance (WR) designed into the component by judicious use of materials and configurations. This can be demonstrated readily by standard contamination tolerance of components in general. These two elements, coupled with the system operating parameters of pressure (P), temperature (T), and speed (N), are the principal determining factors of ω.

It is now possible to demonstrate very simply from Fig. 15 that higher flow rates, better filtration ratios, better fluid lubricity, and more wear resistant materials combined with better methods for preventing the ingression of contaminants and less severe operating conditions will automatically result in increased component service life.

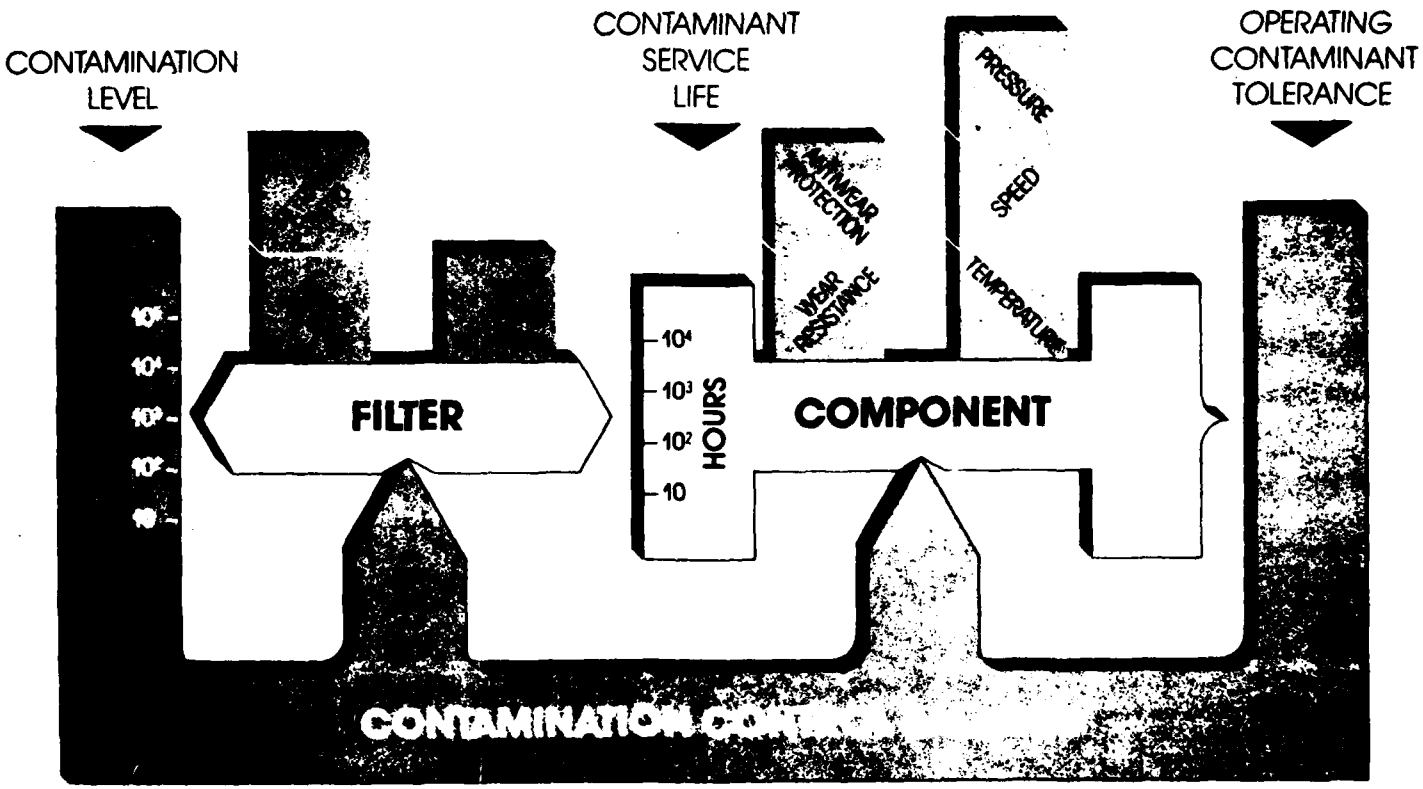

Fig. 15 Contamination Control Balance

Debris Concentration in Terms of Wear Rate

There are three sources of particulate matter in most fluid systems. Contaminant particles can be ingested by the system from the external environment, such as through seals and breathers. In addition, even with extreme care, manufacturing residue can be left in the system during fabrication. Finally, the wear of components will introduce particles into the system - normally called *generated contaminant.*

Because a constant contamination addition from one or all of these sources would cause a progressively increasing contamination level, a filter is used in a hydraulic system to control the particle concentration. Therefore, the system filter is a controller, just as a relief valve is a pressure controller. The amount of contaminant present in a hydraulic system is a function of the material being introduced and the material being removed.

By assuming that the only particles being added to a fluid system are produced by wear, a mathematical relationship can be derived for the concentration of wear debris. Such an analytical expression is based upon a fundamental material balance [11, 12]. On an idealistic basis, such a balance could be written.

$$G_s(t)V_s = G_o V_s + \int g_w\,dt - \int g_R\,dt \tag{10}$$

where: $G_s(t)$ = debris concentration at any time, t, upstream of the filter (mg/litre). V_s = system volume, G_o = initial debris concentration, (mg/litre); g_w = wear rate (mg/min), and g_R = debris removal rate (mg/min).

Eq. (10) can be simplified, however, because the debris removal rate is a function of the efficiency of the filter. Therefore:

$$g_R = (G_s(t) - G_d(t)Q \tag{11}$$

where: G_d = debris concentration at any time, t, downstream of filter (mg/litre), and Q = flow through filter (litres/min).

and:

$$G_d(t) = (1-\epsilon)G_s(t) \tag{12}$$

Substituting Eq. (12) into Eq. (11) and simplifying produces:

$$g_R = \epsilon Q G_s(t) \tag{13}$$

Then, substituting Eq. (13) into Eq. (10) yields:

$$G_s(t)V_s = G_o V_s + \int g_w dt - \int \epsilon Q G_s(t) dt \tag{14}$$

Dividing through by the system volume, V_s, integrating, and rearranging produces the differential equation that describes the wear debris concentration in a hydraulic system:

$$\frac{dG_s(t)}{dt} + \epsilon \frac{Q}{V_s} G_s(t) = \frac{g_w}{V_s} \tag{15}$$

Assuming the parameters of Eq. (15) are time invariant, a closed-form solution can be obtained:

$$G_s(t) = \frac{g_w}{\epsilon Q}\left[1 - e^{-\frac{\epsilon Q}{V_s}t}\right] \tag{16}$$

This equation shows that the final debris concentration achieved after the system has reached equilibrium is directly proportional to the wear rate and inversely proportional to the product of the filter efficiency times the flow. The speed at which the debris concentration attains a steady value is a function of the filter efficiency and the ratio of flow divided by the system volume or the turnover rate. Thus, two hydraulic systems that have exactly the same wear rate would exhibit different debris concentrations if their filter efficiencies were different.

Eq. (16) can be graphically represented, Fig. 16. Here, it was assumed that the system was initially filled with "clean" fluid. Therefore, the initial concentration, G_o, was taken as zero. In cases where the system fluid contains significant amounts of debris so that the initial concentration cannot be ignored, the differential equation - Eq. (15) - will still apply; but, the

solution given by Eq. 16 will not be accurate. The curve shown in Fig. 16 has assumed a constant wear rate for the system of interest. In some cases, such an assumption is not correct. For example, new systems will exhibit a break-in period during which the internal surfaces of the components are aligning themselves. The wear rate may be quite high at the beginning of this period and decrease exponentially throughout the break-in phenomenon. Here again, the differential equation - Eq. (15) - applies, but a solution under this constraint will be different than that given by Eq. (16).

Fluid Sampling

Without a doubt, fluid sampling is the most important and often overlooked aspect of fluid analysis. To obtain a meaningful interpretation of a wear situation through Ferrographic analysis or any other fluid analysis technique, a representative sample is necessary. In this case, representative means that the contamination level in the sample is the same as the system fluid during operation. Basically, there are three critical considerations in acquiring a representative fluid; the condition of the container into which the sample is placed, the time the sample is taken, and the place from which it is removed.

The degree of cleanliness required of the sample containers [13] is associated with the contamination level of the system fluid. That is, if a high concentration of contaminant is in the fluid, then a small amount in the container will never be noticed. In addition, the degree of cleanliness of the sample containers depends upon the type of analysis that will be conducted. For example, because the Ferrograph is capable of separating component wear debris from environmental dust, some of this dust in the sample container is of little concern. However, if a particle count is to be made, such a container would produce erroneous results.

Basically, the International Organization for Standardization (ISO) has defined two simple types of sampling methods - *dynamic* and *static*. Dynamic fluid sampling is the extraction of a sample of fluid from a turbulent section of a flow stream. Conversely, static fluid sampling is the extraction of a sample of fluid from a fluid at rest. Although a representative sample can be obtained through static sampling of the reservoir fluid, great care must be taken to insure against particle settling. A device for acquiring a reservoir sample is shown in Fig. 17. The ISO recommends that the dynamic sampling method [14] be employed to obtain a representative sample. A typical field-type sampling device is shown in Fig. 18 from the ISO standard.

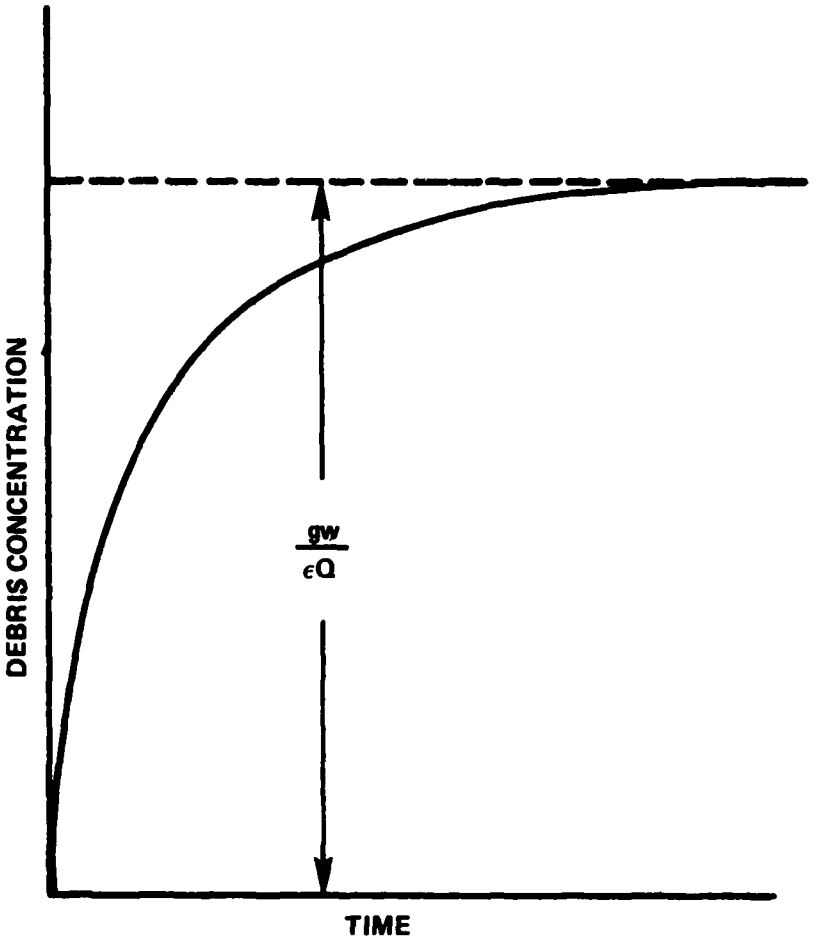

Fig. 16 Debris Concentration as a Function of Time for a Filtered System

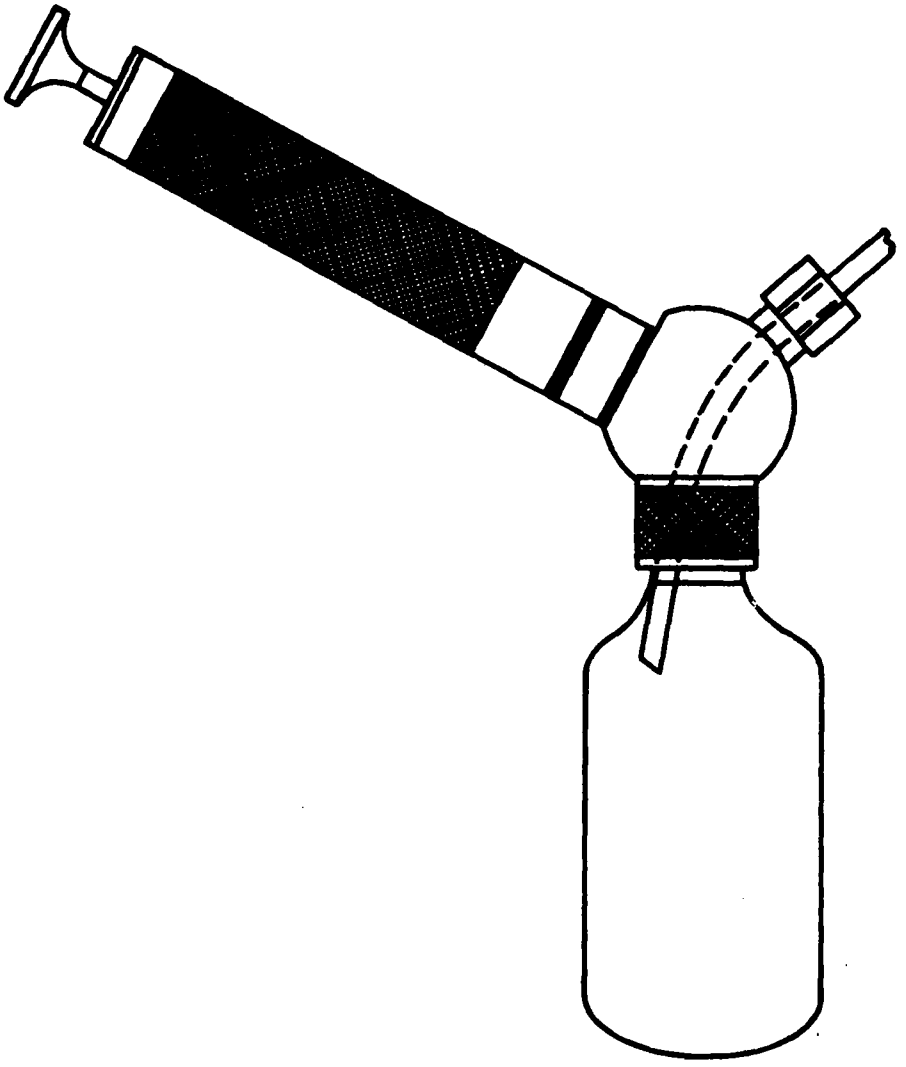

Fig. 17 Hand Operated Vacuum Pump Bottle Sampler

Wear Debris Recovery

In most hydraulic systems, the amount of extraneous material entrained in the oil far exceeds the concentration of the wear debris. Therefore, if a conventional laboratory membrane is utilized to filter the contamination from a sample of fluid extracted from a hydraulic system, the extraneous particles (environmental dust filter fibers, friction polymers, bits of rubber) would cover the wear debris, making any analysis difficult if not impossible. As another example, the contaminant sensitivity of hydraulic components is a critical consideration in their selection and use [7]. To determine the contaminant wear resistance of a hydraulic pump, a test is conducted using a controlled contaminant level of 300 milligrams-per-litre of various particle size ranges of test dust obtained through the classification of AC Fine Test Dust. To analyze the contaminant wear process induced during this test, the wear debris must be adequately separated from the test dust.

Ferrographic oil analysis has been successfully applied to examine the contaminant wear of hydraulic pumps. Typical results from these studies are shown in Fig. 19 and 20 [15]. Fig. 19 shows the results of using the same gear pump tested at various contamination levels, whereas Fig. 20 shows the data acquired using various pump outlet pressures. The most important aspect to note from these figures is that the Ferrographic analysis method was sufficiently sensitive and discriminatory to show small changes in wear rates caused by parameter variations.

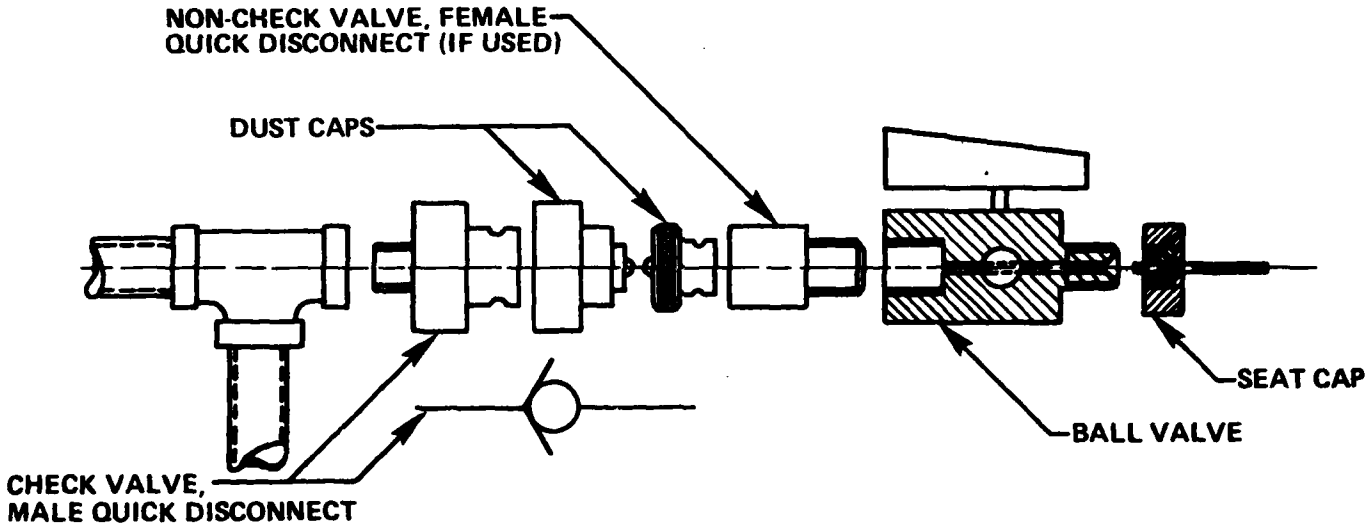

Fig. 18 Typical Field Type Sampling Device

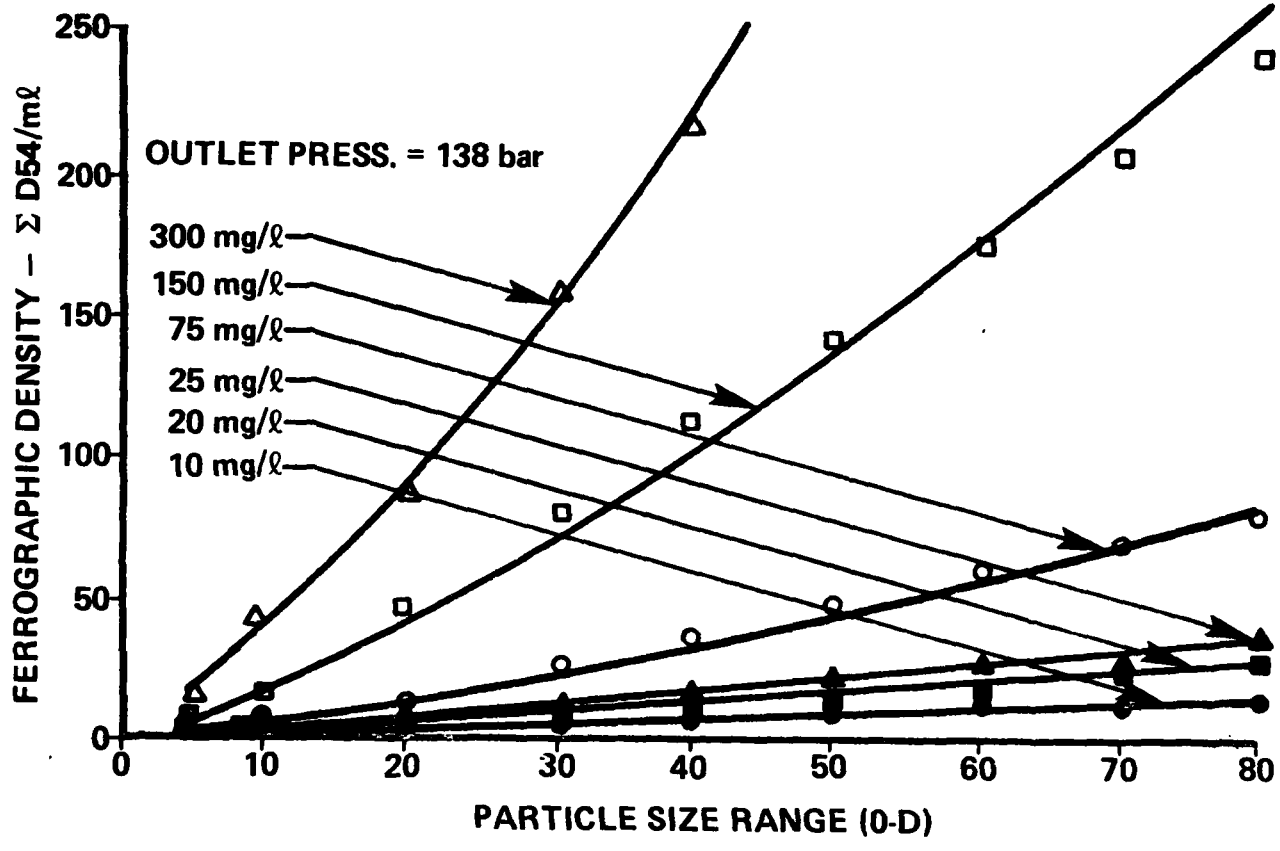

Fig. 19 Summary of Pump Test Results at Various Contaminant Concentrations with a Pump Outlet Pressure of 138 Bars

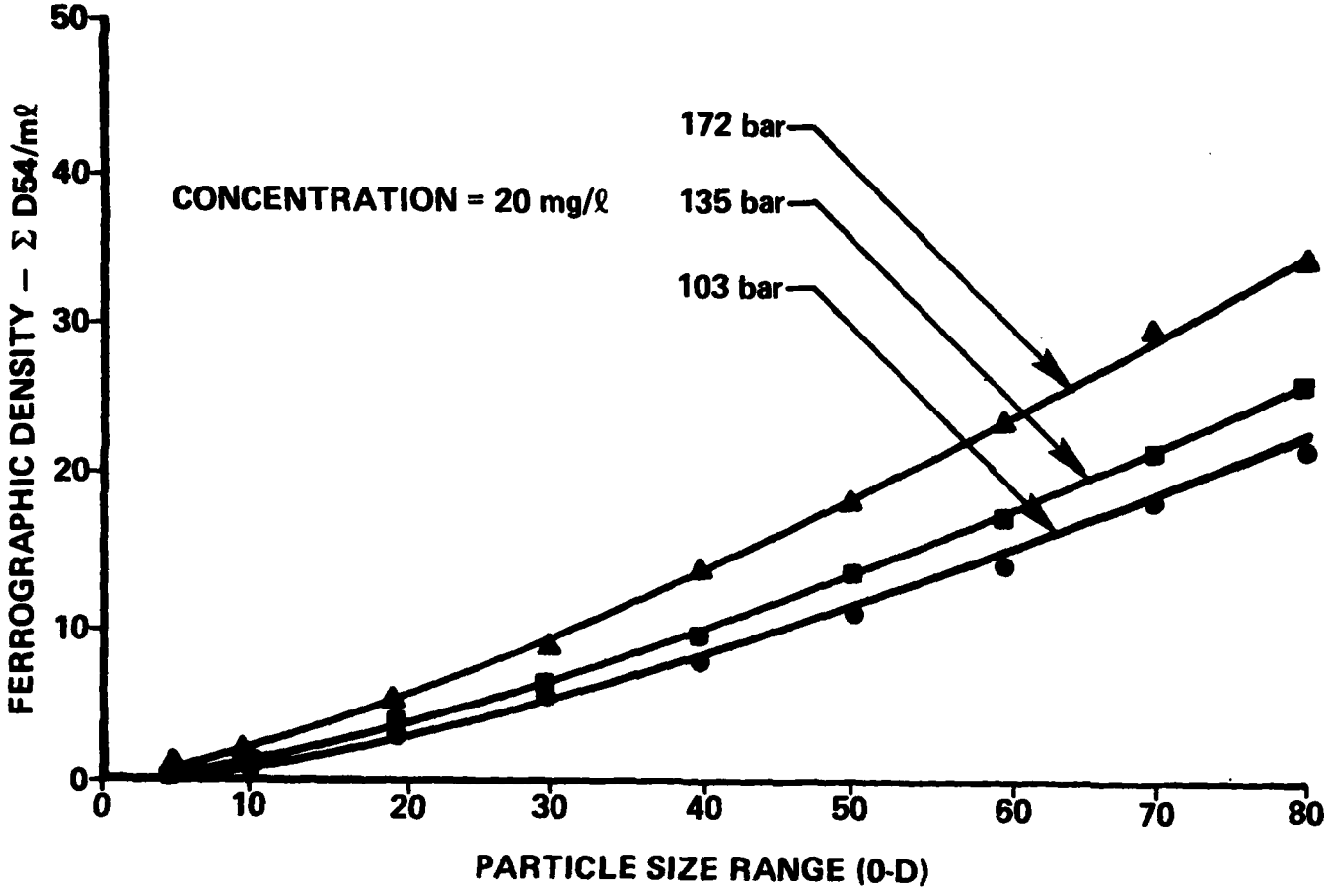

Fig. 20 Summary of Pump Test Results at Various Outlet Pressures with a Contaminant Concentration of 50 Milligrams Per Litre

VII. FERROGRAPHIC STANDARDIZATION

The early life of any newly introduced piece of analysis equipment is normally filled with controversy about its accuracy, repeatability and reproducability. The ferrograph is no exception. Certainly, no such equipment can provide worthwhile and reliable data unless the analysis results can be repeated within a very small tolerance percentage each time a given sample is analyzed. Likewise, if the results cannot be reproduced from one machine or laboratory to the next, there can be no universal acceptance of the equipment because there will be little confidence in it.

A commonly used method for investigating the repeatability and reproducability of equipment is a round robin program in which several laboratories are provided with identical samples which they analyze. The results of these analyses are compared statistically to determine if there are any significant differences. If so, there may be equipment modifications, operator training, procedure refinements, etc., to attempt to reduce the differences and another round robin program initiated. This iterative procedure may be repeated several times until either the desired results are obtained or it is determined that the equipment is not satisfactory.

The Case for Standardization

During the summer of 1979, a round robin ferrograph analysis program was sponsored by the Naval Aircraft Engineering Center (NAEC). The purpose of the program was to investigate the repeatability and reproducability of the ferrographic analysis process. Four laboratories participated in the program - NAEC, FPRC, Michigan Technological University (MTU), and The Foxboro Company, the manufacturer of the ferrographic equipment. Details of the program will be reported by NAEC at a later time, but a brief description is given here.

At the beginning of the project, each laboratory (except Foxboro) prepared several sets of ferrograms from oil samples which they had in their own laboratories. (The ferrograms in each set should have been statistically identical because they were prepared from a common oil sample.) Ferrograms from each set were then distributed to each of the other laboratories where each ferrogram was analyzed three different times using four different methods. The results of these analysis were forwarded to NAEC for evaluation.

NAEC sent a partial tabulation of the results to the FPRC. A detailed statistical analysis using the Analysis of Variables technique was performed on these data. The analysis showed that,

almost without exception, there was a statistically significant difference among the results on any given sample set whether compared by laboratory, method, or a combination of variables. In some cases, there were even significant differences within a laboratory on consecutive analysis of the same sample. The results showed statistically that the ferrographic technique was neither repeatable or reproducable enough to be used as a decision-making method for analyzing oil samples.

At first sight, this appeared to be rather damning evidence that ferrography is not the beneficial tool it was originally thought to be. However, a further analysis of the entire program and the ferrographic equipment itself revealed a number of problems which probably contributed to the differences in the results.

Several of these problems were procedural and pointed out the absolute necessity for a rigidly followed procedure which includes details on sample agitation and dilution. Such a universal procedure is required for any scientific analysis method if comparable results are to be achieved. It is not at all unusual for a new analysis tool to be poorly received at its introduction because of procedural differences in its use.

Other causes of problems were found with the ferrograph itself. One of these is the very common problem of trying to determine a fixed point from a variable reference, in this case, finding the D54 reading. It has been determined that the most significant indication of the debris level of the sample is found at the point which is 54 mm from the exit end of the ferrogram. This is based on the premise that the distance from the point at which the oil first contacts the ferrogram is always the same distance from the point at which the oil exits the ferrogram. This premise fails, however, because of two purely mechanical problems.

The first is that when the clean glass slide is placed on the ferrograph, its fixed end is the entry end. This means that any variation in the nominal slide length of 60 mm--and such variations are common--causes a like variation in the distance from the entry point to the exit point. Consequently, the significance of the D54 reading can be distorted by the variance in its actual location.

The second problem is the possible variation of the initial point at which the oil contacts the slide. This can occur because there are no mechanical stops which limit either the length of the feeder tube protrusion from the tube holder or the amount of travel of the tube holder itself. In normal practice, the tube

is simply lowered until it "contacts" the slide. The angle, location, and force of such contact is not defined, although it is obvious from the analysis of the trajectories of magnetic particles shown in Appendix A that all three are significant to the deposition pattern.

Fortunately, these problems are fairly easily overcome by ignoring the original meaning of "D54", i.e., the density reading obtained 54 mm from the exit end of the slide, and using a position based on the observed entry point of the oil. This entry point is readily identifiable visually by the relatively large (in both diameter and depth) deposit of debris. By measuring 2 mm toward the exit end from the observed center of that deposit, the truly significant "D54" position can be located.

The fact that repeatable and reproducable ferrographic results can be obtained by carefully repeating a well-formulated procedure has been demonstrated numerous times by the FPRC. The curve shown in Fig. 21 is typical of the repeatability of the results normally obtained at the FPRC. In this case, a sample of fluid was taken from a hydraulic system in which contaminant wear had been induced. Three ferrograms were made from each of the following sample volumes--0.25, 0.50, 0.75, 1.0, 2.0, and 3.0 millilitres. The density readings (D54) for each of the 18 ferrograms are shown. The maximum coefficient of variation exhibited by these data is about 5% (using the range to estimate the standard deviation). [16]

NOTE: The change in the slope of the curve at a density reading of about 40 indicates that some type saturation occurs at that point. Consequently, for a ferrogram which has density readings greater than 40, the fluid sample should be diluted and reprocessed.

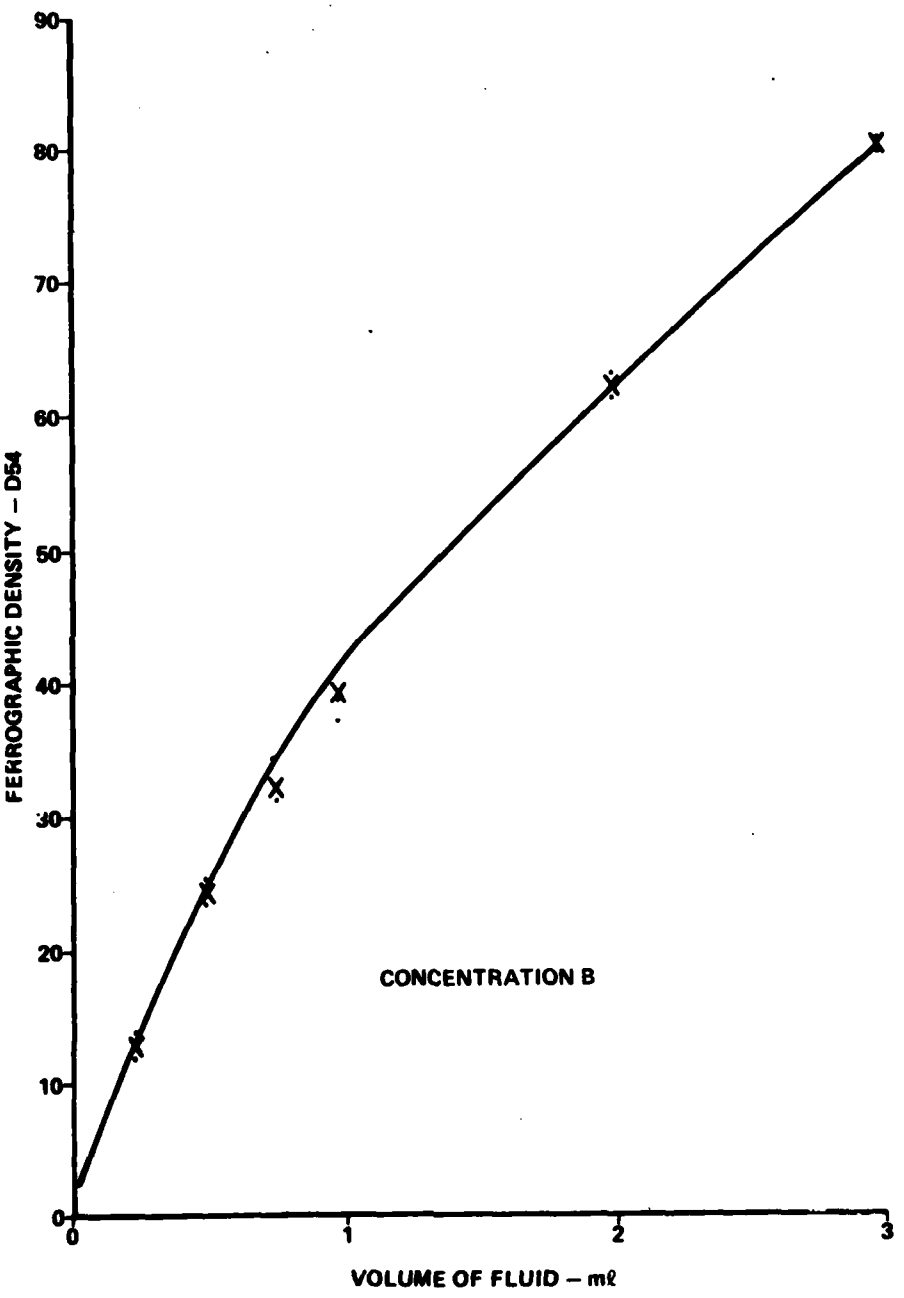

Fig. 21 Repeatability and Saturation Characteristics of Ferrographic Techniques

TTCP Participation

During the period covered by this report, the FPRC has fully and actively participated in two meetings of the Technical Cooperative Program (TTCP), Sub-Group P, Technical Panel 1, Action Group 4. The purpose of this participation was to help solve the operational and interpretation problems of ferrographic analysis and to promote the formulation of an internationally accepted analysis procedure. Significant progress has been made toward these goals. A comprehensive procedures document has been assembled and interpretative techniques have been developed.

Although valuable technical work has been done, by the Group, the promulgation of International Standards is not considered to be within the pervue of the Group. Therefore, it will be necessary to promote the standardization through other channels. The mechanism for this promotion has already been set up through the Society of Automotive Engineers, (SAE), ORMTC/Sub-Committee 4/Working Group 6/Task Group 3. A Task Group has been organized with Mr. Dick Dietrich and Mr. Peter O'Donnell of the Naval Air Engineering Center as co-chairmen. A highly advanced first draft document is available to this Task Group as a result of the TTCP activities.

Once the document has been approved by SAE, it will require sponsorship through the American National Standards Institute (ANSI) and the International Standards Organization (ISO).

Because of the work already accomplished by the FPRC and because of the positions held in all three of the standards organizations cited above by Dr. E.C. Fitch, FPRC Director, continued FPRC participation in this activity is highly desireable. However, such participation will depend upon the securing of sponsorship for the FPRC which will provide the funding necessary for attendance at meetings, participation in survey and round robin activities, etc.

VIII. SUMMARY AND CONCLUSIONS

The behavior of particles--both magnetic and non-magnetic--in the fluid stream can be accurately predicted. These predictions indicate that few magnetic particles are lost from the ferrogram. These predictions have been experimentally verified.

Wear in pumps is easily detected. The predictions of pump life and contaminant sensitivity can be made with significantly less degradation than through the normal contaminant sensitivity test methods. This means that a single item can be used in several different tests.

System health can be successfully monitored by periodic sampling and ferrographic analysis.

Ferrographic analysis can be acceptably repeatable and reproducable, but careful adherence to standardized procedures will be required before the ferrograph will be suitable as a critical decision-making tool.

The TTCP activities have provided a well advanced draft of the required standardization document for the ferrographic procedures. However, this document now needs to be progressed through the appropriate SAE, ANSI, and ISO committees to become recognized nationally and internationally.

The FPRC should receive additional sponsorship from the ONR to support the promotion of the ferrographic procesures through SAE, ANSI, and ISO.

REFERENCES

1. Air Force Materials Laboratory, AFML-TM-MB-79-01, *"Characteristics of Fluid Samples from Multi-Pass Test Stand from Hydraulic Research on Air Force Contract No. F33657-77-C-0277,"* 1979.

2. Bensch, L.E., and E.C. Fitch, *"A New Theory for the Contaminant Sensitivity of Fluid Power Pumps,"* Sixth Annual Fluid Power Research Conference, Oklahoma State University, Stillwater, Oklahoma, 1972.

3. Inoue, R., and E.C. Fitch, *"The Omega Pump Rating System,"* The BFPR Journal, 1979, 12:131-139.

4. Seifert, W.W., and V.C. Westcott, *"A Method for the Study of Wear Particles in Lubricating Oil,"* Wear, Vol. 21, 1972, pp. 21-42.

5. Scott, D., W.W. Seifert, and V.C. Westcott, *"The Particles of Wear,"* Scientific American, Vol. 230, No. 5, May 1974, pp. 88-97.

6. Kitzmiller, D.E., and R.K. Tessmann, *"The Capabilities and Limitations of Ferrographic Wear Analysis--1976,"* The BFPR Journal, 1978, 11:87-94.

7. *"Method of Establishing the Flow Degradation of Hydraulic Fluid Power Pumps When Exposed to Particulate Contaminant,"* T3.9.18-1976--National Fluid Power Association, Milwaukee, Wisconsin, 1976.

8. Bensch, L.E., and G.A. Roberts, *"Classified Test Dust Description and Control,"* Fluid Power Research Conference, Paper No. P76-10, Oklahoma State University, Stillwater, Oklahoma, October, 1976.

9. *"Hydraulic System Diagnostics,"* Section III, MERADCOM/OSU Hydraulic System Reliability Program, Annual Report, Contract No. DAAK02-75-C-0137, 1976.

10. *"Hydraulic System Diagnostics,"* Section V, MERADCOM/OSU Hydraulic System Reliability Program, Annual Report, Contract No. DAAK02-75-C-0137, 1977.

REFERENCES

11. Tessmann, R.K., *"Repeatability of Ferrographic Measurements,"* The BFPR Journal, 1978, 11:305-308.

12. Fitch, E.C., and R.K. Tessman, *"Practical and Fundamental Descriptions for Fluid Power Filters,"* Paper No. 730796, SAE Trans., Society of Automotive Engineers, New York, 1974.

13. Tessmann, R.K., *"The Effect of System Configuration on Filtration Performance,"* Paper No. P75-23, 9th Annual Fluid Power Research Center, Oklahoma State University, Stillwater, Oklahoma, 1975.

14. American National Standard, *"Procedure for Qualifying and Controlling Cleaning Methods for Hydraulic Fluid Power Fluid Sample Containers,"* ANSI B93.20-1972, American National Standards Institute, 1972.

15. International Standard, *"Hydraulic Fluid Power-Particulate Contamination Analysis-Extraction of Fluid Samples from Lines of an Operating System,"* ISO 4021-1977 (E).

16. Tessmann, R.K. and E.C. Fitch, *"Contaminant-Induced Wear Debris for Fluid Power Components,"* Tribology 1978-Materials Performance and Conservation, University College of Swansea, Sponsored by I Mech E, Wales 3-4 April 1978.

17. Tessmann, R.K., *"Ferrographic Measurement of Contaminant Wear in Gear Pumps,"* The BFPR Journal, 1979, 12:379-384.

APPENDIX A

An Appraisal of the Analytical Ferrographic Method

The BFPR Journal, 1980, 13, 3, 281-294 Basic Fluid Power Research Program

AN APPRAISAL OF THE ANALYTICAL FERROGRAPHIC METHOD

K. Nair Editorial Managers: R. K. Tessmann & E. C. Fitch *A Research Documentary*

REFERENCE: Nair, K., "An Appraisal of the Analytical Ferrographic Method," The BFPR Journal, 1980, 281-294.

ABSTRACT: Ferrography has become an important tool for the tribologist in identifying the degree and mode of wear in a machine. Now that the technique is beyond the curiosity stage, an analytical base must be established which accurately simulates its operation. Such a base is needed to make improvements in design and procedural methodology for the development of world standards.

This paper has attempted to strip away the mystical aspects of the process and look at the physics which govern deposition on the Ferrogram. Although the mathematical model derived to represent the process is for an ideal case, it is a powerful tool for making judgement calls on various aspects which exist during the operation. A companion paper covering the Direct Reading Ferrograph has also been written which should also prove valuable to those interested in this subject.

***KEY WORDS:* Ferrogram, Ferrography, mathematical model, analytical assessment, parameter sensitivity, accuracy of readings, wear reduction**

INTRODUCTION

Ferrography [1, 2] is a relatively new technique developed to separate wear debris from lubricating and hydraulic oils, primarily by means of magnetic separation. A high gradient magnetic field separates the wear particles from a fluid sample flowing over a glass substrate and arranges them more or less according to size. After the entire sample volume has been pumped over the substrate, a fixer solution is passed over the slide and wear particles which remain fixed to the slide are used for further analysis by optical or other techniques.

The information obtained from the slide (the Ferrogram) has been extensively used for studying wear phenomena and for diagnosis and prognosis of wear situations in machines [3, 4, 5]. The Fluid Power Research Center at Oklahoma State University has extended the utilization of the Ferrograph to study the wear in hydraulic systems [6, 7, 8]. Quantitative information obtained from these studies is primarily in terms of the optical densities at or near the entry point. Optical densities at other locations also have been utilized for evaluating the Severity Index [28]. Qualitative information on particles is obtained by direct microscopic examination or heating of the Ferrogram along with other chemical processes.

Ferrography has been shown to be an extremely good analytical tool for studying wear situations in machines. Occasionally, small amounts of data scatter are seen in the density readings of the Ferrogram. It would be helpful for a complete and realistic analysis of the wear process if the Ferrographic process was properly understood from an analytical point of view. Kitzmiller [9] has reported an extensive study on the Ferrograph and, based on a number of controlled experiments, proposed an operating procedure. Similar studies on the subject are dealt with in Ref. [10], [11], and [12]. This paper presents an analytical development of the expressions and functions which control the Ferrographic process. The purpose of the effort was to identify and isolate those parameters which are influential and to evaluate their effectiveness. Based on this information, a discussion is advanced for the consideration of parametric control of the Ferrographic technique. In this manner, an analytical foundation can be formed for the standardization of Ferrographic analysis and interpretation.

IDEAL FERROGRAPH

For formulation purposes, it is convenient to conceive an idealized Ferrograph. Deviation of any parameter from ideal situation can be studied by its effect on the Ferrographic process. The following assumptions are made for the modeling of the Ferrograph:

1. The sample fluid consists of evenly distributed particles. (The particles may be ferrous, nonferrous, or any other contaminant.)
2. The particles are spherical in nature.
3. The peristaltic pump delivery onto the slide is at a uniform rate and free from pulsations.
4. The flow over the slide is steady, one-dimensional laminate flow from entry to exit of the sample on the slide. (There is no initial disturbance to the flow at the entry.)

5. The particle concentration is low enough that the flow properties are unaffected by the presence of the particles.

6. The fluid is Newtonian

7. The ferrous particles in the sample do not interact with one another and do not join together to form "larger" particles.

8. Brownian forces do not act on the particles and their motion can be idealized based on fundamental fluid mechanics and magnetic phenomena.

The foregoing concept is used for the analysis given in this paper. The difficulty in developing a mathematical model for an innovation based only on experiment is overcome by using reasonable engineering idealization. The influence of various parameters affecting the idealized operation of the equipment is discussed in detail and possible solutions are suggested based on the model developed.

MODEL OF THE FLUID FLOW

Fig. 1 shows a schematic diagram of the Analytical Ferrograph. The sample fluid is pumped onto the substrate by a peristaltic pump. The flow through the pump is assumed to be constant. By virtue of the peristaltic operation, there will be fluctuations in the output of the pump; however, this will be of minor influence at the delivery end of the tube, where a reasonably steady flow is obtained.

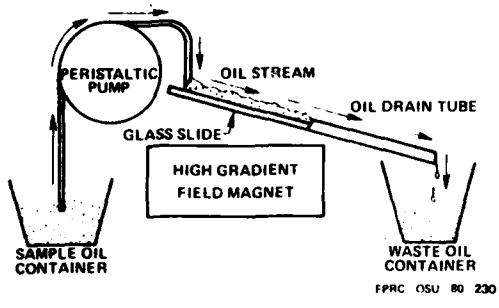

Fig. 1. Schematic of Slide Ferrograph. [9]

In an Analytical Ferrograph, according to measurements, the flow rate (Q) is of the order of 0.25 to 0.5 mℓ per minute. The viscosity of fluids flowing over the slide (without fixer added) may vary from about 216 centistokes for mineral-based lubrication oil formulated for use in aircraft engines to about 13 centistokes for some hydraulic fluid at 20°C. Fluid densities may vary from 0.75 to 0.9 gm/cc. Based on these data, it can be reasonably assumed that the flow over the slide is ripple free laminar. Appendix 1 shows the analytical approach to prove this assumption.

The slide over which the sample fluid flows is made of a rectangular thin glass sheet of about 60 millimetres in length. Oil enters the slide at about 55.5 to 56.5 mm from the exit end where fluid leaves the slide. The gravity flow over the slide is contained in a U-shaped boundary. Fig. 2 shows a slide with its major dimensions.

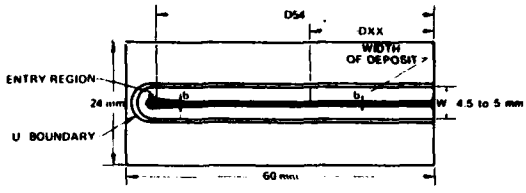

Fig. 2. Major Dimensions of Slide and Deposit.

The sample fluid flows as a rivulet on the slide. Flow of this rivulet is controlled by the inclination of the slide to vertical, surface tension, fluid viscosity, and density of the sample fluid. Towell and Rothfeld [13] have developed the hydrodynamics of such a flow as a one-dimensional laminar flow and have solved simple cases. Using the theory developed by them for the purpose of modeling the Ferrograph suffers from two disadvantages: firstly, it requires numerical techniques denying a closed-form solution; and secondly, on the Ferrogram, the flow is not allowed to expand laterally by the presence of the U-boundary on the slide. Since there is no full bounding wall on either side of the fluid flow as in the case of a channel, and since the width of the flow film is not large, the flow is not of the "open channel" type. Thus, the flow tends to be somewhere in between an open channel flow and a fully developed rivulet flow. Fig. 3 shows the difference between the cross-section of the fluid film under these conditions. On the Ferrogram, however, the major interest is in the central region of the fluid flow, where the ferrous particles are deposited. Ferrous particles in the fluid are attracted towards the center of the slide due to the existence of lateral field gradient of the magnet. Thus, this central region reasonably represents an open channel flow.

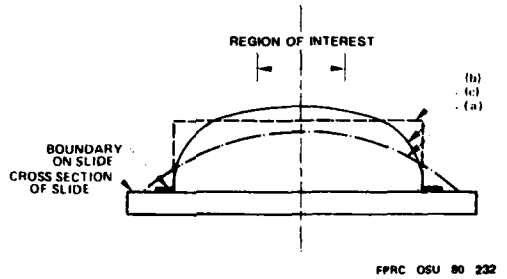

Fig. 3. Fluid Cross Section and Region of Interest.
In Figure:
(a) Fluid Flows as a Free Rivulet.
(b) Fluid Flows in an Open Channel Without Surface Tension.
(c) Fluid Flows Within the Boundary on Ferrogram.

Fig. 4 shows the coordinates selected for analyzing the fluid flow. In this diagram, the positive X-direction is measured vertically upwards from the slide, where fluid contacts the substrate. The Y-direction is measured in a lateral direction from the center line, while the Z-direction is measured along the flow from the point of entry of the fluid on the slide.

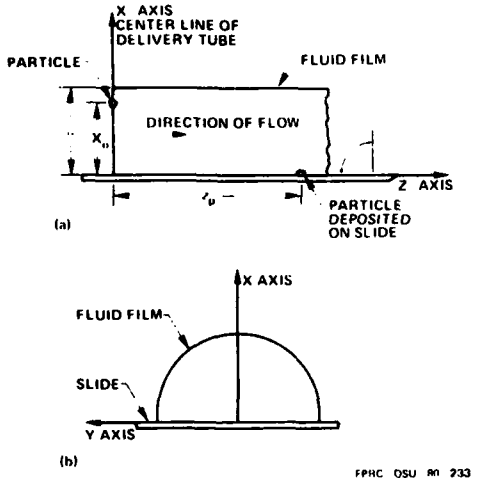

Fig. 4. Coordinate Axes and Particle Location.
(a) In the Direction of Flow.
(b) Cross Section of Fluid Film.

With the assumption of open-channel flow, the velocity profile of the fluid flow over the slide is parabolic. This velocity in the Z-direction can be represented by [14, 15]:

$$U_z = \frac{\rho_f g \cos\beta}{2\mu}(2\delta x - x^2) \qquad (1)$$

where: U_z = the fluid velocity along the flow direction, ρ_f = the density of the fluid, β = the inclination of the slide to the vertical, μ = the viscosity of the fluid, x = the height of the streamline above the slide where velocity is evaluated, and δ = the maximum height of the flowing film.

The maximum value of velocity, as shown by Eq. (1), is at the interface between the air and the sample fluid and this is obtained by substituting $x = \delta$ in Eq. (1). Maximum velocity, U_z (max), is given by:

$$U_z(max) = \frac{\rho_f g \delta^2 \cos\beta}{2\mu} \qquad (2)$$

Limited experiments at the Fluid Power Research Center showed agreement with the theoretical maximum velocity at the interface.

Volume rate of flow over the slide is given by:

$$Q = \frac{\rho_f g w \delta^3 \cos\beta}{3\mu} \qquad (3)$$

where: Q = the volume rate of flow of fluid over the slide, and W = the width of the U-boundary on the slide.

Again, the average velocity of the fluid flow, U_z (ave), on the slide is given by:

$$U_z(ave) = \frac{\rho_f g \delta^2 \cos\beta}{3\mu} \qquad (4)$$

Eq. (1) through Eq. (4) show the general nature of the flow over the slide. The flow rate (Q) is constant in a given situation and is controlled by the pumping system. For a given sample, it could vary slightly depending on the change in delivery tube dimensions and its ovality. Once the flow rate is known, the velocity profile can be evaluated. It should be noted that, in the above equations, it is assumed that the section of the fluid film does not change in shape throughout the flow over the slide.

PARTICLE DYNAMICS

It was assumed earlier that in an ideal situation the particles are spherical in nature. This is far from reality with any wear particles. Describing a non-spherical particle by an equivalent sphere also poses problems since, for example, the magnetic force on them will be a function of the volume of the particle while drag force depends on the shape and projected area of the particles. Hence, deviation from sphericity would be dealt with as a variation from an ideal situation.

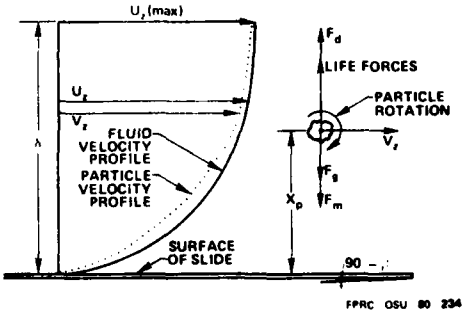

Fig. 5. Effect of Lift Force in Producing Log on Particle Velocity Profile.

The particles are assumed to be suspended uniformly in the fluid. When they flow over the slide, they are subjected to gravity force, buoyant force, drag force due to fluid flow, and magnetic force. Since the flow is of a low Reynolds number, laminar type, particle acceleration will be resisted by the fluid. However, along the X-direction, that is, across the depth of the fluid film,

the velocity profile is parabolic; and, hence, the particle experiences slightly higher velocity on its top surface compared to that at the bottom surface. This, in turn, produces a torque on the particle making it rotate. This causes an energy transfer to the particle, resulting in a lag in particle velocity with respect to the fluid velocity. A lift force could be created by this mechanism tending to create an upward force on the particle. Since the particles are of micronic size and the length of flow over the slide is short, this effect can be neglected. (The above "circulation" or lift effect is shown in Fig. 5.) Thus, it can be assumed that the particle and the fluid have the same velocity distribution in the Z-direction. This is given by Eq. (1). Eq. (1) is rewritten below by replacing U_z by V_z, giving the velocity of the particle in the Z-direction.

$$V_z = \frac{\rho_f g \cos\beta}{2\mu} (2Bx_p - x_p^2) \qquad (5)$$

Eq. (5) gives the velocity of particles in the Z-direction. Another equation in the X-direction is required to describe the complete dynamics of the particles. Since, the inclination of the slide to vertical (β) is approximately 90°, the forces in the vertical direction can be assumed to be the same as in the X-direction.

For wear particles which are heavier than the sample fluid, a net downward force from gravity and buoyancy acts on them and this is given by:

$$F_g = \frac{g\pi D^3}{6} (\rho_p - \rho_f) \qquad (6)$$

where: F_g = the net downward force due to gravity and buoyancy, D = the diameter of the particle, and ρ_p = the density of the particle.

Since the Reynolds number is low, the drag force in the vertical direction can be represented by Stoke's Law as given below:

$$F_d = 3\pi\mu\, DV_x \qquad (7)$$

where: F_d = the drag force in the X-direction, and V_x = the velocity of the particle in the X-direction.

In addition to the above forces, the magnetic particles are subjected to an additional force due to the presence of the high gradient magnet below the slide. This can be represented by:

$$F_m = \frac{\pi D^3}{6} K.H. \frac{dH}{dx} \qquad (8)$$

where: F_m = the magnetic force in the X-direction, K = the volume susceptibility of the material, H = the field strength of the magnet at the point of interest, and dH/dx = the field gradient at point of interest.

Eq. (6), (7), and (8) can be combined to give the net force acting on the particle. The particle is accelerated by the net force acting in the X-direction. This can be represented by:

$$F_g - F_d + F_m = \frac{\pi D^3}{6} \rho_p \cdot \left(\frac{dV_x}{dt}\right) \qquad (9)$$

where: dV_x/dt = the acceleration of the particle in the X-direction.

Substituting the various expressions for forces into Eq. (9), we have

$$\frac{\pi D^3}{6} \left| g(\rho_p - \rho_f) + KH \frac{dH}{dx} \right| - 3\pi\mu D\, V_x =$$

$$\frac{\pi D^3}{6} \rho_p \cdot \left(\frac{dV_x}{dt}\right) \qquad (10)$$

The particle accelerates in the fluid according to Eq. (10), until the gravity and magnetic forces balance the drag force. At this stage, the particle reaches its settling velocity (V_T). Hereafter, the particle travels with uniform velocity (V_T) in the X-direction. The settling velocity can be computed by setting the right-hand side of Eq. (10) equivalent to zero, and replacing V_x by V_T. Settling velocity (V_T) can, then, be represented as:

$$V_T = \frac{D^2}{18\mu} \left| g(\rho_p - \rho f) + KH \cdot \frac{dH}{dx} \right| \qquad (11)$$

From Eq. (11),

$$g(\rho_p - \rho_f) + KH \frac{dH}{dx} = \frac{18\mu}{D^2} V_T$$

Substituting the above expression into Eq. (10) and simplifying,

$$V_T - V_x = \frac{D^2 \rho_p}{18\mu} \left(\frac{dV_x}{dt}\right) \qquad (12)$$

Eq. (12) is a linear, first-order, differential equation in V_x, and its solution is:

$$V_x = V_T \left| 1 - \exp.(-18\mu / D^2 \rho_p) t \right| \qquad (13)$$

From Eq. (13), the time required for particle velocity to reach 98% of the settling velocity (V_T) can be evaluated as ($4D^2\rho_p/18\mu$). For a magnetic spherical particle of 20 μm diameter in a very thin fluid such as water (viscosity of water is 1 centipoise), this time would be:

$$\frac{4(20 \times 10^{-4}\text{cm})^2 (8\ \text{gm/cm}^3)}{18(0.01\ \text{gm/cm-sec})} \approx 7 \times 10^{-4}\ \text{seconds}$$

Thus, the particle velocity reaches 98% of its settling velocity in a fraction of a second; and, hence, it can be assumed that the particle dynamics in the X-direction, that is, along the depth of the film thickness, is con-

trolled by the settling velocity. If x_p is the position of the particle from the slide at any time, then,

$$\frac{dx_p}{dt} = -V_T \tag{14}$$

The negative sign for V_T is introduced as per the sign convention, since V_T acts in the negative X-direction. Eq. (5) and (14) define the dynamics of the magnetic particles in the flowing fluid. They can be combined by eliminating the variable time (t). Dividing Eq. (5) by Eq. (14) and rearranging

$$dz_p = \frac{-\rho_f g \cos\beta}{2\mu}(2\delta x_p - x_p^2)\frac{dx_p}{V_T}$$

Integrating this equation, we have:

$$z_p = -\frac{\rho_f g \cos\beta}{2\mu V_T}(\delta x_p^2 - x_p^3/3) + C \tag{15}$$

where: C = the constant of integration.

The particle may enter the slide at any height above the slide in the fluid film. Denoting this height as x_o (See Fig. 4.), the initial condition in the above equation would be: $x_p = x_o$ at $z_p = 0$.

Setting this initial condition, in the above equation,

$$C = \frac{\rho_f g \cos\beta}{2\mu V_T}(\delta x_o^2 - x_o^3/3)$$

We are interested in evaluating the position of a given particle when it is deposited on the Ferrogram slide, that is, the position z_p when x_p is forced to zero. Substituting $x_p = 0$ in Eq. (15), we have:

$$z_p = C = \frac{\rho_f g \cos\beta}{2\mu V_T}(\delta x_o^2 - x_o^3/3) \tag{16}$$

Substituting the value of V_T from Eq. (11) and that of δ from Eq. (2) into Eq. (16), we have:

$$z_p = \frac{9\,\rho_f g \cos\beta \left| (3\mu Q/\rho_f g\, w\cos\beta)^{1/3} x_o^2 - x_o^3/3 \right|}{D^2 \left| g(\rho_p - \rho_f) + KH\frac{dH}{dx} \right|} \tag{17}$$

Eq. (17) defines the location of a particle on the Ferrogram, if x_o and D are known. However, this equation is derived assuming that the magnetic term, KH (dH/dx) remains constant along the Ferrogram. The high gradient magnet used in the Ferrograph has its field strength and field gradient, dH/dx, varying along the length of the Ferrogram. (Variation of these parameters is assumed to be small along the fluid film thickness, δ.) Accordingly, Eq. (17) should be modified to take care of the variation of magnetic properties.

In the Ferrogram, it is observed that large size particles (particles whose sizes are larger than 15 μm in diameter) are deposited within 5 mm from entry point. If representative values are substituted for various parameters in Eq. (16) and (17), the relative values of the gravity term, g (ρ_p ρ_f) and the magnetic term, KH (dH/dx) can be evaluated such that a particle of 15 μm gets deposited within 5 mm from entry point. Typical values of the parameters are:

fluid density, ρ_f = 0.8 gm/cc
particle density, ρ_p = 8 gm/cc
acceleration due to gravity, g = 980 cm/sec^2
inclination of slide with respect to horizontal, $\beta \simeq 88.5°$
film thickness, $\delta = (3\,\mu Q/\rho_f g\, w\cos\beta)^{1/3}$ = 0.1 cm (assume)
particle diameter, D = 15 x 10^{-4} cm
position of particle deposition, z_p = 0.5 cm

Further, assume that the particle enters the slide at the maximum film height location, that is, $x_o = \delta$. With these parameters substituted into Eq. (17), and solving for KH (dH/dx), KH (dH/dx) = 1.25 x 10^5 dynes/cc. The value of g (ρ_p ρ_f) would be g (ρ_p ρ_f) = 0.07 x 10^5 dynes/cc.

Thus from this illustration, it can be concluded that the contribution of the magnetic forces in the Ferrographic process is much stronger than that from the gravity term. This can be further illustrated by considering the particle as nonmagnetic. In such as case, the term, KH (dH/dx), is zero and, using Eq. (17), the value of the position of deposition of the particle, z_p, can be evaluated. This can be calculated as: $z_p \cong 9$ cm.

Total operating length of the Ferrogram is about 5.7 cm and, hence, it can be observed that this nonmagnetic particle escapes deposition on the slide.

Based on the results of the foregoing analysis, we can now represent the settling velocity, V_T, in Eq. (11) as containing only the magnetic term, that is,

$$V_T = \frac{D^2 KH\frac{dH}{dx}}{18\mu} \tag{18}$$

It is seen from Eq. (18) that the effect of increasing H (dH/dx) along the Ferrogram is to directly increase the settling velocity. But if Eq. (18) is to be modified to this effect, then the variation of H (dH/dx) and, hence settling velocity, V_T, should be known. As such, this variation is not available for the high gradient magnet. However, it should be mentioned here that to evaluate the magnitude of H (dH/dx) or its variation in such a magnet is extremely difficult, if not impossible. Even experimental measurements may not give these values to an acceptable accuracy because of the short range of effective magnetic field and smaller force magnitudes on micronic particles [17, 18, 19, 20, 21, 22, 23]. Moreover, this value can be expected to vary across the thickness of the falling fluid film. The trend of the variation of (dH/dx) along the slide is indicated by Lt. R. S. Miller [24] as a polynomial function of x. (See Fig. 6.)

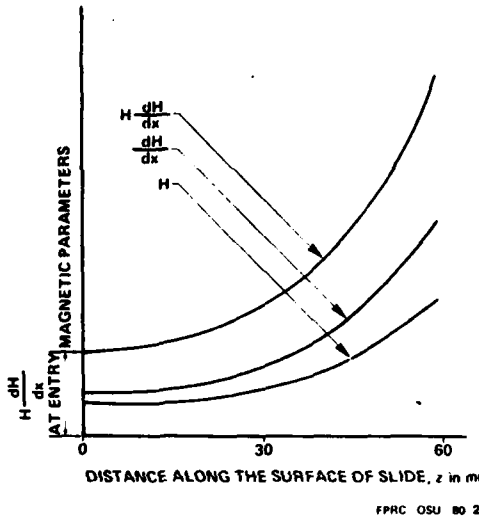

Fig. 6. Assumed Variation of Magnetic Properties Along the Ferrogram. H (dH/dx) is Assumed to Vary as an Exponential Function Along Z-Direction.

It is assumed that the field strength H also varies in similar fashion; then, the product H (dH/dx) can be approximated to be an exponential function H (dH/dx) e^{mz} along the Z-direction (m is a constant.). Subsequently, the settling velocity at various locations on the slide, that is, as z_p varies, will have an exponential variation. This can be represented as: $V_s = V_T\, e^{mz}$.

where: V_s = the settling velocity of the particle as a function of its location along the Ferrogram; V_T = the settling vleocity of the particle as given by Eq. (18); m = a constant; and z = the distance along the Z-direction, where V_s is required to be evaluated. (Note that the magnetic term, KH (dH/dx), in Eq. (18) represents its value only at or near the entry location.)

Now, the motion of the particle along the depth of fluid film, that is, X-direction, as given by Eq. (14) must be modified to take care of the change in settling velocity along the Ferrogram. This can be expressed as:

$$\frac{dx_p}{dt} = V_s = -V_T(\text{exp. } mz) \qquad (19)$$

Now Eq. (5) and (19) represent the complete dynamics of the particles anywhere along the length of the fluid film. Dividing Eq. (5) by Eq. (19) and rearranging, we have:

$$e^{mz_p}\, dz_p = -\frac{\rho_f g \cos\beta}{2\mu V_T}(2\delta x_p - x_p^2)\, dx_p$$

Integrating this equation between the entry point and the point where the particle gets deposited on the slide (that is, x_p, from x_o to 0; z_p, from 0 to z_p).

$$\frac{1}{m}(e^{mz_p} - 1) = \frac{\rho_f g \cos\beta}{2\mu V_T}(\delta x_p^2 - x_p^3/3)$$

From this equation, the location of the particle, z_p, is

$$z_p = \frac{1}{m}\ln\left\{1 + m \cdot \frac{\rho_f g \cos\beta}{2\mu V_T}(\delta x_p^2 - x_p^3/3)\right\} \qquad (20)$$

Eq. (20) is similar to Eq. (16), except that it includes the effect of the variation of magnetic properties along the length of the slide. Note that z_p in the above equation is the location of a magnetic particle on the slide in an idealized situation, presented in the beginning of the paper.

The purpose of the derivation of the above equation was solely to demonstrate the effect of the variation of magnetic forces on particle deposition rather than absolute evaluation. Eq. (20) clearly indicates that the effect of increasing magnetic gradient along the exit end of the Ferrogram is to deposit the larger size particles as close as possible to the entry location. It is seen that the effect of various parameters like x_o, μ, Q, etc., are masked by the equation because of the logarithmic function; however, this need not be true in general. This is because, firstly, in the case of bigger particles, Eq. (16) gives the correct picture of z_p since they are deposited near the entry. Secondly, smaller particles get saturated magnetically as they have only one or at best few magnetic domains [2, 17]. Accordingly, Eq. (16) should be valid for any magnetic particle in the sample fluid. Hence, it could be stated that the effect of variation in the magnetic properties, H (dH/dx), of particles is to confine larger size magnetic particles to the upper region of the Ferrogram. And finally, in the case of particles less than 0.1 μm in size, Brownian motions may become effective and the particles will disobey the equations derived earlier. The Ferrograph does not give full information about such particles (for whatever they are worth) as would be given by a spectrometric analysis.

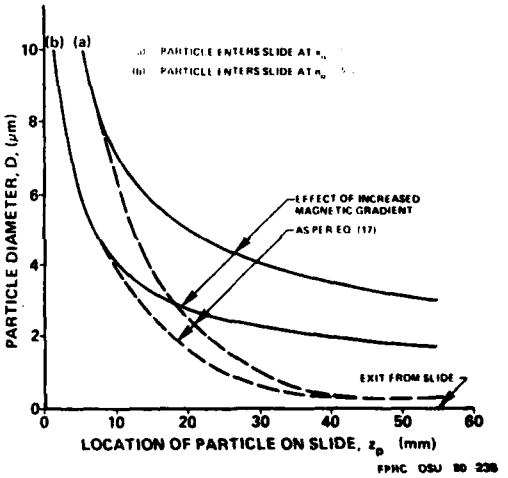

Fig. 7. Particle Diameter Versus Location on Slide.

Eq. (17) indicates that, with a given fluid sample, it is possible to predict the location of deposition of a known

particle if the parameter, x_o (the height at which the particle enters the slide), is kept constant. In such a case, other parameters remaining constant, the location of the particle is inversely proportional to the square of the particle diameter, D. Fig. 7 shows a graph reflecting this relation. The angle of inclination, β, to the vertical is of the order of about 88°. A change in this value due to improper leveling of the equipment or due to incorrect fixing of a slide (by the locking pin provided on the Ferrograph) could affect the reading, though not too drastically.

The strongest parameter which affects the location on the Ferrogram of a particle of given diameter turns out to be the position of the particle, x_o, above the slide as it enters the Ferrogram. This needs further elaboration. Eq. (16) which gives the position of the particle on the Ferrogram can be used to demonstrate the effect of x_o on that position. This is illustrated below.

Representative values of the various parameters in Eq. (16) are computed or assumed as follows:

Fluid density: $\rho_f = 0.8$ gm/cc
Acceleration due to gravity: $g = 980$ cm^2/sec
Cosine of the inclination of slide with respect to vertical: $\cos\beta = 0.03$
Viscosity: $\mu = 0.2$ poise (MIL-H-5606 fluid)
Flow rate: $Q = 0.01$ cm^3/sec
Width of U-boundary: $W = 0.45$ cm

The value of the fluid film height, δ, is evaluated as follows from Eq. (3).

$$\delta = \left| \frac{3\mu Q}{\rho_f\, g\, \cos\beta} \right|^{1/3}$$

Substituting the various values into the above equation yields

$$\delta = \frac{3\times(.2)\times(0.01)}{(0.8)\times(980)\times(0.45)\times(0.03)}$$

$$= 0.083\ \text{cm}$$

If we consider a particle of diameter 15 μm (that is, D = 15 μm), then the only other parameter required in Eq. (16) is the settling velocity, V_T, of the particle. Settling velocity is given by Eq. (11) in which the magnetic term, KH (dH/dx), is unknown. Hence, an approximate evaluation of settling velocity must be performed.

The average velocity of fluid flow is given by Eq. (4). Substituting various values given above into Eq. (4)

$$U_z(\text{ave}) = \frac{(0.8)\,(980)\,(0.083^2)\times(0.03)}{3\times(0.2)}$$

$$= 0.27\ \text{cm/sec}$$

If it is assumed that the magnetic particle of 15 μm diameter gets deposited within the first 5 mm of its travel on the slide, then the time for which it travels in the fluid is given by:

$$\text{Time of travel} = \frac{\text{distance traveled in cm}}{\text{average velocity in cm/sec}}$$

$$= \frac{0.5}{0.27}$$

$$= 1.85 \text{ seconds}$$

If the particle enters the slide at top of the film height (that is, $x_o = \delta$), then the settling velocity is:

$$\text{Settling velocity, } V_T = \frac{\text{film height } \delta}{\text{time to travel the distance}}$$

$$= \frac{0.083 \text{ cm}}{1.85 \text{ sec}}$$

$$= 0.045 \text{ cm/sec}$$

An alternate method to find settling velocity is to use Eq. (18) in which the value of the magnetic term, KH (dH/dx) evaluated for deriving this equation is used. This value was: KH (dH/dx) = 1.25×10^5 dynes/cc.

Using Eq. (18), settling velocity, V_T, is:

$$V_T = \frac{D^2 KH \frac{dH}{dx}}{18\mu}$$

$$= \frac{(15\times10^{-4})^2\ \text{cm}^2\ (1.25\times10^5 \text{gcm}^{-2}\text{sec}^{-2})}{18\times(0.2\ \text{gm cm}^{-1}\text{sec}^{-1})}$$

$$= 0.078\ \text{cm/sec}$$

Clearly, the value of settling velocity, V_T, obtained by this method is more than the value obtained using the average velocity. Since the exact value of KH (dH/dx) is unknown, the value of settling velocity as 0.045 cm/sec will be used for illustration purposes.

To demonstrate the effect of the initial position of the particle, the various values evaluated above are substituted into Eq. (16). Eq. (16) can be normalized in terms of film height, δ, as given below:

$$z_p = \frac{\rho_f\, g\, \cos\beta\, \delta^3}{2\mu V_T} \left| \left(\frac{x_o}{\delta}\right)^2 - \frac{1}{3}\left(\frac{x_o}{\delta}\right)^3 \right| \quad (21)$$

Substituting various values into Eq. (21) yields,

$$z_p = \frac{(0.8)(980)(0.03)(0.083)^3}{2(0.2)(0.045)} \left[\left(\frac{x_o}{\delta}\right)^2 - \frac{1}{3}\left(\frac{x_o}{\delta}\right)^3 \right]$$

$$= 0.75 \left[\left(\frac{x_o}{\delta}\right)^2 - \frac{1}{3}\left(\frac{x_o}{\delta}\right)^3 \right] \quad (22)$$

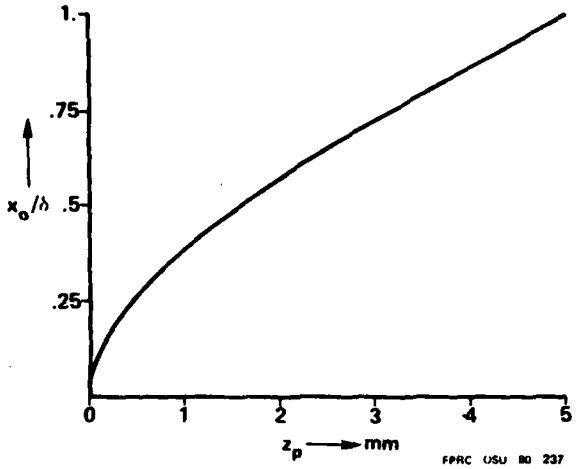

Fig. 8. Effect of Initial Position of Particle, X_o, on Final Deposit Location, z_p (For Large Particles).

Thus, if the particle enters the slide at the top of the falling film, that is, $x_o/\delta = 1$, then $z_p = 0.5$ cm or 5 mm from the point of entry on the slide. The variation of z_p as a function of x_o is given in Fig. 8. From the figure, it is seen that a particle may be deposited anywhere on the length of 5 mm, depending upon its initial position, x_o. It is also seen that if equal probability is assigned to a particle to have its location, x_o, then 50% of the particles in the sample ($x_o/\delta \leq 0.5$) get deposited within 20% of its maximum possible travel. This explains why a large deposit of larger particles is always observed at the entry point. Thus, it appears that the location of a particle on the Ferrogram is strongly affected by its initial height above the slide. However, as mentioned earlier, the effect of the increasing magnetic field gradient is to force the particle not to travel farther from the near-entry region, especially in case of larger particles. In the case of smaller particles, if they are magnets by virtue of their few domains, they may get deposited anywhere on the Ferrogram, scattered over a larger length of the slide.

The foregoing section demonstrated that the initial location of the particle as it enters the slide has a strong influence over the final location of the particle on the Ferrogram. This, in turn, affects the other analytical results in terms of optical density readings. The next section covers the optical density readings as affected by the Ferrographic process discussed so far.

OPTICAL DENSITY READINGS

The primary tool for quantitative and fast assessment of the wear situation is measuring the optical density on the slide [1, 2]. The optical density reading is essentially a function of the percent area covered by the wear particle deposited on a specific location on the slide and is measured by the amount of light blocked by the wear particles in the aperture of the optical densitometer. Details regarding these optical methods are available elsewhere and are not discussed in this paper. The primary interest here is how the modeling discussed above affects the density readings in terms of particle deposition.

A fluid sample used in the Ferrographic process contains different sizes of particles and, as has been seen earlier, they can get deposited in a random fashion as illustrated in Fig. 8. The statistical nature of the deposition of particles renders the analysis difficult. However, an analytical expression can be derived for the density readings to identify and investigate the effect of deposition of the particles as given by Eq. (16).

Let there be n_1 particles of diameter D_1, n_2 particles of diameter D_2, etc., so that the total number of particles, n, is:

$$n = \sum_{i=1}^{k} n_i \tag{23}$$

where: k = the total number of different particle sizes in the sample.

Location of these magnetic particles on the slide is governed by Eq. (21). As given by Eq. (16) for a given fluid sample, the parameters which control the location of the particles are its initial position at then entry, x_o, and the settling velocity, V_T. Settling velocity is, in turn, controlled by the daimeter, D, and density, ρ_p, of the particle. If the analysis is restricted to particles of the same material, say, ferrous particles, then Eq. (16) and (17) can be presented as:

$$z_p = \frac{9\rho_f g \delta^3 \cos\beta \left[\left(\frac{x_o}{\delta}\right)^2 - \frac{1}{3}\left(\frac{x_o}{\delta}\right)^3 \right]}{D^2 \left[g(\rho_p - \rho_f) + KH \frac{dH}{dx} \right]}$$

$$= \frac{A}{D^2}\left[\left(\frac{x_o}{\delta}\right)^2 - \frac{1}{3}\left(\frac{x_o}{\delta}\right)^3 \right] \tag{24}$$

where:

$$A = \frac{9\rho_f g \delta^3 \cos\beta}{g(\rho_p - \rho_f) + KH \frac{dH}{dx}}$$

A is a constant of the Analytical Ferrogram for a given fluid and material of the particle.

Eq. (24) shows that, in an ideal case, a particle of given diameter gets deposited from entry point to a maximum distance of $(2/3)A\delta^3/D^2$ from the entry point. This maximum distance is achieved when the particle enters the slide at the maximum film height, that is, $x_o = \delta$. It was shown earlier that 50% of the particles would get deposited in 20% of its maximum possible distance as described above. If the diameter of the various n_i particles in the fluid sample as given by

Eq. (23) is D_1, D_2 . . . (so that there are n_1 particles of D_1 diameter, n_2 particles of D_2 diameter, etc.), then each size particle will get deposited on the slide within a specified maximum distance corresponding to that size, as given by Eq. (24). Fig. 9 shows an illustration of this situation. Alternately, it can be said that a given location on the slide would consist of different types of particles and number of particles of each size for that location, decreasing as the particle size decreases. It should be noted that this conclusion is based on the assumption that the particles have equal probability to occupy the initial position x_o at the entry position as they enter the slide.

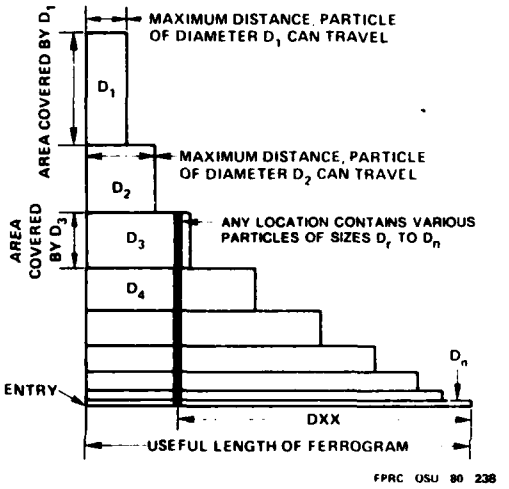

Fig. 9. Maximum Particle-Travel and Its Effect On Area Covered.

Optical density readings are taken at a specified location on the slide, say, the point upstream 54 mm from exit end (designated as D54). Density readings correspond to the area covered by the particles in the aperture of the densitometer (normally 1-mm diameter). For a 1-mm length of the Ferrogram slide along the direction of the flow, then the aperture of the densitometer corresponds to this length by the following relation:

$$\frac{\pi}{4}\,\frac{(dz_p)}{b} \qquad (25)$$

where: dz_p = the 1-mm length considered along the length of the Ferrogram where density readings are taken, and b = the width of the Ferrogram deposit measured laterally.

Fig. 10 shows how this area is represented. Also shown in Fig. 10 is how particles of various diameters form trajectories to get deposited in this particular location as given by Eq. (24). From Fig. 10, it can be seen that a particle of diameter D_1 should enter the slide within a certain specified band of height, dx_{o1}.

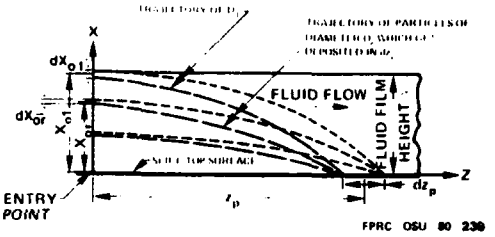

Fig. 10a. Particle Deposition at Any Location. At a Location dz_p, Any Particle of Diameter D_r Can Get Deposited, If They Enter the Slide Within a Band of Height dxo_1.

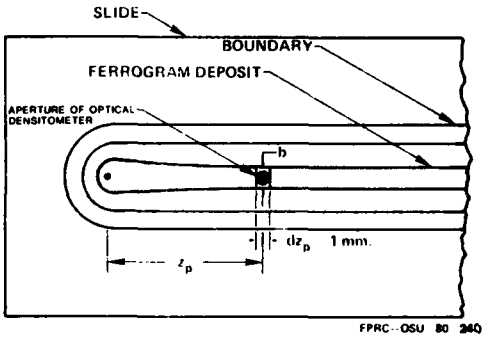

Fig. 10b. Measurement of Area Covered by Densitometer. Area Covered by Aperture = (π/4) (Area Covered in dz_p/b).

above the slide if it is to be deposited within the 1-mm distance selected. Similarly, another particle of diameter D_2 would take another band of height dx_{o2}. This value can be evaluated by differentiating Eq. (24) and setting dz_p = 1 mm or 0.1 cm, that is,

$$dz_p = \frac{A}{\delta^3 D^2}\,(2\delta x_o - x_o^2)\,dx_o \qquad (26)$$

or

$$dx_o = \frac{\delta^3 D^2 dz_p}{A(2\delta x_o - x_o^2)}$$

Consequently,

$$dx_{oi} = \frac{\delta^3 D_i^2 dz_p}{A(2\delta x_o - x_{oi}^2)} \qquad (27)$$

where: $i = \gamma$ to k gives the different particle diameters that could get deposited in the specified location.

In Eq. (27), dz_p is the length of 0.1 cm at a specified location z_p (for example, 54 mm from exit end of Ferrogram). In this equation, x_{oi} should be evaluated for the given location z_p using Eq. (24). This involves

the solution of a cubic equation in x_o and hence is tedious. An approximate method is to linearize Eq. (24). It was shown earlier that 50% of the particles which happen to arrive at the bottom half of the film height at entry (that is, $x_o/\delta < 0.5$) get deposited within 20% of the maximum distance a particle can travel. For example, 50% of 15 μm particles will get deposited within 1 mm of its entry, if the maximum distance such a particle can travel is 5 mm. If a particle can travel a maximum of 50 mm in the fluid before getting deposited (that is, when it enters the slide at maximum height, $x_o = \delta$), then 50% of those particles get deposited approximately in the first 20 mm on the slide. However, their contribution to the optical density readings could logically be assumed to be negligible due to their scatter in location and lesser diameter. Consequently, it can be assumed that the particle which enters the top half of the film height contributes more to the optical density readings. Strictly, this assumption will be more valid in a severe wear situation, when the number of larger particles is greater. Accordingly, Eq. (24) can be approximated as:

$$z_p = \frac{A}{D^2}\left(\frac{x_o}{\delta} - 0.31\right), \frac{x_o}{\delta} > 0.5 \qquad (28)$$

In the general case,

$$z_p = \frac{A}{D_i^2}\left(\frac{x_{oi}}{\delta} - 0.31\right) \qquad (28a)$$

where: z_p = the location where density readings are taken (say, D54).

From this equation,

$$x_{oi} = \delta\left(\frac{D_i^2}{A} z_p + 0.31\right)$$

Differentiation of this equation yields

$$dx_{oi} = \frac{\delta D_i^2}{A} dz_p \qquad (29)$$

where: dz_p = the length 0.1 cm at location z_p where density readings are taken, and dx_{oi} = the band of height at entry from where particles could travel to within the length dz_p.

If equal probability is assigned to n_i particles of diameter D_i in the sample liquid to enter at any height x_{oi}, then the number of particles which enters the band of height dx_{oi}, designated as P_i, is

$$P_i = \frac{(dx_{oi})}{\delta} n_i$$

Substituting for dx_{oi} from Eq. (29) in the above equation yields

$$P_i = \frac{D_i^2}{A} n_i \, dz_p \qquad (30)$$

If there is no overlapping of the deposited particles on the Ferrogram, then the area covered, S, by these particles is given by:

$$S = P_i \frac{\pi D_i^2}{4}$$

Substituting for P_i from Eq. (30) gives

$$S = \frac{\pi}{4A} D_i^4 \, n_i \, dz_p$$

Total area covered by all the particles of different diameters in the particular location selected is

$$S_t = \sum_{i=\gamma}^{k} \frac{\pi}{4A} D_i^4 \, n_i \, dz_p \qquad (31)$$

where: S_t = total area covered by the particles in location selected for optical density reading, D_i = the particle diameter, n_i = the number of particles of diameter D_i, and dz_p = 0.1 cm corresponds to aperture of the densitometer.

If the particles are deposited uniformly in the width, b, of the Ferrogram deposit, then the area covered under the densitometer will be:

$$S_o = \frac{\pi}{4} \frac{S_t}{b}$$

$$= \frac{\pi^2}{16Ab} \sum_{i=\gamma}^{k} D_i^4 \, n_i \, (dz_p) \qquad (32)$$

where: S_o = the area covered by the particles in the aperature of the optical densitometer.

At a given location away from the entry region (say, D30), the maximum size of the particle which can be deposited is again governed by Eq. (24). So in finding the total area covered by particles as given by Eq. (32), only those particles which can get deposited there should be considered instead of all sizes of particles. In other words, the suffix "i" in Eq. (32) varies from some intermediate number γ to k instead of 1 to k like in the near-entry region.

Eq. (32) indicates that the optical density readings are directly proportional to the number of particles and to the fourth power of diameter of the particles. Thus, in a severe wear process, when large particles are greater in number, the influence of small particles near the entry region (D54, D50, etc.) is insignificant. This makes Ferrography a powerful tool in analyzing a serious wear situation.

From the foregoing modeling of the Ferrogram, it could be stated that optical density readings near the entry are the most accurately measureable quantity since the diameter of the particles is larger and the trajectory of the particles is smaller. From experience at the Fluid Power Research Center at Oklahoma State University, the position D54 has been found to be the best location for taking a fairly accurate density reading.

This position avoids the entry deposit congestion and the high statistical dispersion towards the exit end. The measurement of D50 is subjected to more scatter than D54. In any case, an average of three readings, including two other close locations on either side of the desired location, could be used to identify the corresponding optical density readings. Density readings at the lower end of the Ferrogram are subject to high statistical variations which diminish their usefulness.

VARIATION FROM IDEAL FERROGRAPHIC PROCESS

So far the Ferrographic process has been analyzed considering it as an ideal case. In an actual situation, a number of parameters are uncontrollable. For example, wear particles are rarely spherical. Magnetic particles interact with one another and, accordingly, the analytical concept presented on an individual particle basis needs realistic interpretation. Variations from ideal assumptions and their effect on the process will now be discussed.

Flow Properties

The flow, as it enters the slide, is not fully developed laminar flow. In this unsteady condition, particles which move downward due to the momentum of entering fluid, may not move up towards the fluid surface even if the fluid has a component velocity in that direction. This is due to the opposition from the magnetic forces. The result could be that the lower portion of the film height can have a higher particle density than the higher portion. This would tend to change the particle deposition nearer the entry location.

Magnetic Properties

The magnet used in the Ferrograph uses a high gradient field to obtain sufficient forces to attract the particles. The force on the particle is governed by Eq. (8). Apart from the volume of the particle, the other parameters are the volume susceptibility of the material of the particle (K), field intensity (H), and the rate of change of field strength with respect to vertical distance (dH/dx). The value of susceptibility is dependent on the field intensity (H), composition of the particle, mechanical process and residual stress during the wearing operations, etc. [17]. The permeability and hence volume susceptibility of the material (permeability, $\mu = (K - 1)/(4\pi)$ in C. G. S. units) is found to change with aging and thermal cycling. The particles in a sample kept for long periods may have a decreased permeability. An iron particle, for example, with all the effects mentioned above, may have its susceptibility changed by a factor of more than 100%. In such a case, density readings near the entry region of the Ferrogram may be subject to variations.

One of the methods to produce a high gradient field is to introduce small magnetic material in a magnetic field [20, 21, 22]. The higher gradient produced near this magnetic material is used to trap other smaller particles in a flowing fluid. Based on this, it is reasonable to expect that, in a Ferrogram, larger size particles "catch hold" of smaller particles. However, such "togetherness" may not affect the density readings appreciably.

Spherical particles as in "fatigue wear" and plate-like particles as in normal wear form strings or flux patterns in the direction of magnetic field, as seen on a Ferrogram. It could be assumed that the strings are formed while the particles are travelling in the fluid where they have more mobility. This could result in a higher equivalent diameter of the particle and may amount to an increased settling velocity and a forward speed which is lagging behind the fluid velocity [25]. The net result would be for the string of particles to settle earlier on the slide. In the case of spherical particles [25], they can move on the Ferrograph due to the slightest fluid disturbance and due to the component of magnetic forces on the forward direction of motion. In case of rolling fatigue wear particles, density readings could be affected by this movement of particles over the slide. Formation of strings could be expected to reduce this effect. However, since particles can form layers when they are in strings, this could alter the density readings at a given location.

Effect of Shape of the Particles

Particles exhibiting a flaky or plate-like shape, when they settle under the influence of magnetic or gravitational forces, can experience a change in drag forces by a ratio of three or four times if they fall on the edge. Irregularly shaped particles like large chunks or curled, propeller-type particles with random shape as developed in cutting wear processes would rotate as they travel in the fluid [26] and may show more drag than otherwise possible. They could settle in any fashion on the Ferrogram since hydrodynamic forces would be a predominant factor and they could travel well beyond the entry location. In general, non-spherical particles exhibit more drag and such particles settle at locations further downstream than if they were spherical in shape.

Effect of Fluid Flow and Viscosity

Viscosity of the fluid samples used in Ferrographic analysis cannot be standardized to a constant value due to the wide variety of fluids in systems of interest. Also, in preparing the sample for running a Ferrogram, dirty oil from the machine is mixed with a solution primarily to obtain a uniform distribution of particles in the sample. Such solutions added tend to reduce the viscosity of the sample drastically. Thus, it is worthwhile to investigate the effect of viscosity on the density readings.

Eq. (32) was shown to be representing the area covered by the particles at a given location. In this equation, the constant of an Analytical Ferrogram, A, is given by Eq. (24).

$$A = \frac{9\rho_f g \delta^3 \cos\beta}{g(\rho_p - \rho_f) + KH\frac{dH}{dx}}$$

Substituting for δ^3 from Eq. (3),

$$A = \frac{27\mu Q}{w\left[g(\rho_p - \rho_f) + KH\frac{dH}{dx}\right]}$$

Substituting the value of A into Eq. (32) yields the area covered by particles in the aperture of the densitometer, S_o, as

$$S_o = \left(\frac{1}{\mu Q}\right)\frac{\pi^2 w}{432b}\left[g(\rho_p - \rho_f) + KH\frac{dH}{dx}\right]\sum_{i=r}^{k} D_i^4 n_i (dz_p) \quad (33)$$

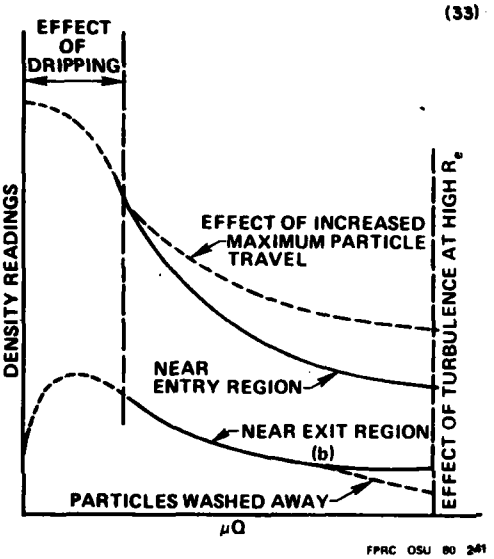

Fig. 11. Effect of μQ on Density Readings. At Near Entry Region, As μQ Increases, Higher Size Particles Start Arriving, Which Otherwise, Were Constrained to Upstream Location. See Eq. (33).

If an experiment is conducted with particle distribution and sizes known, it appears from Eq. (33) that the area covered and, hence, the optical density is inversely proportional to μQ. Anywhere along the Ferrogram, where H (dH/dx) is higher (say, beyond 20-25 mm from exit), the variation in μQ will not have an appreciable effect on density readings, since the particles are magnetically saturated. Hence, the locations mostly affected by changes in viscosity and flow are the few millimetres from the entry point. Fig. 11 shows the effect of μQ on the density readings at various locations on the Ferrogram. The nature of the curve is, however, strongly affected by the particle distribution in the sample. When a combination of various sizes and numbers of particles is present in the sample, the area covered will still be controlled by the largest particles and, hence, the above arguments hold good. It follows that in a severe wear process when the viscosity is low, as in some hydraulic fluids (for example, MIL-H-5606), the particle deposits are subjected to less scatter and readings at the D54 and D50 points will be more accurate. When experiments are conducted with different fluids, the total areas covered over a certain initial length, say, first 10 mm from entry, could be selected for comparison purposes. When the viscosity increases, flow through the peristaltic pump decreases. If these changes are small, it could be assumed that μQ remains constant. Hence such changes need not be considered.

When the viscosity is low, however, the flow Reynolds number would increase and, consequently, there would be more disturbance at the entry region. This causes the entry and D54 readings to increase and D50 or lower readings to be reduced. In this respect, the dilution of less viscous oil with solvent could cause problems. A qualitative assessment of this situation is difficult due to the random nature of the motion of the particles in the initial entry location.

Effect of Delivery Tube

The fluid sample is delivered to the slide through a tube of about 1.5-millimetres diameter which is fixed to a turret tube arm. It is reasonable to believe that the position of the fluid exit from the tube has a strong influence over the "quality" of the Ferrogram. If the pipe end is not touching the fluid flowing over the slide, fluid may drip onto the slide and the flow will be unsettled in the initial region of the slide. If the pipe end is immersed in the fluid, or "just touching" the slide, the initial value of x_o for the particles in the fluid is small. Subsequently, a higher density reading at the entry and D54 could be expected. Further, due to low velocity of fluid near the tube wall, the entry deposit would be more in the periphery region of the tube, primarily towards the U-end of the slide. If a bevelled edge is used at the tube end, then one large entry deposit near the U-end and a statistical distribution of the initial height of the particles could be the result. Further experiments are necessary to determine whether an optimum tube configuration and a method for a controlled particle entry are possible.

Effect of Sample Volume and Concentration

From an ideal Ferrogram point of view, sample volume and particle concentration have no effect on the location of the deposition of a particle on the slide. However, a large concentration or uneven distribution of particles in the sample promotes particle agglomeration and subsequent deposition at an earlier location on a Ferrogram. They may decrease the density of the Ferrogram by forming layers and by a shift of position. Increasing the concentration or sample volume further may make the densitometer reading saturate due to the property of the instrument [27]; hence, the volume of the sample is adjusted by diluting the fluid so that the density reading is in between 10 and 40. Details regarding the densitometer and its functioning are available in Ref. [1, 2, 9].

DISCUSSION

It has been pointed out that there are a number of variables associated with the flow particles in the fluid film. It has been mentioned that the position near D54 would be the best position (based on experiments men-

tioned in references and based on the theory presented here) for a quantitative appraisal in terms of density readings. D50 readings are subjected to more scatter than D54. However, when the wear situation becomes critical, particle size and number increase and, accordingly, the density readings. A definite relation between the increase in density readings and particle concentration is difficult to predict. But, based on the increased density readings, the wear situation can be assessed. Qualitative examination by means of optical and electron microscopes and other methods, like heating the Ferrogram for identification of particles, etc., would further expand the study of wear phenomena. Further, if a method to control the initial positon of the particle on the Ferrogram could be devised, that would help decrease the scatter of density readings.

It may be worthwhile to investigate the degradation rate of the magnet used in the Ferrograph. It is possible that there may be "aging" of the magnetic material as a function of time, especially if it is subjected to temperature variations. Handling of the equipment has to be extremely careful in that if a weight or other objects accidently fall on the magnet, its magnetism may deteriorate. In any such circumstance, it should be noted to ensure that density readings at a location are not affected by the magnet.

In view of the scatter possible on the density readings, the concept of Severity Index poses some problem. Severity Index (I_S) as proposed in Ref. [29] is given by:

$$I_S = A_L^2 - A_s^2$$

where: A_L and A_s are the percent area covered at 54 and 50 mm from the exit end, respectively.

Considering the scatter in density readings, as the state-of-the-art of Ferrography stands today, it seems more reasonable to have a Severity Index which integrates all density readings in between a certain distance over the Ferrogram (say, from D50 to entry) with due weighting for near entry locations. Such an index can be represented as:

$$I_S = \sum_{D50}^{entry} (Dxx)\ell$$

where:

$$\ell = xx - 49$$

For example, at 53 mm from exit, ℓ would be 53 - 49 = 4. Such a description of Severity Index will tend to nulify the effect of scatter in density readings.

CONCLUSION

A detailed analysis of the physics of an Analytical Ferrograph was presented in this paper. Various factors affecting the density readings in a Ferrogram were discussed. A different Severity Index approach was suggested.

Ferrography remains the best method available for wear debris analysis in spite of the various factors involved for its efficient operation. Development of a new method to control the initial position of the particle in the falling film has the best promise in reducing the scatter and making Ferrography more of a science than an art.

* * *

REFERENCES

1. Scott, D., et al., "*Ferrography An Advanced Design Aid for the 80's,*" Wear 34, 1975, pp. 251-260.

2. Seifert, W. W., and V. C. Westcott, "*A Method for the Study of Wear Particles in Lubricating Oil,*" Wear 21, 1972.

3. Westcott, V. C., "*The Investigation and Interpretation of the Nature of Wear Particles,*" Trans-Sonics, Inc., Prepared for the Office of Naval Research, 1974.

4. Jones, W. R., et al., "*Ferrographic Analysis of Wear Debris Generated in a Sliding Elastohydrodynamic Contact,*" NASA.

5. Hofman, M. V., and J. H. Johnson, "*The Development of Ferrography as a Laboratory Wear Measurement Method for the Study of Engine Operating Conditions on Diesel Engine Wear,*" Wear 44, 1977, pp. 183-189.

6. Tessmann, R. K., "*Monitoring Wear in Hydraulic Systems,*" Presented at the International Conference on Fundamentals of Tribology, MIT, Cambridge, Mass., June 1978.

7. Smith, R. J., and R. K. Tessmann, "*The Magnitude of Wear Debris Generation in Hydraulic Systems of Mobile Equipment,*" The BFPR Journal, Vol. 12, No. 2, 1979, pp. 163-168.

8. Tessmann, R. K., "*Non-Intrusive Analysis of Contaminant Wear in Gear Pumps through Ferrography,*" Ph.D. Thesis, Mechanical Engineering Dept., Oklahoma State University, Stillwater, Okla., 1977.

9. Kitzmiller, D. E., "*The Development of a Calibration Technique and Standard Operating Procedures for a Ferrograph,*" M.S. Thesis, Oklahoma State University, Stillwater, Okla., 1977.

10. "*Sample Preparation / Ferrogram Procedure / Ferrogram Analysis,*" Naval Air Engineering Center, Tribology Laboratory, September 1978.

11. Ruff, A. W., "*Study of Initial Stages of Wear by Electron Channeling - Part 2: Quantitative Methods on Wear Debris Analysis,*" Institute of Material Research, National Bureau of Standards Report No. NBSIR 76-1141, September 1976.

12. Hofman, M. V., and J. H. Johnson, *"The Development and Application of Ferrography to the Study of Diesel Engine Wear,"* SAE Paper No. 70181, Presented at the Congress and Exposition, Detroit, Mich., February-March 1978.

13. Towell, G. D., and L. B. Rothfeld, *"Hydrodynamics of Rivulet Flow,"* A. I. Ch. E. Journal, September 1966, pp. 972.

14. Bird, R. B., et al., *"Transport Phenomena,"* John Wiley & Sons, Inc., 1960, pp. 2.2-1.

15. Giles, R. V., *"Fluid Mechanics and Hydraulics,"* 2nd Edition, Schaum Publishing Company, 1962, pp. 164.

16. Taggart, A. F., *"Handbook of Mineral Dressing Ores and and Industrial Minerals Ch. 13,"* John Wiley & Sons, Inc., 1945.

17. Bozorth, R. M., *"Ferromagnetism Ch. 19,"* D. Van Nostrand Co., Inc., 1951.

18. Luborsky, F. E., *"High Field-High Gradient Magnetic Separation: A Review,"* 21st Annual Conference on Magnetism and Magnetic Materials, Philadelphia, 1975.

19. Barrett, W. T., et al., *"Rapid Method of Evaluating Magnetic Separator Force Patterns,"* Transactions of the Society of Mining Engineers, AIME, Vol. 247, September 1970, p. 231.

20. Gardini, A., et al., *"Magnetic Filter for Small Particles,"* Nuclear Engineering and Design 1, North Holland Publishing Co., Amsterdam, 1967.

21. Watson, J. H. P., *"Magnetic Filtration,"* Journal of Applied Physics, Vol. 44, No. 9, September 1973.

22. Oberteufter, *"High Gradient Magnetic Separation,"* IEEE Transactions on Magnetics, September 1973.

23. Oberteufter, J. A., *"Magnetic Separation: A Review of Principles, Devices and Applications,"* IEEE Transactions on Magnetics, Vol. MAG-10, No. 2, June 1974.

24. Miller, R. S., Lt., U.S. Navy, Office of Naval Research, Discussions During the Paper by M. B. Peterson, et al., *"Wear Control,"* Progress in Tribology Workshop, Report No. PB-2412-53, April 1974.

25. Parsons, D. A., *"Speed of Sand Grains in Laminar Flow Over a Smooth Bed,"* Sedimentation, Published by Hsieh Wen Shen, Prof. of Civil Engineering, Colorado State University, 1972, pp. 1-1.

26. Happel, J., and H. Brenner, *"Low Reynolds Number Hydrodynamics,"* Noordnoff International Publishing, Leyden, 1965.

27. Kitzmiller, D. E., and R. K. Tessmann, *"The Capabilities and Limitations of Ferrographic Wear Analysis,"* The BFPR Journal, 1978, Vol. 11, No. 1, pp. 87-94.

28. Hofman, M. V., and J. H. Johnson, *"Development of Ferrography as a Laboratory Wear Measurement Method for the Study of Engine Operating Conditions on Diesel Engine Wear,"* Wear 44, 1977, pp. 183-189.

* * *

APPENDIX–FLOW REYNOLDS NUMBER

The model developed in the paper was derived on the assumption that laminar ripple free flow existed. The flow will be ripple free laminar, if the Reynolds number is less than 4. (According to Ref. [14], flow is ripple free laminar when Reynolds number is less than 4-25.)

Reynolds number, R_e, is given by [14],

$$R_e = \frac{4\delta U_z(ave) \cdot \rho_f}{\mu}$$

where: δ = the maximum film height as given by Eq. (3), ρ_f = the fluid density, μ = the fluid viscosity, and $U_z(ave)$ is given by Eq. (4).

Substituting for δ and $U_z(ave)$ from Eq. (3) and (4), respectively, into the above equation,

$$R_e = \frac{4\rho_f Q}{\mu}$$

The following values are assumed for the variables in the above equation.

$Q = 0.01$ cc/sec
$\rho_f = 1$ gm/cc
$\mu = 0.01$ poise

The value of Q selected is higher than normally occurring in the Ferrograph. ρ_f and μ are that of water, so that these values give a conservatively high Reynolds number. Substituting these values into the equation for R_e,

$$R_e = \frac{4(1)(.01)}{(.01)} = 4$$

As stated at the beginning of the Appendix, when the Reynolds number is around 4, the flow over the Ferrogram is ripple free laminar.

* * *

APPENDIX B

An Appraisal of the Direct Reading (DR) Ferrograph

AN APPRAISAL OF THE DIRECT READING (DR) FERROGRAPH

K. Nair Editorial Managers: E. C. Fitch & R. K. Tessmann *A Research Documentary*

REFERENCE: Nair, K., "An Appraisal of the Direct Reading (DR) Ferrograph," The BFPR Journal, 1980, 13:319-328.

ABSTRACT: The Direct Reading (DR) Ferrograph was initially conceived as a means for screening fluid samples in order to identify those which should be studied by the Analytical (glass slide) Ferrogram. In practice, the DR unit has been plagued with a host of operational problems and an indepth analysis of its future potential was deemed necessary.

This paper represents the results of a significant effort at the FPRC to give an unbiased appraisal of the DR system. To maintain an unbiased posture, a mathematical model of an idealized unit was formulated. Based upon this model and various considerations of non-ideal conditions, an insight was gained with direction for improvements which could not be garnered by any other way. This paper represents the full report of the study.

KEY WORDS: Direct Reading (DR) Ferrograph, influencing parameters, mathematical model, analytical readings, wear prediction

INTRODUCTION

Monitoring lubricating oil for wear particles has been accepted as a realistic and economic nondestructive method for diagnosis and prediction of machine malfunction [1, 2]. Among the many methods available, the Direct Reading (DR) Ferrograph, developed by Trans-Sonics, Inc., provides rapid monitoring of wear without the need for time-consuming analytical procedures [3]. In operation, the DR Ferrograph magnetically precipitates the wear particles from a representative fluid sample and provides digital readings of both large (> 5 μm) and small (1 to 2 μm) particles present in the fluid. These numerical readings and their relative values indicate the condition of the wearing machine. When the DR Ferrograph indicates an abnormal wear situation, detailed analysis for size, shape and material of the wear particles can be done on an Analytical Ferrograph [4].

Fig. 1 shows a schematic diagram of the DR Ferrograph. Sample oil in the vial flows under gravity (by siphoning) through a precipitator tube. Magnetic wear particles are deposited on the bottom wall of the tube under the action of a high gradient magnet. The particles are deposited on the tube according to their size with larger particles near the entry side of the precipitator tube. Two fibre-optic sensors are provided in the equipment to measure the optical density readings. The first is located near the entry of the precipitator tube where large, L, particles (> 5 μm) are located, and the second beam crosses the tube where the smaller, S, particles (1 to 2 μm) are deposited. An electro-optical system senses the attenuation of light by the wear particles and indicates the attenuation in terms of DR units on a digital display. Fig. 2 gives a schematic of the optical system. Absolute and relative values of L and S are used to interpret the wear situation in the machinery. More information can be found on the system in Ref. [3, 5, 6, 7].

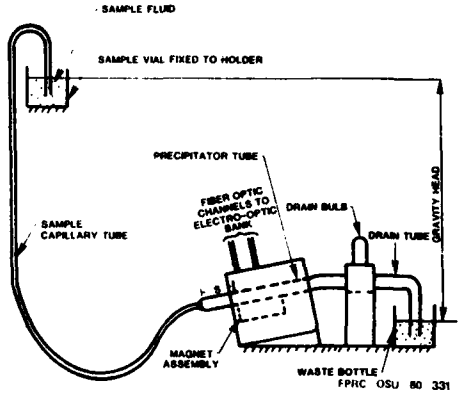

Fig. 1. Schematic Diagram of DR Ferrograph.

A great advantage of the DR Ferrograph is the speed and ease of analysis of a wear situation. Additionally, it requires little specialized training for operation. Prediction of incipient failure by the DR Ferrograph or decision to go for detailed analysis depends on the accuracy and reliability of the instrument. The Fluid Power Research Center at Oklahoma State University has used the DR Ferrograph for analyzing the wear in hydraulic systems since August, 1975. During this period, it was observed that large variations were present in the DR readings from the same sample. An analysis of this Ferrographic process will assist in defining the nature of

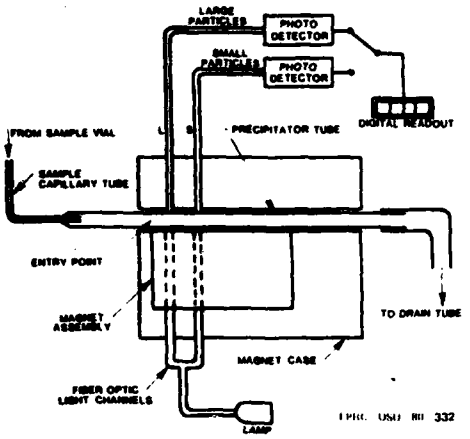

Fig. 2. Schematic of the Optical System.

the variation by identifying critical parameters which control the behavior of the analysis system.

Ref. [8] describes the effect of the fluid sample volume on DR readings. In this paper, an analytical approach to the DR Ferrographic process will be presented. Based on the model developed, discussions are advanced on the effect of various parameters on the DR readings and on improvements possible for reducing the scatter in the readings.

BASIC PROCESS OF THE DR FERROGRAPH

The basic DR Ferrographic process can be summarized as:

1. Preparation of sample.
2. Flowing the fluid through the precipitator tube.
3. Precipitation of particles under the action of a high gradient magnetic field.
4. Measurement of the density as DR units by the electro-optical system.

For the analysis presented here, it is assumed that the sample is prepared according to the procedure given in Ref. [5]. It is further assumed that the sample has a uniform and even distribution of particles and there is no agglomeration of particles. Normally, the "dirty fluid" from the system is mixed with a solvent solution to reduce viscosity and to reduce the agglomeration of particles. The solvent would further help in dissolving some of the unwanted contaminant of non-wear origin. The sampling process will not be discussed further in this paper. However, the flow process and the particle dynamics will be analyzed in detail and the effect of these parameters on the electro-optical system output, that is, DR readings, will be investigated.

BASIC ASSUMPTIONS

The following assumptions are made to derive the mathematical model. This leads to an idealized situation. Any deviation from the assumptions made and its effect on the Ferrographic process will be considered in detail.

- The fluid is Newtonian.
- The particles in the sample are spherical in shape.
- Particle concentration is low enough not to affect the fluid flow or its viscosity.
- The particles in the sample do not interact under the presence of the magnetic field.
- Brownian forces are negligible and the particle motion can be idealized based on fundamental fluid mechanics and magnetic properties.

The assumption that the particles are spherical in shape is far from reality. Effect of particle shape and size will be dealt with in detail in the discussion part of the paper.

MODEL OF FLUID FLOW

Sample fluid is siphoned through a capillary to the precipitator tube and then to the waste bottle through an exhaust tube. The flow of the fluid is normally about 5 cc/minute, but measurements have shown large flow variation. Since the flow is low, the Reynolds number is far less than 200 and, hence, it is laminar. For example, with MIL-H-5606 petroleum fluid, the Reynolds number, R_e, in the precipitator tube will be:

$$R_e = \frac{\rho_f d}{\mu}\left(\frac{Q}{A}\right) = \left[\frac{(0.8)\times 0.15}{0.1}\right]\left[\frac{5}{60\times\frac{(0.15)^2}{4}}\right] \approx 5.6$$

where: ρ_f = density of fluid = 0.8 gm/cc; d = diameter of the precipitator tube = 0.15 cm; Q = flow through the precipitator = 5 cc/minute; μ = viscosity of the sample fluid = 0.1 poise; and, A = area of the precipitator tube = $\pi d^2/4$.

In the capillary tube (internal diameter of the capillary is approximately 0.5 mm on the average), the Reynolds number would be about three times that in the precipitator tube. If we take into account the influence of solvent added to the fluid, assuming the same flow rate, Q, the Reynolds number would be double the value as mentioned earlier (assuming solvent reduces viscosity by half). In any case, the flow in the tube is a low Reynolds number laminar type.

The path of the fluid flow is shown in Fig. 1. It consists of a capillary tube section, precipitator tube and a delivery section. If the capillary tube is assumed to be circular in cross-section and uniform in diameter, then the flow under gravity through the system with the help of the Hagen-Poiseuille equation can be predicted. However, since the effect of losses at entrance and exit of the tube sections must be considered, this makes it a tedious effort to obtain an analytical expression. In principle, the system works like a Rankine visco-

meter [10] used to measure viscosity of fluids, with the major head loss being in the capillary portion of the flow path. Another parameter which controls the flow is the reduction of gravity head as sample fluid is emptied from the vial. Finally, the cross-section of the capillary is not perfectly circular and may vary along its length. With all these effects, the flow does not remain inversely proportional to the fluid viscosity as would be expected from the Hagen-Poiseuille equation.

An alternate method could be to calibrate the system with known fluid viscosity and find the calibration constant. This constant could be used for other samples assuming "average" dimensions of the capillary tube remain constant. (After a sample is run, the used tube assembly is rejected.) *In futher analysis, the assumption is made that the flow, Q, is inversely proportional to the* viscosity of the fluid, or:

$$Q = \frac{C}{\mu} \qquad (1)$$

where: C = a constant.

At this point, a word of caution about very low Reynolds number flow should be given. Ref. [10] proposes that the effect of higher order terms of viscosity on the flow rate, Q, will be more predominant when the Reynolds number is less than 0.5. In such cases, as with highly viscous lubricating oils, the Reynolds number should be checked to avoid erroneous results.

Fluid entering the precipitator tube from the capil*lary is decelerated since the precipitator tube is larger in* cross-section. It is assumed that the flow will be fully developed laminar when the wear particles come under the influence of the magnetic field. For an approximate evaluation of the length required to develop the laminar flow, the value given in Ref. [11] can be adopted. That is, the length required for fully developed laminar flow, L_e, is given by:

$$L_e = 0.035\ d\ R_e.$$

where: d = the diameter of precipitator tube, and R_e = the flow Reynolds number in the precipitator tube.

Using the values for d and R_e given earlier in the paper,

$$L_e = 0.035\ (0.15\ cm)\ (5.6) \approx 0.03\ cm \approx 0.03\ cm$$

Clearly, this is a smaller length compared to the length of the precipitator tube outside the magnetic assembly. (See Fig. 1.) Thus fully developed laminar flow exists at the section where the particles become influenced by the magnetic field.

At this point, a set of coordinate axes is established to define the fluid flow and later the motion of the wear particles. Fig. 3 shows the coordinate axes chosen. The origin chosen is the junction of the tube bottom inner surface and end of the magnetic assembly with the X-axis perpendicular to the axis of the tube and Z-axis along the direction of flow. The Y-axis is selected laterally, as shown in Fig. 3.

Using classical analysis, the velocity distribution in *the pipe cross-section is parabolic [11], with maximum*

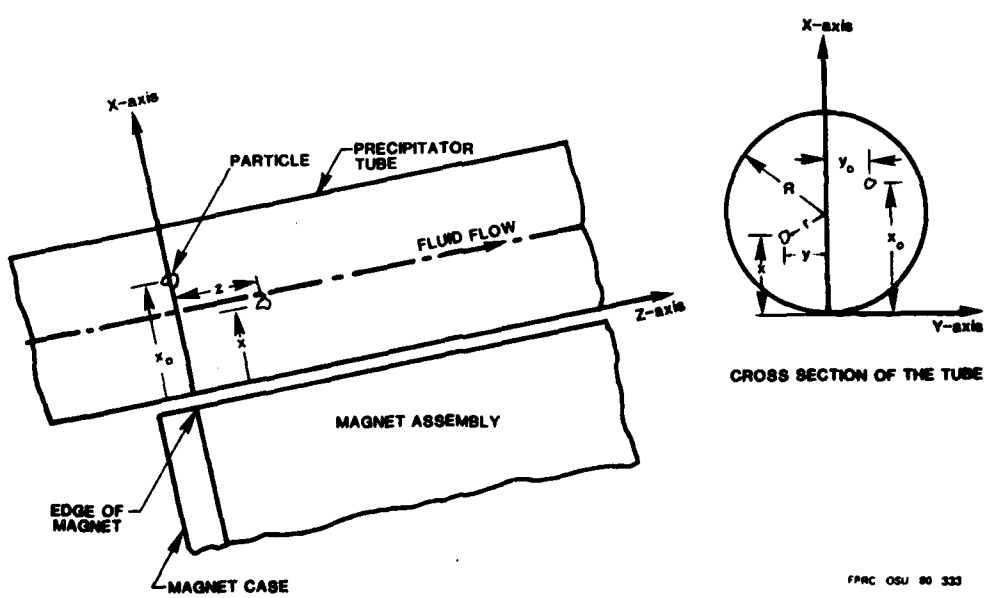

Fig. 3. Coordinate Axes.

velocity at the center of the pipe, as shown in Fig. 4. The velocity in the Z-direction, U_z, at any point in the tube cross-section is given by:

$$U_z = 2\,U_{(av)}\left[1-\left(\frac{r}{R}\right)^2\right] \qquad (2)$$

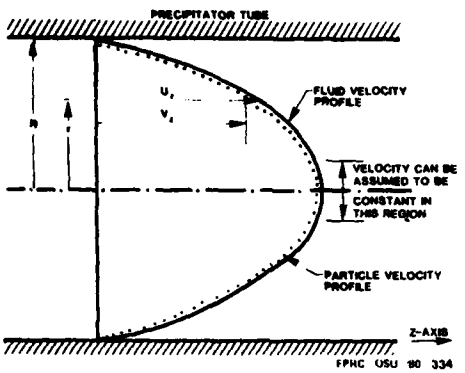

Fig. 4. Fluid and Particle Velocity Profile.

where: U(av) = average fluid velocity in the precipitator tube, r = radius at any point where velocity is measured, and R = the radius of the precipitator tube.

The average velocity, U(av), is given by,

$$U_{(av)} = \frac{Q}{A} \qquad (3)$$

where: Q = flow rate through the precipitator tube, and A = area of the precipitator tube = πR^2.

The purpose in developing the model is to find how the fluid flow affects the wear particle deposition in the precipitator tube under the influence of the magnet. The next section discusses these aspects of the particle dynamics.

PARTICLE DYNAMICS

Magnetic particles entering the "magnetic region" travel toward the bottom of the precipitator tube under the action of the magnetic forces. The forces acting on the particle are gravity force, magnetic force, fluid drag, and lift forces. Reference is made to a companion paper by the author on the analysis of an Analytical Ferrograph [12] in which a detailed discussion of these various forces is presented. In Ref. [12], it was shown that the gravity forces are much smaller than the magnetic forces and these forces can be safely neglected for the analysis. In other words, in the absence of a powerful magnet, there would be very few wear particles deposited inside the precipitator tube. It is further shown later in this section that, in the absence of a magnet, the chance of any particle getting deposited is nil due to lift forces acting on the particles.

Fig. 5 shows the various forces acting on a magnetic particle. Neglecting gravity and buoyancy, the various forces acting on the particles are discussed below:

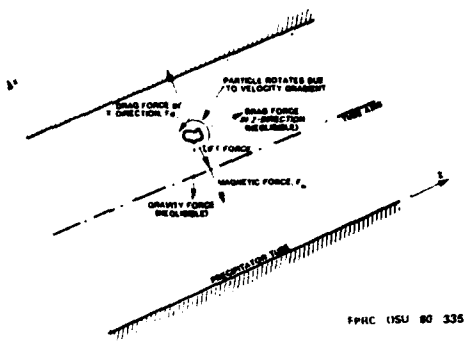

Fig. 5. Forces on the Magnetic Particle.

Magnetic force, F_m, is given by:

$$F_m = \frac{\pi D^3}{6}\,K \cdot H \cdot \frac{dH}{dx} \qquad (4)$$

where: D = diameter of the particle, K = volume susceptibility of the particle, H = field intensity of the magnet, and dH/dx = field gradient of the magnet in the X-direction.

At any cross-section of the tube, the values of H and dH/dx change, however, it can be assumed that this value remains constant along a given cross-section. The magnet in the DR Ferrograph has its value of H (dH/dx) varying along the direction of fluid flow.

The drag force acting on the particle can be divided into two components one in the X-direction and the other in the Z-direction. The drag forces for the low Reynolds number flow are given by Stokes Law.

Drag in the X-direction by Stokes Law is:

$$Fd_x = 3\pi\cdot\mu\, D\, V_x \qquad (5)$$

where: Fd_x = the drag force on the particle in the X-direction, μ = absolute viscosity of the fluid, and V_x = velocity of the particle in the X-direction (towards the magnet).

Another force acting in the X-direction is the hydrodynamic lift, which will be small compared to the magnetic forces. It will be shown that the hydrodynamic lift on the particle has a strong effect on the initial entrance of a particle in the tube.

In the Z-direction, the forces acting on the particles are the component of gravity trying to move the particle against the flow and the fluid drag trying to move the fluid along the flow. In practice, these forces are small enough so that the particle velocity is approximately

the same as the fluid velocity. This assumption stems from the basic flow visualization techniques in fluid mechanics measurements [13]. Consequently, in Eq. (2), we can replace fluid velocity, U_z, by the particle velocity, V_z. Thus, the particle velocity in the Z-direction at any point in the fluid can be given by:

$$V_z = 2U_{(av)}\left[1-\left(\frac{r}{R}\right)^2\right] \qquad (6)$$

Differences in fluid velocities on top and bottom surfaces of the particle (due to parabolic velocity profile) cause it to rotate, deriving energy from the fluid stream. Subsequently, particles lag behind the fluid velocity, lag being maximum near the walls due to a higher velocity gradient. This difference in velocity is shown schematically in Fig. 4. Even though this velocity difference is small, it develops lifting forces on the particles.

Eq. (6) gives the motion of the particle in the Z-direction. Expressing Eq. (6) in terms of Cartesean coordinates, (See Fig. 3.),

$$V_z = \frac{dz}{dt} = 2\cdot\frac{U_{(av)}}{R^2}\left[R^2-(x-R)^2-y^2\right] \qquad (7)$$

from which

$$\frac{dz}{dt} = \frac{2\,U_{(av)}}{R^2}\,(2xR-x^2-y^2)$$

Eq. (7) defines the velocity of a particle at any point in the precipitator tube in the Z-direction. One more equation (assuming no particle dynamics in the Y-direction) is needed in the X-direction to define the particle motion. From Eq. (4) and (5) by Newton's Law,

$$\frac{\pi D^3}{6}\,KH\frac{dH}{dx} - 3\pi\mu D V_x = \zeta_p\left(\frac{\pi D^3}{6}\right)\frac{dv_x}{dt} \qquad (8)$$

where: ρ_p = the density of the particle, and $dV_x = dt$ = acceleration of the particle in the X-direction.

According to Eq. (8), the particle accelerates toward the bottom of the tube; however, the resulting increase in velocity, V_x, increases the drag monotonically. After a lapse of time, the drag force becomes equal to the magnetic force, and the particle can no longer accelerate. From there on, the particle travels in the X-direction with a uniform velocity, V_T (known as the settling velocity). It can be shown that the time required to achieve this settling velocity is a minute fraction of a second [12] and, hence, the motion of the particle in the X-direction can be completely defined by the settling velocity.

$$V_x = \frac{dx}{dt} = -V_T \qquad (9)$$

The negative sign for V_T is due to the downward motion of the particle. The magnitude of V_T in Eq. (9) is obtained by forcing the acceleration, $dV_x/dt = 0$, in Eq. (8) and replacing V_x by V_T. Subsequently, from Eq. (8),

$$V_T = \frac{D^2}{18\mu}\,K\cdot H\cdot\frac{dH}{dx} \qquad (10)$$

Substituting Eq. (10) into Eq. (9) yields:

$$\frac{dx}{dt} = -\frac{D^2}{18\mu}\,KH\cdot\frac{dH}{dx} \qquad (11)$$

Now Eq. (7) and (11) define the complete motion of the particle in the fluid. The parameter time, t, can be eliminated from Eq. (7) and (11). Dividing Eq. (7) by Eq. (11) and rearranging,

$$dz = \frac{-36\,\mu\,U_{(av)}}{R^2D^2KH\,\frac{dH}{dx}}\,(2xR-x^2-y^2)\,dx \qquad (12)$$

It may appear from Eq. (12) that y is also a variable in the particle path in the fluid before it gets deposited. However, it can be observed that the position of the particle should not change laterally (in an ideal situation without considering the effect of lift or tube wall), since there are no lateral forces acting on the particle in the Y-direction. Hence, in Eq. (12), the lateral position of the particle, y, can be considered as a constant depending on the initial position of the particle as it enters the "magnetic region." Thus, by integrating Eq. (12) with appropriate limits of integration, the final position of the particle inside the tube wall can be obtained. To find the limits of integration, the starting point is at the edge of the magnetic assembly where $z = 0$. The particle enters this region at some point (x_o, y_o) at $z = 0$. After travelling through the fluid as per Eq. (12), the particle gets deposited at some distance, z_p, from the entry region. But, now, the magnitude of z_p cannot be selected as a fixed value for any initial position (x_o, y_o) due to the curvature of the wall. That is, particles near the wall (laterally) would touch the wall earlier than the particle which happened to be in the central region. Thus, it is necessary to integrate the equation with the variable limits.

Fig. 6 shows a schematic of the effect of the tube curvature on particle deposition. Particles which hit the bottom side curvature of the wall, as shown in Fig. 6, would be expected to roll down to the bottom of the tube. Such particles will obviously occupy an earlier position in the bottom of the tube compared to a position, z_p, if its initial position were in the central region. The result could be a wide range of scatter in the output density reading of the equipment. However, the situation is not all that bad, since most of the wear particles, if not all, will enter the "magnetic region" at the central region of the tube. To substantiate this, it is necessary to look more closely at the role of lift on particles and the geometry of the capillary tube in controlling the location of the wear particle in the fluid.

RADIAL MIGRATION OF PARTICLES

In the previous section; the motion of the magnetic particles, once they entered the region of magnetic influence was presented. The initial position of the particle in this region was assumed to be an arbitrary value (x_o, y_o). In this section, a look into the previous

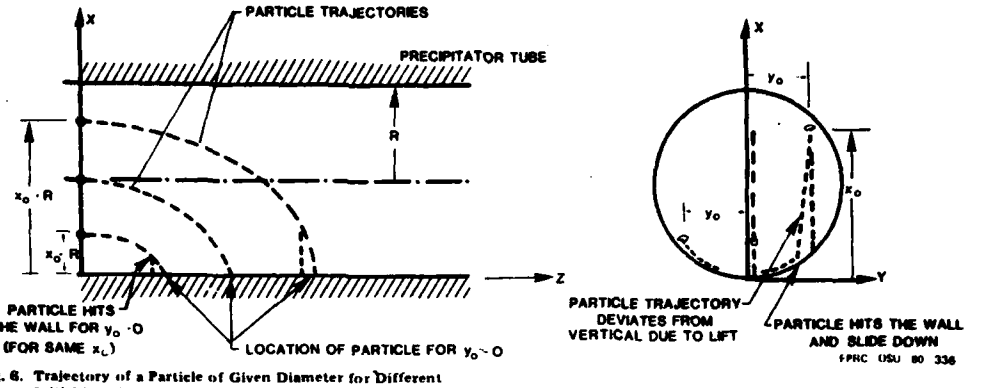

Fig. 6. Trajectory of a Particle of Given Diameter for Different Initial Position (X_o, Y_o).

history of the particle before it reaches the "magnetic region" will be given.

The motion of a mixture of solid particles and fluid in a pipe is found in many engineering and natural situations. Transportation of solids through pipes or the travel of blood corpuscles in blood are typical examples. It has been found by many observers that fluid particles migrate to a certain region in the pipe [13, 14, 15]. The reason for this lateral migration is said to be the lift forces acting on the particle. Gravity has a strong effect over the direction of migration of the particle. There exists considerable differences of opinion among various authors on the magnitude of the migrative forces and velocities. Thus, it is necessary to restrict this discussion to the qualitative results of the above observation in controlling the Ferrographic process.

The radial migration of particles can be summarized as follows: if the particle is denser than the fluid medium and if the flow is upward (not necessarily vertical), the particles try to concentrate in the form of a ring between the center and wall of the pipe. If the particles are lighter than the fluid, they move toward the wall. If the flow direction is reversed, this tendency is reversed with buoyant particles occupying the same position. This situation is shown in Fig. 7. In the fluid sample being analyzed, it can be assumed that the particles of wear origin or non-wear origin are denser than the fluid. Consequently, during the initial travel of the particle in the capillary tube, the flow is downward (See Fig. 1.) and, hence, wear particles which are denser than the fluid try to move to the wall of the tube. In a later stage, the flow is upward and particles tend to try and move to the center of the pipe. It is difficult to predict the net effect of this phenomenon; however, it can be presumed that, when the particles reach the exit of the capillary tube, there will be a denser region of wear particles in the central area of the capillary.

Fig. 2 shows the entrance of the capillary to the precipitator tube which accommodates it (capillary tube) approximately at the center. Considering the fact that the velocity of fluid entering the precipitator is higher and the initial disturbances die out fast, we can assume that the denser particles are around the central region of the tube when they enter the magnetic region. In other words, the initial position (x_o, y_o) of the particle can be approximated as $x_o = R$, the radius of the tube.

Based on the above assumption that particles enter the precipitator tube at the center, the location of deposition of the particle can be established.

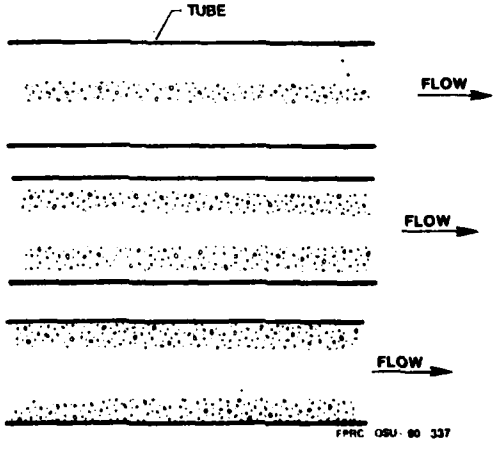

Fig. 7. Migration of Particles in a Flowing Fluid.

DEPOSITION OF WEAR PARTICLES

Eq. (12) gives the dynamics of the particles as shown earlier. Integrating this equation between limits 0 to z_p and x_o to 0 for x (y is taken to be y_o) yields the location, z_p, of the magnetic particle on the bottom of the precipitator tube, that is,

$$\int_0^{z_p} dz = \frac{-36\mu U(av)}{R^2 D^2 KH \frac{dH}{dx}} \int_{x_o}^{0} (2xR - x^2 - y_o^2)\, dx \qquad (13)$$

or

$$z_p = \frac{36\mu U(av)}{R^2 D^2 KH \frac{dH}{dx}} \left(Rx_o^2 - \frac{x_o^3}{3} - x_o y_o^2\right)$$

If y_o is small compared with x_o, that is, the particles are initially at the central region of the tube, then,

$$z_p = \frac{36\mu U(av)}{R^2 D^2 KH \frac{dH}{dx}} \left(Rx_o^2 - \frac{x_o^3}{3}\right) \quad (14)$$

Substituting for U(av) from Eq. (3) into Eq. (14),

$$z_p = \frac{36\mu Q}{\pi R^4 D^2 KH \frac{dH}{dx}} \left(Rx_o^2 - \frac{x_o^3}{3}\right) \quad (15)$$

Substituting for Q from Eq. (1) into Eq. (15) yields:

$$z_p = \frac{36C}{\pi R^4} \left(\frac{Rx_o^2 - \frac{x_o^3}{3}}{D^2 KH \frac{dH}{dx}}\right) \quad (16)$$

Eq. (13) through (16) are the various forms for expressing the location of the particle on the bottom of the precipitator tube.

In the DR Ferrograph, the magnetic parameter, H (dH/dx), varies along the Z-direction. In the absence of any other data (Ref. [16]) shows a schematic of the variation of dH/dx along the Z-direction as a polynomial function of z), it is assumed that the variation of the magnetic parameters is:

$$H \frac{dH}{dx} e^{mz}$$

where: H (dH/dx) = the magnetic parameter at the entrance region of the particles, and m = a constant.

Accordingly, Eq. (11) can be modified as:

$$\frac{dx}{dt} = \frac{D^2}{18\mu} KH \frac{dH}{dx} e^{mz} \quad (17)$$

and, subsequently, Eq. (12) will be modified as:

$$e^{mz} dz = \frac{-36\mu U(av)}{R^2 D^2 KH \frac{dH}{dx}} (2xR - x^2 - y^2) dx \quad (18)$$

Eq. (18) can be integrated for z, varying from 0 to z_p and x varying from x_o to 0 as in the derivation of Eq. (13). Integrating Eq. (18) with the limits above and solving for z_p yields:

$$z_p = \frac{1}{m} \ln \left|1 + \frac{m \cdot 36\mu U(av)}{R^2 D^2 KH \frac{dH}{dx}} \left(Rx_o^2 - \frac{x_o^3}{3} - x_o y_o^2\right)\right| \quad (19)$$

Comparing Eq. (13) and Eq. (19), it can be seen that if a particle is travelling farther from the entry point, then the effect of increased magnetic force is to influence the particle to get deposited at a faster rate. In other words, according to Eq. (19), larger size particles will not be deposited very faraway from the entry region. In the DR Ferrograph, the optical density readings for large particles, L, and smaller particles, S, are taken near the entry and a few millimetres (say, 5 mm) from the entry point. In this region, the variation of H (dH/dx) is not appreciable; and, hence, Eq. (13) through (16) will be used for further discussion.

OPTICAL DENSITY READINGS

As mentioned at the beginning of the paper, the density readings near the entry, where large particles, L, are deposited and at another location near the entry where smaller particles, S, are deposited, give the raw data for analyzing the wear situation. The electro-optical system measures the amount of light blocked by wear particles and expresses this as (direct) DR readings on a digital meter. The maximum reading that can be obtained without losing linearity according to the manufacturer is 100 DR units on large or small particles. In the absence of data on electro-optical systems, it will be necessary to present general comments on the density readings based on the model developed.

Eq. (16) shows that the location of a particle, z_p, is inversely proportional to the square of the diameter of the particle, D^2, if x_o remains constant. If $x_o = R$, that is, the particle enters the magnetic region at the center of the tube, then Eq. (16) is:

$$z_p = \frac{24C}{\pi R KH \frac{dH}{dx}} \left(\frac{1}{D^2}\right) \quad (20)$$

If we assume that at the central region of the tube, the fluid velocity remains constant (See Fig. 4.), then Eq. (20) approximately represents the deposition of all the particles entering this area. Subsequently, particles of a given diameter, D, entering in a small area around the axis of the tube will get deposited in a specific location. (The particles will be deposited in a specific ellipse). Fig. 8 shows this situation. The smaller the diameter of the particle, the larger the area of deposition. Alternately, if it is assumed that equal numbers of particles of any diameter exist in the sample then the number of particles in a given field of the optical system, say, L or S, will be nearer the entry region. Accordingly, the density readings increase sharply toward the entry region. Note that this increased density reading near the entry region is due to the larger diameter of the particle (area = $\pi D^2/4$) as well as the increased concentration of the particles. However, a difficult situation arises if the machine wear produces more smaller particles. Since smaller particles cannot get deposited (as per Eq. (16)) near the entry, a condition may exist when reading S will be greater than L. In other words, the DR Ferrograph is more efficient in detecting a severe wear situation when larger particles are being generated by the machinery.

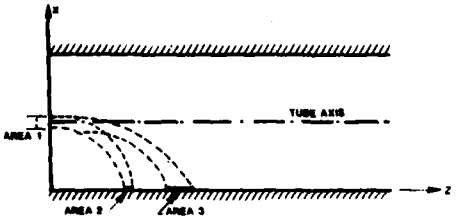

Fig. 8a. Figure Showing the Trajectory of Particles.

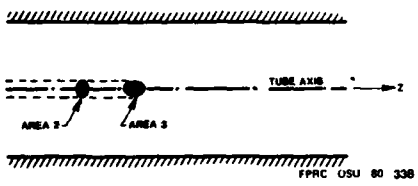

Fig. 8b. Figure Showing the Deposition of Particles Entering Area "1."

Fig. 8. Deposition of Particles.

So far the discussion has been based on the assumption that the particles enter the "magnetic region" in the central region of the tube. If some of the particles enter farther from the center, but are not laterally shifted (that is, x_o any position but $y_o \cong 0$), then those particles with $x_o > R$ will get deposited farther from its ideal position, as discussed earlier, while those particles with $x_o < R$ will get deposited before the ideal position. If an equal probability for x_o to be less than or more than R is assumed, then the contribution for density readings from these particles at any location can be assumed to be approximately the same. In another case, the lateral initial position, y_o, will be comparable to x_o. In such situations, the particles would travel toward the magnetic field, but keeping the same lateral position until they touch the tube wall from where they will roll down to the side of the deposition. The contribution to density readings from such particles are similar for large and smaller particles on an equal probability basis. This argument is valid, even if the trajectory of these particles bends toward the axis due to the influence of hydrodynamic lift. (See Fig. 6.) In conclusion, the model developed, as given by Eq. (16), can be used for qualitatively assessing the Ferrographic process.

VARIATION FROM IDEAL FERROGRAPHIC PROCESS

When various samples from different machinery are analyzed, many of the parameters like fluid viscosity, flow, particle size and shape, etc., are uncontrollable. The following pages describe how these parameters could affect the DR readings.

Eq. (16) indicates that the Ferrographic process will be unaffected by the viscosity of the fluid and magnitude of the fluid flow. This result is not surprising since, if flow increases due to viscosity, the settling velocity should be higher due to reduced drag and the particle gets deposited at the same location. However, if the Reynolds number becomes less than 0.5, the flow may be a function of higher powers of viscosity and then density readings will be affected by both μ and Q. In actual practice, this situation may not occur at all. Other factors which affect the flow are the height of the sample vial (This should be kept constant when comparing different readings.) above the delivery point. Variation in the cross-section of the capillary can cause a change in flow properties.

Optical density is read when the last portion of the sample fluid flows through the precipitator tube [5]. As per the operating instructions by the manufacturer, the reading, L and S, should be set equal to zero (by operating adjustable potentiometers) when the fluid sample initially passes through the tube. Thus, it is assumed that the cleanliness of the fluid is uniform so that the light attenuation by the fluid will remain the same. In the case of "dirty fluid," a different method must be used for density readings. This method employs a clean fluid as reference before and after the "dirty sample" is run. This, being a subjective rather than an objective decision, could cause considerable error in density readings. For example, water present in oil may make it hazy or cloudy if the water content is above the saturation level [18]. Further, growth of micro-organisms [19] could be accelerated by the presence of water which could again contaminate the fluid and make it turbid. These reasons, together with the effect of other non-wear origin contaminants, could influence the oil quality in terms of light attenuation. Hence, it is advisable to assess the sample before it is run whether it appears to be a "dirty fluid" or not.

Magnetic Properties

The location of a particle, z_p, as given by Eq. (16) is inversely proportional to the volume susceptibility, K, of the particle. This is a property of the material and the magnitude depends on many factors, such as the material, field intensity (11), mechanical and chemical processes due to wear, residual stress in the particle, and aging [17]. These variations are difficult to generalize and may depend on the machine under investigation and its current wear stage.

Spherical particles as in "fatigue wear" and plate-like particles as in "normal wear" form strings in the magnetic field (as seen on an Analytical Ferrogram). This causes agglomeration of the particles and forces them to be deposited earlier on the tube, as if they were larger particles.

Effect of Shape of the Particles

Most of the wear particles have non-spherical shapes (except "fatigue wear" particles) which can be described as fibrous, flaky, irregular and angular. Their behavior in the fluid flow can be different from that of spherical particles. In general, they have higher drag and lift forces acting on them with the result that they could

travel farther in the fluid than if they were spherical. Hence, it should be accepted that scatter in density readings can be critical in wear situations where both spherical and non-spherical particles are being generated.

Effect of Non-Magnetic Particles

It was shown earlier that particles having the same density as the fluid would migrate to form an annular ring in the capillary tube. Insoluable contaminants may have more or less the same density as the fluid. Subsequently, they would be washed away with the fluid without being deposited in the precipitator tube. Other non-magnetic particles, like brass or aluminum which have not been stressed by the wear process, might migrate to the center of the tube and get washed away. Thus, in the DR Ferrograph, a deposit of primarily magnetic particles can be expected.

Effect of Sample Volume and Concentration

In an ideal situation, the sample volume or concentration of particles in the fluid should not affect the model developed. (Extreme concentrations cannot be achieved in any wear situation; hence, fluid properties can be assumed to remain unchanged.) However, at higher concentrations or sample volumes, an exorbitant number of particles may be deposited in the tube and the density readings will show nonlinear and saturated characteristics [8]. At lower values of concentrations and sample volumes, the density readings may not be large enough to be statistically accurate. In such cases, the sample volume has to be adjusted to get the density readings in the operating range of the equipment. However, another factor with a high concentration of particles could be an inordinate scatter of density readings. This is due to the crowding of particles near the center of the tube as a result of the lift forces and their possible agglomeration in the magnetic region.

DISCUSSION

From the model developed and from its interpretation presented in the previous chapters, it is apparent that the DR Ferrograph should effectively predict the wear situation in a machine based on the density readings of large, L, and small, S, particles. The results of the paper so far can be summarized as follows:

1. Density readings near the entry region (say, L) will be greater than the readings downstream of the region (say, S) by virtue of larger particle sizes and higher concentration of particles in that area.

2. A particle of a given diameter is deposited in a specific location of the tube. A change in viscosity (by using a more viscous fluid or by adding more solvent) and a corresponding change in flow does not affect this deposit location.

3. Non-magnetic particles are not deposited in the tube due to the lift forces.

Scatter in density readings would be noticeable when:

1. There are considerable variations in the shape and size of the capillary tube which would create different flow effects.

2. The liquid Reynolds number is very low (highly viscous, thick fluid).

3. A wear situation in the machine produces very few large particles.

4. Wear particles in the sample contain a considerable amount of magnetically weak (low volume susceptibility, K) particles like oxides.

5. The sample fluid is "dirty" with carbon particles, water, micro-organisms or other metallic particles. (Assuming a clean fluid was not used as a reference.)

It may be noted that some of these factors can be taken into consideration by the operator, while others are dependent on the nature of the wear process.

It has been shown that the lift forces and the location of the capillary tube in the precipitator tube force the wear particles to enter the "magnetic region" at the center of the precipitator tube. Any deviation from this initial location to a non-axial position would cause the particles to be deposited at a different location. The contribution to density readings from such particles may not affect the density readings, if the relative number of such particles is small. Also, the influence of such particles could be eliminated all together if all the particles were axially located at the entry point. It has been further shown that wear particles are forced to the center of the tube (by the lift forces), if the flow is in an upward direction. Thus, if the capillary flow is always in an upward direction and the length of the capillary were increased, then the wear particles would indeed be expected to be axially located when they enter the precipitator tube. This could be achieved by using a siphoning action with the delivery tube kept lower than the sample vial for a gravity head or by mechanical action.

In Ref. [6], the degree of wear in a machine was expressed by a Severity Index (I_s) factor. This Severity Index is given by:

$$I_s = A_L^2 - A_S^2$$

where: A_L = the density reading at location L, and A_S = the density reading at location S.

This index is affected by the location of the particles being shifted due to the difference in shape of the particles, as mentioned earlier. Also, in a normal wear mode, density readings at location L could be considerably reduced. However, if readings are taken at three or four locations, along the flow path instead of two locations, the magnitude of the readings at these locations may produce a better prediction reference. If R_1, R_2, R_3, and R_4 are the density readings at four locations from the entry in that order, an expression for the Severity Index could be given as:

$$I_e = \sum_{i=1}^{4} l_i R_i$$

where: l_i = a weighting factor for the density readings near the entry region so that the value of l_i decreases along the length of the tube at the four locations.

Such an index may more accurately identify a serious wear situation by de-emphasizing the influence of smaller particles. By controlled experiments with known particle distributions, the weighting parameter, l_i, could be evaluated.

CONCLUSION

A detailed analysis of the DR Ferrograph was presented in this paper. The various parameters influencing particle deposition and optical density readings were identified.

It was shown that the DR Ferrograph actually grades the wear particles according to size by depositing location in the tube and the instrument exhibits considerable promise in predicting severe wear conditions. Methods have been suggested to reduce the possible scatter in the density readings.

* * *

REFERENCES

1. Aronson, Robert, *"Wear Particles Predict Machine Malfunction,"* Machine Design, July 24, 1976, pp. 84-89.

2. Tessmann, R. K., *"Monitoring Wear in Hydraulic Systems,"* International Conference on Fundamentals of Tribology, Massachusetts Institute of Technology, June 1978.

3. *"D. R. Ferrograph System,"* Manufacturers Catalogue, Foxboro/Trans-Sonics, Inc.

4. Seifert, W. W., and V. C. Westcott, *"A Method for the Study of Wear Particles in Lubricating Oil,"* Wear, 21, 1972, pp. 27-42.

5. *"D. R. Ferrograph Calibration and Operating Instructions,"* Foxboro/Trans-Sonics, Inc., Manufacturers Catalogue.

6. *"Calibration of D. R. Ferrograph,"* Foxboro/Trans-Sonics, Inc., Manufacturers Catalogue, August 12, 1977.

7. Bowen, R., et al., *"Ferrography,"* Tribology International, June 1976.

8. Kitzmiller, D. E., and R. K. Tessmann, *"The Capabilities and Limitations of Ferrographic Wear Analysis,"* The BFPR Journal, 11, 1, 1978, pp. 87-94.

9. Popgoshev, Daniel, and Raymond Valori, *"Effectiveness of the Real Time Ferrograph and Other Oil Monitors as Related to Oil Filtration,"* Report No. NAPC-PE-2, Naval Air Propulsion Center, New Jersey, November 1977.

10. Kestin, J., et al., *"Theory of Capillary Viscometers,"* Applied Scientific Research, Vol. 27, February 1973, pp. 241-264.

11. Bird, R. B., et al., *"Transport Phenomena,"* John Wiley and Sons, Inc., 1960, pp. 42-48.

12. Nair, K. S., *"An Appraisal of the Analytical Ferrographic Method,"* The BFPR Journal, 1980, pp. 281-294.

13. Merzkirch, W., *"Flow Visualization,"* Academic Press, New York, 1974, pp. 20-30.

14. Lawler, M. T., and P. C. Lu, *"The Role of Lift in the Radial Migration of Particles in a Pipe Flow,"* Paper 3, Advances in Solid-Liquid Flow in Pipes and Its Applications, I. Zandi (Ed.), Pergamon Press, 1971, pp. 39-57.

15. Brenner, Howard, *"Hydrodynamic Resistance of Particles at Small Reynolds Number,"* Advances in Chemical Engineering, T. B. Drew, et al. (Eds.), Vol. 6, Academic Press, New York, 1966, pp. 287-438.

16. Miller, Lt. R. S., Discussion During the Paper, *"Wear Control,"* by M. B. Peterson, et al., Progress in Tribology Workshop, Report No. PB-2412-53, April 1974.

17. Bozoroth, R. M., *"Ferro-Magnetism,"* D. Van Nostrand Co., Inc., 1951.

18. Jones, L. J., *"The Measurement and Control of Water Contamination in Mineral Oil Hydraulic Systems,"* Contamination in Fluid Power Systems, Institute of Mechanical Engineers, Conference Publications, April 1976.

19. Myers, M. B., *"Effects of Microbial Contamination on Hydraulic System Performance,"* Fluid Power International, January-February, 1974, pp. 36-40.

* * *

APPENDIX C

The Effect of Non-Magnetic and Weakly Magnetic Particles on the Ferrographic Process

THE EFFECT OF NON-MAGNETIC AND WEAKLY MAGNETIC PARTICLES ON THE FERROGRAPHIC PROCESS

K. Nair Editorial Manager: E.C. Fitch *A Research Documentary*

ABSTRACT: Non-magnetic and weakly magnetic particles occasionally get collected in a scattered fashion on the Ferrograph and affect the density readings. When it is known that the particles are of non-wear origin, the efficiency of the equipment can be increased if the particles are separated before the Ferrographic analysis. Various methods to separate the non-magnetic particles from the fluid samples are presented in the paper.

KEY WORDS: Ferrography, non-magnetic particles, weakly magnetic particles, magnetic separator, fluid sample storage.

INTRODUCTION

Ferrography [1, 2] is a newly developed technique to evaluate wear phenomena in machines utilizing the analysis of wear debris. The method is nondestructive and involves the analysis of lubricating or hydraulic oil samples from the machines. The operating principle of the equipment utilizes the magnetic properties of the wear particles in the oil sample. Commercially, two types of Ferrographs are available: the Analytical Ferrograph and the Direct Reading (DR) Ferrograph. A variation of the DR Ferrograph is used for 'on-line' wear monitoring, the equipment being designated as the Real Time (RT) Ferrograph. In all the equipment, a high gradient magnetic field is used to trap the magnetic particles in the fluid sample. In the case of Analytical Ferrograph, the fluid passes over a glass slide below which the magnet is located while in the DR Ferrograph the fluid passes through a tube located above the magnetic field. Fig. 1 and 2 show a schematic of the two Ferrographs. It is assumed that the reader is conversant with the operation and applications of the equipment and, hence, further details of the instrument are avoided. More details on the equipment can be found in Ref. [3, 4, 5, 6, 7, 8, 9, 10, 11].

It is evident from the principle of operation of Ferrography that the essential criterion for proper functioning of the equipment is that the material should be magnetic. In such a case, the machine can function at its best if all the wear particles have the same magnetic properties. However, there are many situations where the particles in the fluid are either weakly magnetic or non-magnetic. In some instances, wear particles from the same machine can have different magnetic properties due to mechanical working other environmental effects. Presented in this paper is a consider-

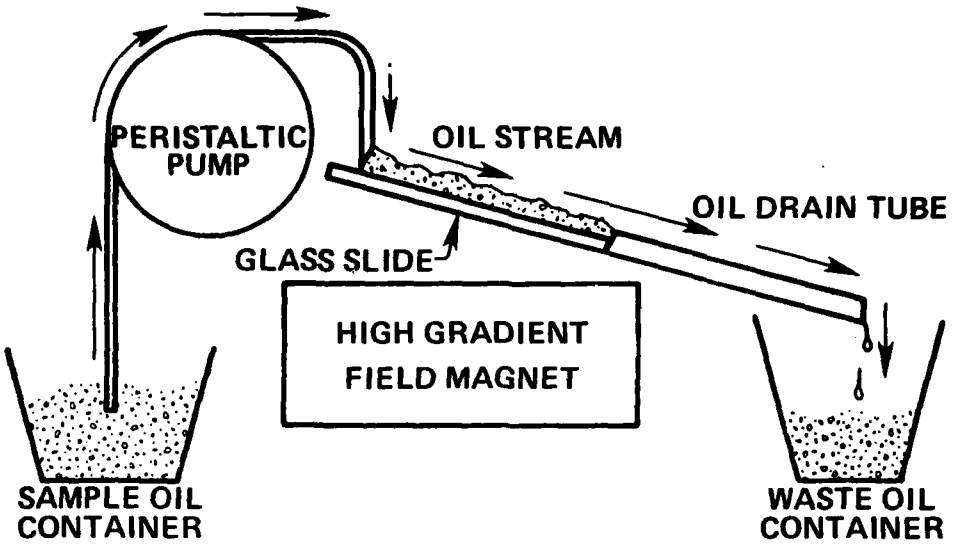

SCHEMATIC OF SLIDE FERROGRAPHIC

© FPRC—OSU—80—230

Fig. 1 Schematic of Slide Ferrograph

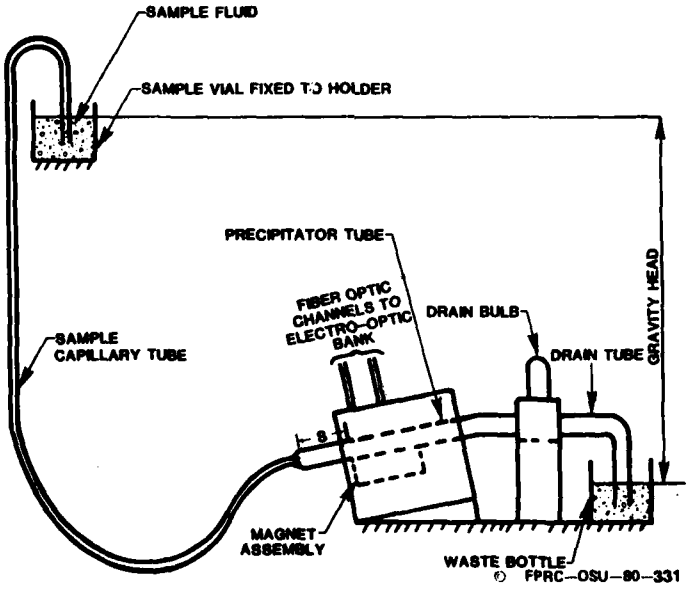

© FPRC—OSU—80—331

Fig. 2 Schematic Diagram of D.R. Ferrograph

ation of the effect of the weakly magnetic or non-magnetic particles on the Ferrographic process. Also, a detailed test program is advanced for the evaluation of the effect of non-magnetic particles on the efficiency of the Ferrographic equipment. As mentioned earlier, there are situations when non-magnetic particles in the sample may not be of wear origin. (Typical examples are particulate contaminants or other non-magnetic metals when it is known that the mating parts in the machine are made of only steel or other magnetic materials). In such cases, it is proposed that suitable means be provided to divert non-magnetic particles from the fluid sample before it is passed through the Ferrograph.

BACKGROUND

The Fluid Power Research Center at Oklahoma State University, seeing the potential of the Ferrography, has acquired the equipment for diagnostic and prognostic studies of hydraulic equipment. Tessmann [12] has shown how Ferrography can be effectively used to evaluate the contaminant wear in hydraulic pumps. Smith and Tessmann [13] have shown that Ferrography can accurately diagnose impending failures in hydraulic systems of mobile equipment. It was observed that, occasionally, there was some amount of scatter in the density readings on the Ferrograph from similar fluid samples. Subsequently, Kitzmiller [14] conducted a series of experiments and proposed a standardized test procedure. Nair [15, 16] further developed analytical methods for predicting the deposition of wear particles on the Ferrogram slide as well as that in the precipitator tube of the DR Ferrograph.

Limited experiments were conducted at the Fluid Power Research Center for evaluating the performance of the Analytical Ferrograph when non-magnetic particles were present in the sample fluid. Fluid samples containing 0-10 μm AC Fine Test Dust and 50-400 μm aluminum particles were separately prepared and Ferrogram slides were made using these samples. It was found that some of these particles got deposited on the slide and gave unacceptable density readings. However, when fluid samples from wear tests on hydraulic components were used for making the slide, the number of AC Fine Test Particles were none or few. It is hypothesized that the magnetic particles get deposited faster on the bottom of the slide and non-metallic particles (AC Fine Test Dust, for example), if they happen to get deposited on the slide, roll down the slide since they will be away from the boundary layer (where velocity of the fluid is non-zero). Analysis presented in Ref. [15] reveals that the probability of non-magnetic particles getting deposited on the slide is fairly low. This aspect will be discussed later in the paper.

It is interesting to note the experience of others who have successfully used Ferrography for wear monitoring. Ruff [5] states

that "a large non-metallic particle" was seen at the entry in one of the Ferrographic readings. Also, among the deposits, organic coatings around metallic particles were observed in the same experiment. This was thought to be due to chemical reactions in the fluid when it was stored for long periods. In the same reference, it is mentioned that sodium, potassium, calcium, etc., were found on the slide and presumably originated from the oil. Ref. [6] reports similar organic compounds on the slide. Ref. [7] suggests that waxes and gels are formed on the bottle-surfaces (when in storage) and particles get trapped onto them. Jones [8] reports the deposition of carbanaceous particles (due to the decomposition of lubricating oil) on the slide in his experiments. Most interesting experiments were due to Ruff [9] who conducted a number of tests for evaluating the ability of the Ferrograph for recovering non-magnetic materials. He reports: "An equal volume mixture of SiO_2 and Ni/SiO_2 (nickel impregnated SiO_2 used for the manufacture of silica magnets) microspheres were prepared. Very few SiO_2 spheres were deposited. The SiO_2 spheres were usually found at random locations on the substrate."

It was mentioned that organic materials might be formed in the sample fluid if it was kept for a longer period at room temperature. Also it is possible that, in such conditions, chemical reactions and corrosion of wear particles might occur during storage. Ref. [10] suggests keeping the sample at $-20^{o}F$ while Ref. [11] suggests a temperature is expected to retard the possible chemical reactions.

The foregoing discussion was presented to bring forth the following aspects of Ferrography:

1. Whether Ferrography is accepted by industry as the best method presently available to the tribologist.
2. The magnetic (or non-magnetic) properties of the particles in the sample have a strong influence on the Ferrographic process when optical density is the primary measured output from the machine.
3. Is it worthwhile to investigate the possibility of using some techniques to reduce or nullify the difficulties arising from the non-magnetic particles, especially when it is certain that they are of non-wear origin.
4. Keeping a fluid sample over long periods needs special attention since the magnetic property of the wear particles is likely to change.

Based on these observations, it is thought that a detailed experimental investigation is necessary for further improvement of the Ferrographic process. The details of the proposed experiments are worked out and possible schemes for alleviating the effects of non-magnetic particles are presented in the paper. Before proceeding

AD-A079 654 OKLAHOMA STATE UNIV STILLWATER FLUID POWER RESEARCH --ETC F/G 11/8
WEAR IN FLUID POWER SYSTEMS.(U)
NOV 79 N00014-75-C-1157

UNCLASSIFIED ONR-CR169-004-2 NL

2 OF 2
AD A079654

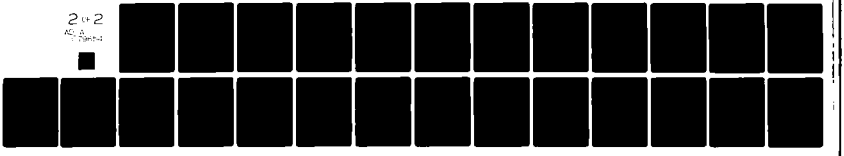

END
DATE FILMED
2 — 80
DDC

into specific details, a brief theoretical appreciation of the effect of magnetic properties of wear particles on the Ferrographic process is presented. It is shown that the theory accurately supports the observations made by the FPRC and many other authors, as detailed above.

EFFECT OF MAGNETIC PROPERTIES

The Ferrograph uses a high gradient magnetic field to trap the magnetic wear particles. The force on a magnetic particle in a magnetic field is given by [1, 17].

$$F_m = V K H \frac{dH}{dx} \qquad (1)$$

where: F_m = the magnetic force on the particle

V = the volume of the particle

K = the volume susceptibility of the material of the particle

H = the field intensity due to the magnet

$\frac{dH}{dx}$ = the rate of change of field intensity perpendicular to the slide (or precipitator tube).

Fig. 3 shows a schematic diagram of the forces acting on the particle. When the particles are very small, say less than 0.1 - 0.2 μm, it might consist of only a single or a few magnetic domains and such particles easily get magnetically saturated under the influence of the magnet. The force on such a particle can be expressed as:

$$F_m = I_s \cdot V \cdot \frac{dH}{dx} \qquad (2)$$

where: I_s = the magnetic saturation moment of the material of the particle.

These small particles do not contribute to optical density readings on the Ferrograph. This is primarily due to their smaller sizes. Even if they get deposited, it will be mostly around the exit point on the slide. Moreover, these particles may be more influenced by Brownian forces and are likely to disobey the magnetic forces. Larger size particles (say, greater than 1-2 μm in size) are of major interest in Ferrographic analysis. It may be mentioned here that a severe wear situation is represented by the presence of larger size particles and subsequent increased optical density

readings. In short, Eq. (1) represents the magnetic force on the wear particle.

In Eq. (1), $\frac{dH}{dx}$ and K are the two parameters which strongly control the magnetic force on the particle. Volume susceptibility, K, is the property of the material of the particle while $\frac{dH}{dx}$ is a function of the volume susceptibility and field strength, H. Thus, there can be a widerange of magnitude of magnetic force on any particle of given diameter. The possible reasons for different magnetic properties for various particulate materials in the sample fluid are given below:

1. Nature of the Material of Contaminant in Fluid. Iron, cobalt and nickel, magnetite, are highly magnetic and they have high values of K. They are called ferromagnetic materials. Paramagnetic materials are weakly magnetic, such as hematite, manganite, coal and blood. Materials such as cuprite are very weak magnetically. (Ref. [18] suggests that cuprite has an attractability of 0.08 on the basis of an attractability of 100 for iron). Again, many fluid contaminants are non-magnetic in nature.

2. Mechanical Process of Wear Particles. Wear particles are subject to high stresses, temperature, fast cooling, quenching and annealing. Residual stresses and thermal cycling due to the wear process can reduce the magnetic properties of the material [17].

3. Aging and Age Hardening. Impurities in iron such as carbon and nitrogen can reduce permeability due to aging especially when the sample is kept for a long time. [17].

4. Crystalline shape of the wear particles can affect the magnetic property of the material such that, in some preferred directions, it could be more magnetic.

5. Corrosive environment, oxidation, and other chemical reactions can reduce the magnetic property of the material.

6. Non-magnetic material might trap a small amount of magnetic material during the wear process and could attain weak magnetism.

7. Some materials such as organic compounds and gels will collect wear particles and become magnetic.

8. Very small magnetic particles reach saturation, and magnetic forces on them may be totally independent of field strength.

All the effects combined may change the magnetic property of a particle (of wear or of non-wear origin) considerably. Earlier work on modeling of the Analytical Ferrograph at the Fluid Power Research Center [15] showed that the deposition of a particle on the slide can be represented as:

$$Z_p = \frac{C_1\left[\delta x_o^2 - \frac{x_o^3}{3}\right]}{D^2\left[g(\rho_p - \rho_f) + KH\,\frac{dH}{dx}\right]} \qquad (3)$$

where: Z_p is the location of the wear particle deposition on the slide

C_1 is a constant based on the type of fluid used and geometry of the slide

δ is the fluid film thickness

x_o is the height of a particle as it enters the slide

D is the diameter of the particle

g is the acceleration due to gravity

ρp is the density of the particle

ρf is the density of the fluid

Fig. 3 shows a schematic of the details required to clarify the various terms in Eq. (3).

Similarly, the deposition of the particle in a DR Ferrograph [16] can be given as:

$$Z_p = \frac{C^2}{D^2\left[g(\rho_p - \rho_f) + KH\,\frac{dH}{dx}\right]} \qquad (4)$$

where C^2 is a constant.

Fig. 4 shows a schematic diagram for the explanation of terms in Eq. (4).

From Eq. (3) and (4), it is seen that for a particle of a given diameter, D, the location of the particle on the Ferrogram is dependent on the magnetic parameters. In the case of non-magnetic particles, the term $KH\,\frac{dH}{dx}$ will be absent in Eq. (3) and (4). Subsequently, the location Z_p becomes large. It can be shown that, in a realistic situation with suitable numerical values substituted in the above equations, the length, Z_p, will be higher than the length of the precipitator tube or the slide Ferrograph. Thus, ideally, no non-magnetic particles will be deposited on the Ferrogram. In Ref. [16], it is shown that the probability of deposition of a

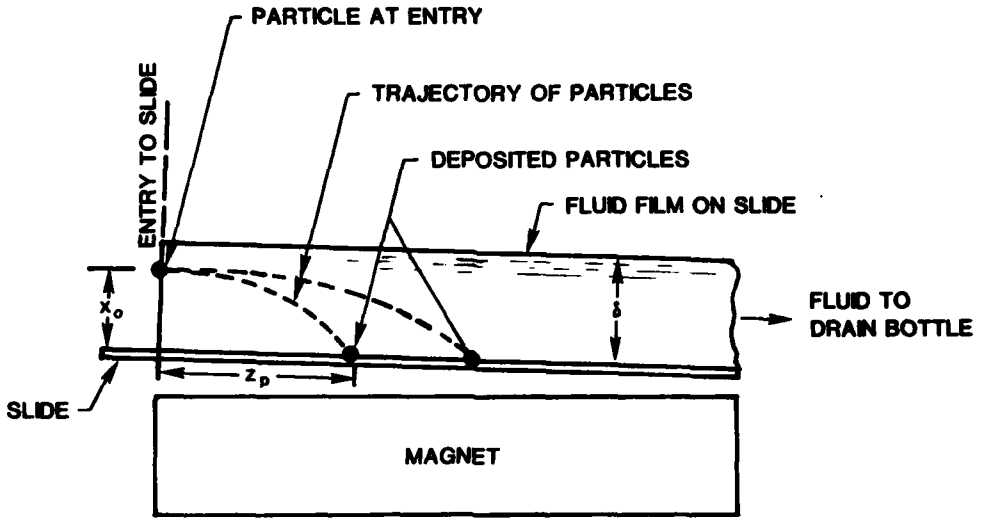

Fig. 3 Trajectory of Particles as defined by Eq. (3)

Note that particles of same diameter can have different trajectories depending on their magnetic properties

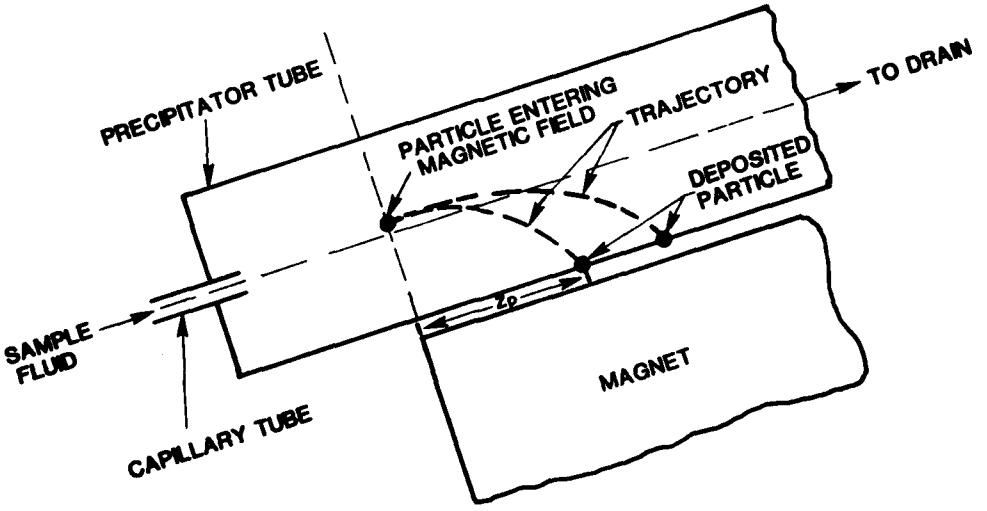

Fig. 4 Trajectory of Magnetic Particle as per Eq. (4)

non-magnetic particle in a DR Ferrograph is much less due to hydrodynamic lift and special nature of the design of the equipment. In the case of the Analytical Ferrograph, as evident from Eq. (3), non-magnetic particles could get deposited on the Ferrogram, if the initial height, x_o, of the particle above the slide is small compared to the film thickness. Fig. 5 shows how non-magnetic particles can get deposited on the slide. This is the reason why scattered non-metallic particles are seen on the slide Ferrograph. Further, it can be said that if the particles are weakly magnetic, they could get deposited in a random fashion on the slide since hydro-dynamic forces can be stronger than magnetic forces. In the case of the DR Ferrograph. Also, large particles which are weakly magnetic might get deposited inside the precipitator tube and, accordingly, the optical density could be affected.

The brief theoretical presentation given here simply illustrates that the experimental observations are duly supported by theory. More information on the modeling can be found in Ref. [15] and [16]. Based on the discussions presented so far, a detailed proposal for the study of the effect of non-magnetic particles on the Ferrographic process is presented in the following pages. Apart from what has been illustrated so far, such a study will be justified by the following practical aspects of any oil analysis program using Ferrography.

1. In most cases, a detailed study of the Analytical Ferrograph (in terms of particle morphology, etc.) is rarely done due to the urgency of the requirement for machine data.

2. Based on the above reasoning, it is better to pre-separate the non-metallic particles from the sample fluid. Even if the tribologist is adamant that he should have the details of the non-magnetic particles, then a second Ferrograph can be made from a separated sample which predominantly will contain non-metallic particles. In such a case, more non-metallic particles will be available on the slide.

3. In the case of DR and RT Ferrographs, there is no visual (by microscope) aid to see the morphology of the particle and, hence, it is logical to avoid unnecessary particles in the fluid sample. Moreover, the readings on the DR Ferrograph are taken when the fluid is still present in the precipitator tube. A cleaner fluid, then, would further decrease the chance of error and, hence, it may be better that unnecessary particles be removed from the sample.

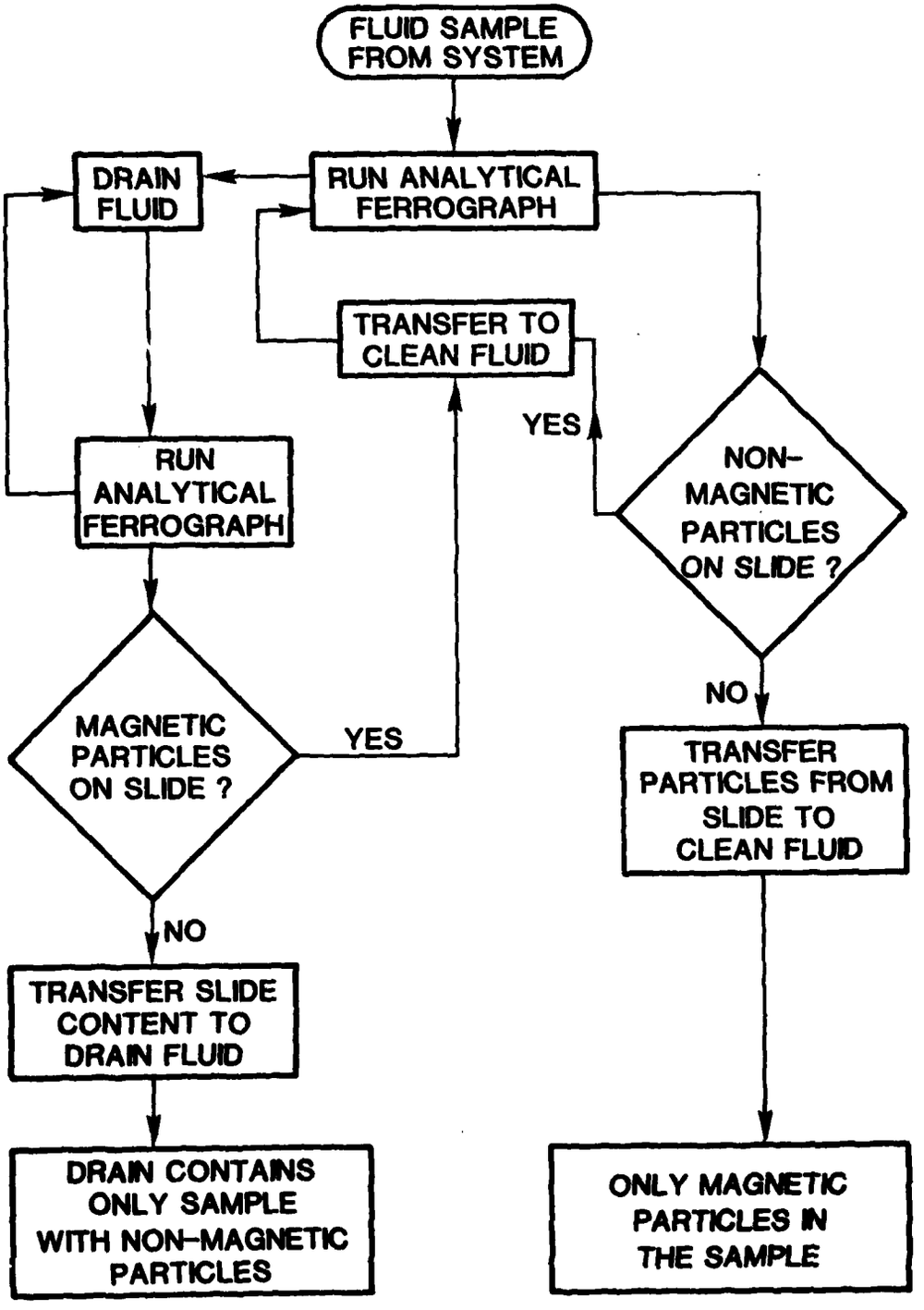

Fig. 5 Flow diagram for separation of magnetic particles

PROPOSED TEST PROCEDURE

Based on the discussions presented so far, the following test procedure is suggested for further investigation.

1. Prepare samples containing known contaminant concentrations. The contaminant can be non-magnetic, magnetic or a combination of both. Typical contaminants can be AC Fine Test Dust, carbonyl iron, aluminum powder. Obtain density readings from these samples using the Analytical Ferrograph and the DR Ferrograph. Observe the deposition of non-magnetic particles on the slide.

2. Separate the non-magnetic particles from a sample containing both non-magnetic and magnetic particles and repeat the Ferrographic process using the separated samples (one sample containing the magnetic particles and other containing non-magnetic particles). Observe the amount of magnetic particles on the slide when the non-magnetic sample was used and vice versa. The details regarding separation techniques are given at the end of the paper.

3. Prepare samples from an actual wear process. This can be economically done at the FPRC since, quite often, wear tests are conducted on hydraulic components. Using the samples, run the Analytical and the DR Ferrograph. Observe the density readings as well as the morphology of the particles. Collect the drained oil from the drain bottles and re-run these "drained" oils for another set of Ferrographic data. The second set of data will show whether (a) the recovery of magnetic particles is complete in the first set of density readings and (b) the recovery of non-magnetic particles is augmented by the absence of magnetic particles in the second set of readings.

4. Separate the original samples used in Step 3 into two samples, one containing only magnetic particles and another containing non-magnetic particles as in Ref. [2]. Run separate Ferrographic data for these two samples.

   As is evident, the original sample fluid has to be recovered from Step 3 for conducting this experiment. This is done by transferring all the particles from the slides and DR precipitator tube into the drain fluid obtained in the second set of experiments in Step 3. Ultrasonic removal of particles should be satisfactory for this process.

5. Collect another set of sample fluid from the wear test. Introduce a known amount of non-metallic particles into the fluid. Repeat Steps 3 and 4. This experiment will reveal the effect of excessive non-metallic particles in fluid samples.

6. Add iron oxide into a sample fluid and repeat Steps 3 and 4. Metallic iron oxide can be ordinary rust particles for which there cannot be any shortage. This experiment will reveal the effect of weakly magnetic particles on Ferrography.

7. Collect a large sample (say, one litre) from a wear test. Run the Ferrograph using fluid from this sample. Divide the remaining fluid into 10 bottles. Keep this fluid stored at $-40^{o}F$, $-30^{o}F$, $-20^{o}F$, up to $40^{o}F$. One of the bottles can be kept at room temperature. Take samples from each of the bottles after storing for one week, two weeks, one month, two months, four months, etc. Run the Ferrograph using the normal techniques. Another set of samples can be run after heating the stored fluid to $150^{o}F$. These experiments will completely define the effect of corrosion and chemical reaction on the fluid. Repeat Step 4 in all these cases. It should be noted that this experimental procedure is much more involved and very careful planning is necessary. The purpose of its presentation here is only to advance the basic approach to the experimentation. Table 1 shows a list of the proposed experiments.

SEPARATION OF NON-MAGNETIC PARTICLES

It was mentioned in the foregoing section that for some of the experiments, non-magnetic particles in the fluid should be separated. This can be achieved in several ways. The Ferrograph, by itself, is a magnetic separator. To use a Ferrograph as a separator, run the fluid sample over the slide again and again until microscopic examination reveals only magnetic particles. The scheme is given in the form of a chart in Fig. 5. It is seen that the process is iterative and might be quite laborious. Further, in a situation where the particles are to be separated before they are to be used on the Ferrograph, this process is not practical. However, if the DR Ferrograph can be designed using an electromagnet instead of the present permanent magnet, then it could be made to work as a separator as suggested below:

1. Run sample through modified DR Ferrograph described in the above paragraph. The electromagnet should be energized.

2. Collect the drain.

S 1 No.	TYPE OF EXPERIMENT	PURPOSE
1	Sample contains known contaminant-magnetic (M) or Non-Magnetic (NM).	Evaluate the effect of standard contaminant.
2	Separate M and NM and repeat the experiment	To evaluate the effect of separation.
3	Sample from wear test.	Evaluate the effect of actual wear particles.
4	Separate M and NM from the sample in 3.	To evauate the effect of separation.
5	Add known contaminant to samples in 3 and 4 and repeat those experiments.	To study the effect of excessive M or NM particles in wear test.
6	Add iron oxide to sample fluid from wear test and repeat 3 and 4.	To evaluate the effect of weakly magnetic particles.
7	Store sample for longer periods at low temperature before experiments.	To study the effect of chemical reaction and corrosion on wear particles.

Table 1. Summary of Proposed Experiments

3. De-energize the electromagnet.

4. Pass clean fluid through the precipitator tube while providing ultrasonic excitation to the tube.

5. Collect the fluid sample along with clean fluid, if the Analytical Ferrography is to be conducted. If the sample is to be used for DR or RT Ferrography, directly, pass the fluid through the respective precipitator tubes. It is assumed that without any iterative process, a fairly good separation will be possible by this technique. It is thought that some other techniques which are already used in industry can be adopted for use in Ferrography. They are described in the following pages.

Ref. [19] reviews a number of magnetic separators, some of which could be used for the application in the Ferrography. One of the possibilities is the use of the Davis Tube separator. Fig. [6] gives the construction of the equipment. The magnetic particles are trapped near the pole edges inside the tube in the equipment. Another device which could be used is a Franz-Isodynamic separator. Fig. [7] gives the schematic of the equipment. The operation of the equipment is self-explanatory. This equipment is used for solid particles, but it is thought that by suitable modification, it can be used for fluids as well. The two output channels for the fluid flow, shown in Fig. [7], consist of sample fluids with magnetic and non-magnetic particles. This separator seems to be ideally suited for Ferrographic applications. Another separator which offers promise is the Jones Separator. Fig. [8] gives the details of the equipment. After the sample fluid has passed through the separator, metallic particles trapped in the grooved plate should be washed out with clean fluid in this equipment.

It is not the purpose of this paper to describe the details of the various separators and, hence, discussion about them is avoided. It is emphasized here that, before attempting to use any particular separator, the effect of the magnetic particles on the Ferrographic process should be well established as per the experimentation proposed in the paper.

DISCUSSION AND CONCLUSION

The Ferrographic technique has a large potential in diagnosis and maintenance of machinery. It has been proven that, using this technique, impending failures in machines can be predicted. It was brought out in this paper that the non-magnetic particles in the fluid sample can cause erroneous results in the readings especially when a real-time monitoring of a wear situation is attempted. Based on this observation, a detailed proposal for investigation

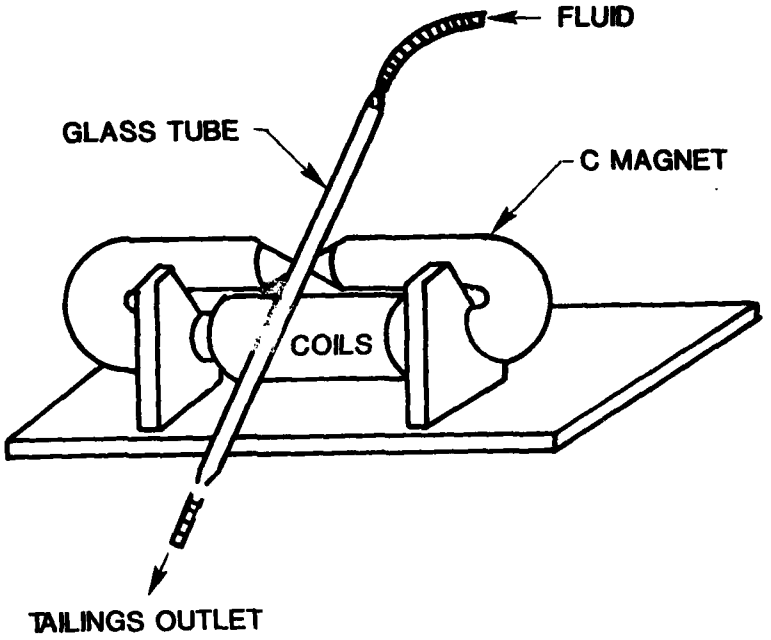

Fig. 6 Davis Tube separator

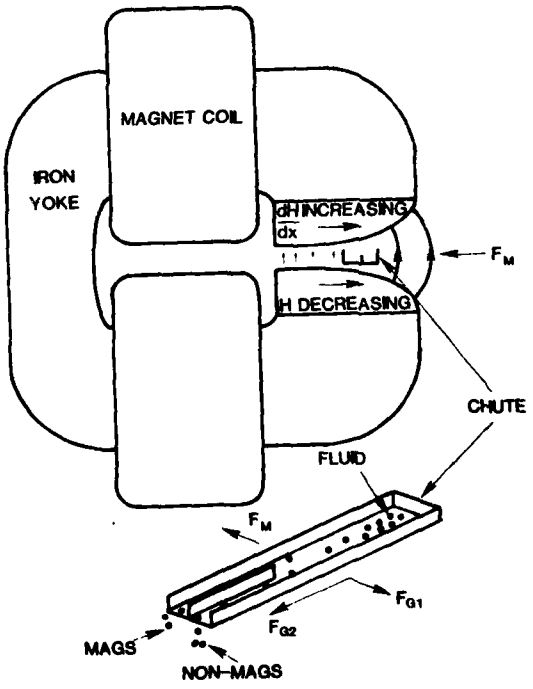

Fig. 7 Frantz-Isodynamic separator

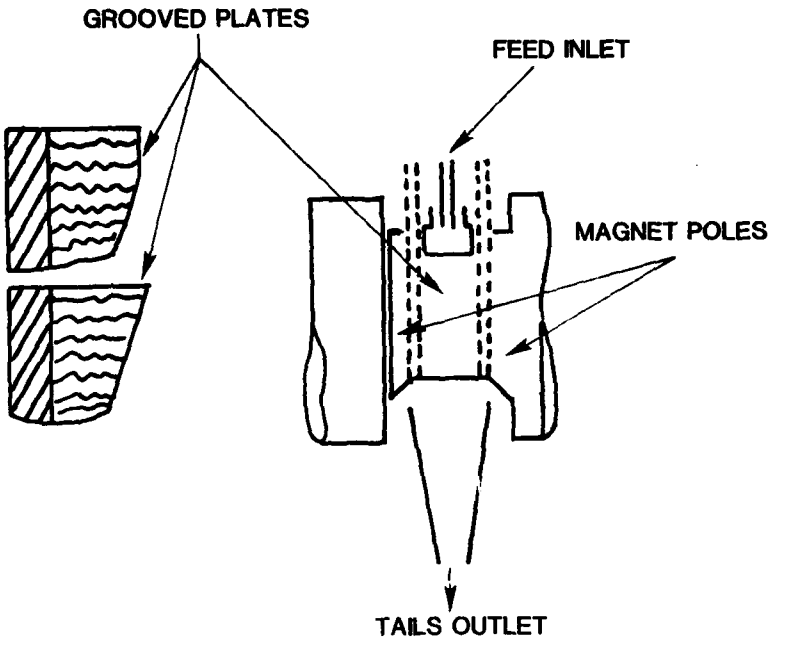

Fig. 8 Jones separator

of the effect of these non-magnetic particles in the fluid sample was presented. It was suggested that suitable separators be used upstream of the Ferrograph so that only the magnetic or fairly magnetic particles pass through the Ferrographic equipment.

ACKNOWLEDGEMENT

The author is grateful to the help and suggestions provided by Mrs. Janice Dobson, the Ferrographic Analyst at the Fluid Power Research Center.

REFERENCES

1. Seifert, W.W., *"A Method for the Study of Wear Particle in Lubricating Oil,"* Wear, 21, 1972.

2. Scott, D. et al., *"Ferrography - An Advanced Design Aid for the 80's,"* Wear, 34, 1975, pp. 251-260.

3. Hofman, M.V. and J.H. Johnson, *"The Development and Application of Ferrography to the Study of Diesel Engine Wear,"* SAE Paper No. 780181, February-March, 1978.

4. *"New Analyzer Ferrets Out Particles in Lube Oil to Get Clues on Machine Wear,"* Power, May 1972, pp. 35-37.

5. Ruff, A.W., *"Metallurgical Analysis of Wear Particles and Wearing Surfaces,"* Interim Report, Prepared for Dept. of Navy, Naval Air Engineering Center, Contract 4-8049, 1975.

6. Peterson, M.B. *"Wear Control"* Progress on Tribology Workshop, Rep. No. PB-241253, April 1974, Comments during discussion by Lt. R.S. Miller of U.S. Navy.

7. Bowen, E.R. and V.C. Westcott, *"Wear Particle Atlas,"* Foxboro/ Trans-Sonics, Inc., Contract No. NO0156-74-1682, 1976.

8. Jones, W.R., Jr., *"Ferrographic Analysis of Wear Debris from Boundary Lubrication Experiments with a Five Ring Polyphenyl Ether,"* ASLE Transactions, Vo. 18, 3, 1974, pp. 153-162.

9. Ruff, A.W. *"Study of Initial Stages of Wear by Electron Channeling,"* Part II: Quantitative Methods in Wear Debris Analysis, Institute of Materials Research, NBS, Report No. N000 14-76-F-002, September, 1976.

10. *"Sample Preparation/Ferrogram Procedure/Ferrogram Analysis,"* Preliminary Report by Naval Air Research Centre, Tribology Laboratory, Sept. 1978.

11. *"MTV Standardized Ferrography Analysis Procedure."*

12. Tessmann, R.K., *"Non-Intrusive Analysis of Contaminant Wear in Gear Pumps Through Ferrography,"* Ph.D. Thesis, Mechanical Engineering Dept., Oklahoma State University, Oklahoma, 1977.

13. Smith, R.J. and R.K. Tessmann, *"The Magnitude of Wear Debris Generation in Hydraulic Systems of Mobile Equipment,"* The BFPR Journal, 12, 2 1979, pp. 163-168.

14. Kitzmiller, D.E., *"The Development of a Calibration Technique and Standard Operating Procedure for a Ferrograph,"* Masters Thesis, Oklahoma State University, 1977.

15. Nair, K.S., *"An Appraisal of the Analytical Ferrograph,"* The BFPR Journal, 1980.

16. Nair, K.S., *"An Appraisal of the Direct Reading (DR) Ferrograph,"* The BFPR Journal, 1980.

17. Bozoroth, R.M., *"Ferromagnetism,"*D. Van Nostrand Company, Inc., 1951.

18. Taggert, *"Handbook of Mineral Dressing,"* John Wiley & Sons.

19. Oberteuffer, J.A., *Magnetic Separation: A Review of Principles, Devices, and Applications,"* IEEE Transactions on Magnetics, Vo. MAG 10, No. 2, June 1974.

APPENDIX D

Summary of Ferrographic Data for Hydrostatic Transmission

SUMMARY OF FERROGRAPHIC DATA

Test Ident. Test Track

Sample Location Case Drain - Pump for left wheel drive

Machine Hydrostatic Transmission

Day 3

Test Time (hrs)	Ferrographic Densities per ml at Indicated Location				Remarks
	Entry	54mm	50mm	30mm	
0	55.5	64.7	35.8	14.2	Pump failure
1	9.4	12.2	9.4	6.1	New oil-New pump/motor
2	8.0	9.7	7.5	4.6	
3	5.2	9.8	8.5	4.8	
4	6.5	8.5	7.2	4.5	
5	5.7	7.5	5.6	4.4	
6	6.4	6.8	5.6	4.1	
7	4.9	6.3	5.1	3.6	
8	5.0	5.5	4.5	3.2	
9	6.2	8.0	6.7	4.3	
10	8.3	9.5	7.5	6.6	Machine down 30 minutes

SUMMARY OF FERROGRAPHIC DATA

Test Ident. Test Track

Sample Location Case Drain - Pump for right wheel drive

Machine Hydrostatic Transmission

Day 3

Test Time (hrs)	Ferrographic Densities per ml at Indicated Location				Remarks
	Entry	54mm	50mm	30mm	
0	72.7	87.0	45.3	15.7	Pump failure
1	9.7	9.8	7.9	4.9	New oil-New pump/motor
2	8.2	9.5	7.0	3.7	
3	9.4	9.2	8.5	4.9	
4	6.3	8.2	7.0	4.6	
5	8.3	9.0	6.9	4.3	
6	6.3	7.0	5.8	3.7	
7	5.2	6.0	4.3	3.3	
8	7.2	8.0	6.2	3.9	
9	6.6	7.2	5.5	4.3	
10	5.1	7.0	5.5	3.3	Machine down 30 minutes

SUMMARY OF FERROGRAPHIC DATA

Test Ident. Level Terrain

Sample Location Case Drain - Pump for left wheel drive

Machine Hydrostatic Transmission

Day 1

Test Time (hrs)	Ferrographic Densities per ml at Indicated Location				Remarks
	Entry	54mm	50mm	30mm	
C	9.5	8.9	7.5	5.2	Taken at Stillwater
0	6.4	6.4	5.7	4.0	Taken during shake down
1	5.3	4.4	4.0	2.9	
2	3.8	3.5	3.4	2.4	
3	3.7	3.5	2.9	2.4	
4	3.4	3.5	2.8	2.2	
5	4.2	4.0	3.1	2.1	
6	3.3	2.7	2.2	1.8	
7	3.2	2.8	2.6	2.1	
8	3.3	2.4	2.1	1.6	
9	3.3	2.5	3.0	1.6	
10	3.8	2.5	2.3	1.8	

SUMMARY OF FERROGRAPHIC DATA

Test Ident. Level Terrain

Sample Location Case Drain - Pump for right wheel drive

Machine Hydrostatic Transmission

Day 1

Test Time (hrs)	Ferrographic Densities per ml at Indicated Location				Remarks
	Entry	54mm	50mm	30mm	
0	7.5	8.3	7.2	5.0	Taken at Stillwater
0	8.4	6.1	5.0	3.7	Taken after shake down
1	8.2	6.1	4.7	3.3	
2	5.0	4.6	3.7	2.5	
3	7.2	5.2	3.8	2.5	
4	4.3	3.8	3.3	2.4	
5	3.5	3.6	2.7	2.4	
6	4.0	3.4	2.9	2.1	
7	3.4	3.2	2.6	2.2	
8	3.6	2.8	2.3	1.8	
9	3.2	2.7	2.2	1.7	
10	4.9	4.1	3.3	1.3	

SUMMARY OF FERROGRAPHIC DATA

Test Ident. Rough Terrain

Sample Location Case Drain - Pump for left wheel drive

Machine Hydrostatic Transmission

Day 2

Test Time (hrs)	Ferrographic Densities per ml at Indicated Location				Remarks
	Entry	54mm	50mm	30mm	
1	5.5	4.6	3.9	2.9	Changed oil before start
2	4.1	3.5	3.2	3.1	
3	4.6	4.4	4.1	3.6	Machine down one hour
4	4.5	3.7	3.2	2.7	
5	3.7	3.3	2.8	2.7	
6	4.3	3.7	3.3	2.2	
7	3.5	3.5	2.8	2.2	
8	3.4	3.3	2.7	2.1	
9	3.0	3.1	2.7	2.1	
10	3.4	2.9	2.8	2.1	

SUMMARY OF FERROGRAPHIC DATA

Test Ident. Rough Terrain

Sample Location Case Drain - Pump for right wheel drive

Machine Hydrostatic Transmission

Day 2

Test Time (hrs)	Ferrographic Densities per ml at Indicated Location				Remarks
	Entry	54mm	50mm	30mm	
1	3.7	4.1	3.5	3.2	Changed oil before start
2	3.6	3.9	3.5	3.0	
3	4.0	4.2	3.8	3.2	Machine down one hour
4	3.9	3.8	3.7	3.0	
5	5.3	4.9	4.6	3.3	
6	3.5	3.7	3.5	2.7	
7	4.5	4.0	3.4	2.4	
8	4.7	3.7	3.3	2.6	
9	4.0	3.4	3.3	2.3	
10	3.2	2.8	2.6	2.1	

DISTRIBUTION LIST

Army Materials & Mechanics Res. Ctr.
Watertown, MA 02172
C. P. Merhib 1

Admiralty Materials Laboratory
Holton Heath Poole Dorset BH16 6JU UK
Dr. G. Pocock 1

Office of Naval Research
800 N. Quincy St.
Arlington, VA 22217
LCDR H. P. Martin, Code 211 6
Dr. R. S. Miller, Code 473 1
Dr. R. Burton, Code 473 1

R&D Representative
Department of Defence
Australian High Commission Australia House
The Strand London WC2 UK
Mr. Ron A. Cummins 1

Aeronautical Research Laboratories
506 Lorimer St. Fishermen's Bend
Box 4331 PO Melbourne Victoria 3001
Australia
Mr. Max L. Atkin 1

Defence Research Establishment Facific
Esquimalt Road Victoria British Columbia
Canada
Mr. Clint A. Waggoner 1

AFAPL/SFL
Wright Patterson AFB, OH 45433
Phillip W. Centers 1

Defense Documentation Center
Building 5, Cameron Station
Alexandria, VA 22314 12

NASA Lewis Research Center
M. S. 23-2
21000 Brookpark Road
Cleveland, OH 44135
Mr. W. J. Anderson 1

Texaco Research Center
POB 509, Beacon, N.Y. 12508
Mr. E. M. Barber 1

Mr. E. Bisson
20786 Eastwood Ave.
Fairview Parks, OH 44126 1

School of Mechanical Engineering
Upson Hall
Cornell University
Ithaca, NY 14850
Prof. J. F. Booker 1

Pratt & Whitney Aircraft
400 Main St.
EB3SW
East Hartford, CT 06108
Mr. P. F. Brown 1

Prof. W. E. Campbell
22 Ledgestone Road
Troy, NY 12180 1

Prof. of Mech. Engrg, and Astronautical
Science
Northwestern University
Evanston, IL 60201
Prof. H. S. Cheng 1

Aero Materials Department
Naval Air Development Center
Johnsville, Warminster, PA 18974
Mr. D. Minuti 1

Dr. R. S. Fain
Texaco Center
P. O. Box 509
Becon, NY 12508 1

General Electric Co., R&D Center
POB 43, Bldg. 37, Rm. 615
Schenectady, NY 12345
Mr. G. R. Fox 1

Engineering Mec. Dept., GMC-GM Research
Lab.,
12 Mile and Mound Roads
Warren, MI 48090
Mr. D. F. Hays 1

Engineering Division, Brown University
Providence, RI 02912
Prof. M. D. Hersey 1

Mr. R. L. Johnson
5304 West 62nd St.
Endina, MN 55436 1

Research Dept., Caterpillar Tractor Co.
Peoria, IL 61602
Mr. B. W. Kelley 1

Dept. of Chemical Engrg.
Pennsylvania State University
University Park, PA 16802
Prof. E. E. Klaus 1

Southwest Research Institute
8500 Culebra Road
San Antonio, TX 78284
Dr. P. M. Ku 1

The Boeing Center
POB 16858
Philadelphia, PA 19142
Mr. A. J. Lemanski, M.S. P32-09 1

Security Div., Dresser Industries
POB 24647
Dallas, TX 75224
Dr. W. E. Littmann 1

Mechanics Div., Rensselaer Polytechnic Inst.
Troy, NY 12181
Prof. J. Tichy 1

Mr. S. J. Needs, Kingsbury, Inc.
19385 Drummond Rd.
Phil., Ind. Park
Philadelphia, PA 19154 1

Mechanical Engineering Dept., MIT
Cambridge, MA 02139
Prof. Nam Suh 1

Army Research Office
POB 12211
Research Triangle Park, NC 27709
Dr. E. A. Saibel 1

Mechanical Eng. Dept., University of Wisconsin
1513 University Avenue
Madison, WI 53706
Prof. A. Seireg 1

SKF Technology Service
1100 First Ave.
King of Prussia, PA 19406
Mr. L. B. Sibley 1

Mechanical Technology, Inc.
968 Albany Shaker Rd.
Latham, NY 12110
Dr. D. F. Wilcock 1

Mechanical Eng. Dept.
University of Massachusetts
Amherst, MA 01002
Prof. W. R. D. Wilson 1

Mechanical Engineering Dept.
Georgia Institute of Technology
Atlanta, GA 30332
Prof. W. O. Winer 1

U. S. Naval Research Laboratories
Washington, DC 20375
Mr. R. C. Bowers 1

Office of Technology Assessment
Congress of the United States
Washington, DC 20510
Mr. M. E. Peterson 1

Air Force Aero Propulsion Laboratory
Wright Patterson Air Force Base, OH 45433
Mr. H. F. Jones 1

MS 23-2, NASA-Lewis Research Center
21000 Brookpark Rd.
Cleveland, OH 44135
Mr. L. P. Ludwig 1

Air Force Materials Lab.
Wright Patterson Air Force Base
Dayton, OH 45433
Mr. F. Brooks 1

Mobil Research & Development Corp.
Box 1025 Princeton, NJ 08540
C. N. Rowe 1

NASA-Lewis Research Center
21000 Brookpark Road
Cleveland, OH 44135
E. V. Zaretsky 1

Commander
Naval Air Systems Command
Washington, DC 20361
Code 340E (Mr. B. Poppert) 1

Naval Air Engineering Center
Ground Support Equipment Department
Lakehurst, NJ 08733
Code 92724 (P. Senholzi) 1

National Bureau of Standards
Department of Commerce
Washington, DC 20234
Dr. W. Ruff 1

Imperial College of Science and
Technology
Dept. of Mechanical Engineering
Exhibition Road
London, England SW7
Prof. P. Macpherson 1

Commander
Naval Sea Systems Command
Code 0484G
Washington, DC 20362
Mr. Tarte 1

Foxboro Analytical
Burlington Center
78 Blanchard Road
P. O. Box 435
Burlington, MA 01803 1

Mechanical Engineering Department
Michigan Technological University
Houghton, MI 49931
Dr. John Johnson 1

Office of Naval Research Branch Office
536 South Clark Street
Chicago, IL 60605
DODAAD Code N62880 1

Office of Naval Research
Room 582 Federal Building
300 E. 8th Street
Austin, TX 78701
Mr. Matial Davoust 1